



Published in final edited form as:

Chem Rev. 2008 November ; 108(11): 4754–4783. doi:10.1021/cr8004422.

Biomimetic Systems for Hydroxyapatite Mineralization Inspired By Bone and Enamel

Liam C. Palmer[†], Christina J. Newcomb[‡], Stuart R. Kaltz[‡], Erik D. Spörke^{‡,§}, and Samuel I. Stupp^{*,†,‡,||,⊥}

[†]*Department of Chemistry, Northwestern University, Chicago, Illinois 60611*

[‡]*Department of Materials Science and Engineering, Northwestern University, Chicago, Illinois 60611*

^{||}*Department of Medicine, Northwestern University, Chicago, Illinois 60611*

Institute for BioNanotechnology in Medicine, Northwestern University, Chicago, Illinois 60611

1. Introduction

1.1. Biomineralization

The study of biomineralization is not only important to gain an understanding of how mineral-rich tissues are created *in vivo* but also because it is a great source of inspiration for the design of advanced materials.^{1–7} Mineralized tissues have remarkable hierarchical structures that have evolved over time to achieve great functions in a large variety of organisms. Organic phases play a key role in templating the structure of mineralized tissues; therefore, their matrices are often hybrid in composition, varying widely in the relative content of organic and inorganic substances. Understanding the complex integration of hard and soft phases that biology achieves in mineralized matrices across scales and its link to properties is knowledge of great value to materials chemistry. At the same time, the synthetic mechanisms used by biology to create mineralized matrices could also offer some useful strategies to create synthetic hybrid materials. Often, the amount of organic material utilized by Nature to modify mechanical properties of mineralized structures is vanishingly small. One example is the role of occluded proteins in the toughness of biogenic calcite.⁸ The study of mammalian bone and teeth in the biomineralization and biomimetic context is particularly interesting since the information derived could contribute a significant biomedical impact on therapies and strategies to repair or regenerate human mineralized tissues. This is an important area given the continually rising average life span of humans. The materials of interest could be highly sophisticated bioactive scaffolds to regenerate bone and possibly dental tissues as well. This review focuses on the formation of hydroxyapatite (HA) in synthetic systems designed primarily in the biomimetic context of bone or enamel mineralization for therapeutic approaches in repair of human tissues. Bone and enamel share the same mineral composition, HA, but have different morphologies and organic content. Enamel is almost entirely inorganic in composition, and bone has a relatively high organic composition. Knowledge acquired in this field may inspire the chemical synthesis of novel hybrid materials, including apatite-based structures for the regeneration of human bone and dental tissues.

*To whom correspondence should be addressed. E-mail: s-stupp@northwestern.edu.

§Current address: Electronic and Nanostructured Materials, Sandia National Laboratories, Albuquerque, NM 87185.

1.2. HA and Related Minerals

The term apatite indicates a mineral structure with the chemical formula $A_4B_6(MO_4)_6X_2$, where A and B are both calcium in many biological tissues, MO_4 is a phosphate group, and X is a hydroxide ion.⁹ Biologically mineralized crystals are typically formed in an organic matrix with precise regulation of synthetic mechanisms through proteins. These proteins are in dynamic equilibrium with their environment, thus resulting in fluctuations and tissue remodeling. Given the unique mechanism involved in apatite crystal formation in biology, biogenic apatite varies in several ways from the corresponding geologically produced mineral. First, biogenic apatite has a smaller crystal size, which generates a higher surface area, thus permitting additional adsorption of ions and molecules on the apatite surface. Biogenic apatite also contains significant carbonate substitutions, OH^- deficiencies, and imperfections in the crystal lattice.¹⁰ For example, F^- ions are readily incorporated into the HA lattice, forming fluoroapatite, a less soluble phase of calcium phosphate as compared to HA. Finally, biological minerals tend to attain high crystallinity and a more organized structure on the time scale of days or months rather than years.¹¹

HA is the calcium phosphate mineral found in vertebrate bones, mammalian teeth, fish scales, and the mature teeth of some chiton species. In the early 1900s, X-ray diffraction patterns identified ground bone to be similar to geological HA $Ca_5(PO_4)_3(OH)$, which has a Ca/P ratio of 1.67.¹⁰ However, later studies have shown that the molar ratios of Ca/P in biomineralized tissues such as bone can vary significantly from this ideal value due to an abundance of substitutions and vacancies. These imperfections occur because the body utilizes bone as a reservoir to maintain homeostasis with respect to calcium, magnesium, and phosphate ions. Carbonated HA, $Ca_{10}(PO_4,CO_3)_6(OH)_2$ (also known as “dahllite”), is the most abundantly produced phosphate mineral in mammals, particularly in bones and teeth.^{12,13} Substitutions of carbonate for hydroxide are known as A type, and carbonate substitutions for phosphate are called B type.¹⁴ These two substitution patterns can be distinguished by Fourier transform infrared (FTIR) spectroscopy.¹⁵ Carbonated HA in enamel and dentin exhibit fewer imperfections and more closely resemble the stoichiometric ratio, since teeth are not typically involved in maintaining ion homeostasis. When in vitro methods of mineralization are combined with biological applications, researchers should recognize the fundamental differences between synthetic and biologically produced HA.

In addition to HA, a number of other calcium phosphate minerals are known (Table 1). For example, octacalcium phosphate (OCP) can be produced under similar conditions that cause formation of HA in vitro. The initially formed OCP mineral displays four resonances by ^{31}P magic angle spinning NMR (0.2, 2.0, 3.3, and 3.7 ppm).¹⁶ Under basic conditions ($pH > 7.4$), this spectrum changes to a single broad resonance at ~ 3 ppm that is characteristic of HA. OCP also can be distinguished by the characteristic 100 diffraction in small-angle X-ray scattering (SAXS) that is absent from HA. Furthermore, these minerals can be distinguished by their Ca/P ratio using EDX. Other common methods for establishing the mineral phase include Raman and FTIR spectroscopy.^{15,17,18} As we will discuss later in this review, the transformation from OCP to HA is complex and may involve dissolution and reprecipitation or the intermediacy of other mineral phases. The intermediacy of OCP in HA mineralization in vivo has been quite difficult to determine and remains controversial.

HA by itself can be prepared artificially using a variety of methods that we will discuss in section 4 of this review. For example, precipitation reactions¹⁹ and sol-gel synthesis²⁰ have been used extensively, but directed growth of HA is key to mimicking biological systems. The key factors that contribute to a well-controlled process of mineralization as seen in biology include solubility, supersaturation, and energetics. Reproducing these parameters in the laboratory can be quite challenging. Before describing the artificial chemical systems designed

to understand or mimic bone and enamel mineralization, we first review the basic structure of bone (section 2) and enamel (section 3).

2. Bone Mineralization

2.1. Introduction to Bone

Bone is a dynamic, highly vascularized tissue that is formed from a composite of 70% mineral (mostly nanoscale HA crystals) and 30% organics (including collagen, glycoproteins, proteoglycans, and sialoproteins) by dry weight.²¹ As the primary structural support of the mammalian body, bones are constantly being remodeled in response to the applied stresses. This continuous regeneration of bone likely serves to repair fatigue damage and prevent excessive aging.²² In addition to its structural functions of load bearing, internal organ protection, and muscle support, bone is also important for the tight regulation of calcium ion concentration through the ongoing resorption and formation of new mineral. There are two cell types that are responsible for the formation, removal, and maintenance of bone tissue. Osteoblasts are mononuclear cells primarily responsible for bone formation. Osteoclasts are multinuclear, macrophage-like cells that resorb bone.

2.2. Hierarchical Organization of Bone

To better understand the complex bone architecture, several hierarchical models have been proposed. Weiner and Wagner have identified seven discrete levels of hierarchical organization in bone (Figure 1), which we describe here.²³ In their model, bone is considered as a family of materials with the mineralized collagen fiber as the primary building block for subsequent higher order architectures. The structure of bone varies greatly among different locations in the skeleton, but the basic nanoscale structure of bone consisting of mineralized collagen remains the same throughout.²³ Mann has presented a similar structural hierarchy containing six levels.²⁴

The first level of hierarchy consists of the molecular components: water, HA, collagen, and other proteins. The crystals of HA are plate-shaped and are among the smallest known biological crystals (30-50 nm long, 20-25 nm wide, and 1.5-4 nm thick, depending on the study) (Table 2). In early studies, apatite needles were observed,²⁵ but more recent studies suggest that platelets are the dominant morphology and that the apparent needles are most likely to be platelets viewed edge-on.²⁶ Collagen is discussed in detail in section 2.3.1. Noncollagenous proteins (NCPs) are also present but make up 10% or less of the total protein content in the bone matrix. The specific functions of the NCPs, which are discussed in more detail below, are still not completely understood. In addition to influencing crystal nucleation and growth, NCPs also play roles in cell signaling and ion homeostasis.²⁷

The second level is formed by the mineralization of collagen fibrils. This platelet-reinforced fibril composite is described by Weiner and Wagner as containing parallel platelike HA crystals²³ with their *c*-axis aligned with the long axis of the fibril.²⁸ The location of these crystals in the fibril was demonstrated in a study by Traub et al. that showed that mineralized collagen fibrils had the same banded pattern as negatively stained collagen fibrils.²⁶ This indicated that mineral is concentrated in the hole zones of the fibril, as described in the next section. It was proposed that these mineral platelets were arranged in parallel like a stack of cards within the interstices of the fibril. Olszta et al. concluded from electron diffraction studies that the mineral plates are not quite as ordered as previously assumed.¹² This imperfect arrangement of nearly parallel crystals has been supported by recent SAXS and transmission electron microscopy (TEM) data from Burger et al.²⁹

The third level of hierarchy is composed of arrays of these mineralized collagen fibrils. These fibrils are rarely found isolated but rather almost always associated as bundles or other

arrangements, often aligned along their long axis. The fourth level is the patterns of arrays that are formed. These include parallel arrays, woven arrangements, plywoodlike structures, and radial arrays like those found in dentin.³⁰

Cylindrical structures called osteons make up the fifth level. Osteons are formed with significant cellular activity and remodeling; osteoclasts resorb bone and form a tunnel, and osteoblasts subsequently lay down lamellae in stacked layers until only a small channel (Haversian canal) is left behind. These channels serve as a conduit for nerves and blood supply to the bone cells. The sixth level of bone organization is the classification of osseous tissue as either spongy (trabecular or cancellous) or compact (cortical). Cancellous bone is extremely porous (75-95% porosity), providing space for marrow and blood vessels, but has much lower compressive strength. Cortical bone is the dense outer layer (5-10% porosity) that allows the many of the support functions of bone. Therefore, the mechanical properties of cortical bone represent the benchmark for synthetic bone.³¹ The seventh level is simply the whole bone on the macroscopic scale, incorporating all of the lower levels of hierarchy. There are 206 bones in the adult human skeleton, the structure of which depends on the location and function.

2.3. Molecular Components of Bone

Bone is composed of a number of biomacromolecules (Table 3). The structural aspects of the matrix are accounted for by framework macromolecules, such as collagen. These framework macromolecules are generally hydrophobic and can be cross-linked to support and localize the water-soluble acidic proteins, which are responsible for directing nucleation and mineral growth by the organization and transport of ions.²⁴

2.3.1. Collagen—Collagens serve as extracellular matrix molecules for many soft and hard connective tissues, including cornea, skin, tendon, cartilage, and bone. The chemistries underlying the formation of these tissues are all quite similar; the fundamental differences depend on their hierarchical fibrillar architectures. More than 20 human collagens have been reported, many of which display a 67 nm periodicity, due to the axial packing of the individual collagen molecules.³² Of these, type I collagen is the most abundant protein in the human body and provides much of the structural integrity for connective tissue, particularly in bones, tendons, and ligaments.

Collagen is composed largely of the amino acids glycine, proline, and hydroxyproline, which together account for more than 50% of the amino acid composition, often as Gly-X-Y repeats (where X and Y are either proline or hydroxyproline).³³ Tropocollagen is the subunit of collagen fibrils formed of three polypeptide strands (each offset by one amino acid), approximately 300 nm long and 1.5 nm in diameter. Each of the three chains forms a left-handed helical polyproline II type helix with three residues per turn. The tropocollagen units assemble in a parallel, quarter-staggered arrangement.³² There is a 40 nm gap, also called the “hole zone”, between the ends of each of these units, with 27 nm of overlap between adjacent units. This spacing gives rise to the basic 67 nm repeat unit and banding observed by electron microscopy, also known as the D-period. This 67 nm repeat unit corresponds to approximately 234 amino acid residues (Figures 2 and 3).³⁴ These “hole zones” are critical in mineralization, as they appear to be the site of mineral nucleation. The crystals appear to grow and proliferate from this area. The size of this gap also appears to constrain the mineral growth. The commonly accepted model of higher order aggregation suggests that five tropocollagen units align longitudinally (overlapping by about one-quarter of the molecular length) into a microfibril. TEM shows an expected bundle diameter of about 3.6 nm. These microfibrils assemble into collagen fibrils 35-500 nm in diameter (Figure 4). Berman and co-workers solved a high-resolution X-ray crystal structure of a collagen-like peptide (Gly→Ala) with 1.85 Å resolution

that helped elucidate the helical conformation as well as the hydration of the polar groups (Figure 5).^{35,36}

Collagen organization within mineralized bone is difficult to study directly but can be imaged by TEM after removal of the mineral.^{37,38} Crystal organization in bone is harder to investigate than collagen organization by TEM, because of the difficulties in preparing thin specimens of the mineral-containing material.³⁹ Therefore, quantitative X-ray texture analysis has generally been more useful for investigating the mineral phase of bone.⁴⁰ It is worth noting that many of the early studies of mineralization on collagen were based on samples from the leg tendon of *Meleagris gallopavo* (wild turkey).^{26,41-43} As noted by Wenk and Heidelbach, textural differences between the tissues suggest that mineralized turkey tendon may not be a good model for bone tissue.

A gel filtration-like procedure has also been used to determine the size exclusion profiles of collagen from demineralized bovine tendon and bone.⁴⁴ It was found that molecules (or potentially apatite crystals) smaller than a 6 kDa protein could diffuse into the hydration shell of the collagen. In contrast, molecules larger than a 40 kDa protein are completely excluded. The exclusion of proteins, aggregates, or crystallites based on size may be extremely important for the highly regulated collagen mineralization processes that take place in vivo. For example, a large protein may nucleate a small HA crystallite (up to the size of about 12 unit cells) that can then diffuse into the collagen fibril.

2.3.2. NCPs—A large area of biomineralization research is focused on the NCPs, including bone sialoprotein (BSP),⁴⁵ osteonectin (ON), osteopontin (OP),⁴⁶ and osteocalcin (OC).⁴⁷ The primary amino acid sequence of these proteins often includes a high density of aspartic acid and glutamic acid residues, which have a high affinity for calcium ions.⁴⁸ These proteins often undergo extensive posttranslational modifications to add additional acidic groups.²⁴ Furthermore, polysaccharides are often added that contain even more carboxylic acid and sulfate groups. Unfortunately, these acidic macromolecules are difficult to isolate from the bone matrix and are therefore not well understood. In fact, even the primary sequence can be difficult to determine precisely. Addadi et al. showed evidence that one of the nucleators of HA may have a β -sheet structure,⁴⁹ a conformation that could allow preferential interactions with certain mineral crystal faces, as demonstrated in a subsequent study.⁵⁰ Collagen, while it is the most prevalent organic component in bone, does not exhibit this secondary structure, suggesting that the actual nucleators of mineral in natural bone may be other proteins bound to the collagen scaffold. Therefore, NCPs are expected to play an important role in biomineralization, as described below.

BSP (also known as BSP-II) is a phosphoprotein that contains large stretches of poly(glutamic acids) as well as the RGD integrin-binding sequence at its carboxy terminus.⁴⁵ Its expression is generally limited to the later stages of osteoblast differentiation and early stages of mineralization. It is also expressed at low levels in osteoclasts, hypertrophic cartilage, and chondrocytes.⁵¹ BSP has a high affinity for calcium ions. ON, also known as “secreted protein, acidic, rich in cysteine” (SPARC), is a glycoprotein found at high concentrations in bone tissue.⁵² It is only slightly phosphorylated and has been shown to both nucleate⁵³ and inhibit⁵⁴ mineralization. Another potentially important feature is the presence of many aspartic acid and glutamic acid residues repeated throughout the structure.²⁴ OP (also known as BSP-I) also contains a string of polyaspartic acid residues as well as a RGDS sequence near the middle of the primary sequence.²⁴ It is an important regulator of osteoclast activity, and the level of phosphorylation of OP has been shown to control the inhibition or nucleation of HA.⁵⁵ It was hypothesized that partially phosphorylated OP can bind to mineral nuclei or small crystals and block growth, but fully phosphorylated OP can nucleate mineral at low concentrations. OC is the most abundant noncollagenous protein in bone and is synthesized only by osteoblasts.

⁵⁶ It has been shown to inhibit bone formation but has no effect on the mineralization of bone.
⁵⁷ However, as the only osteoblast-specific protein, OC has become an essential marker to indicate differentiation into osteoblasts.⁴⁷

2.4. Cellular Components

Osteoblasts are mononuclear cells of mesenchymal origin that are responsible for formation of the osteoid, the organic portion of the bone tissue. Representing about 50% by volume and 25% by mass of the total bone content, the osteoid is composed of collagen, NCPs, and polysaccharides [e.g., chondroitin sulfate (ChS)]. In addition to osteoid secretion, osteoblasts are also involved in the mineralization process. These cells are believed to regulate the local calcium and phosphate concentrations to promote apatite mineralization.^{22,58} As osteoblasts become trapped in the secreted matrix, they terminally differentiate into osteocytes (Figure 6).⁵⁹ These star-shaped cells compose 90-95% of all cells in mature bone and are connected to one another and to cells on the bone surface through dendritic processes, similar to those of neurons. The primary function of these cells appears to be signaling for matrix resorption or formation in response to mechanical stress.⁶⁰ Mature osteocytes can be difficult to isolate in pure form, so many mineralization studies have used osteoblasts in place of osteocytes. However, it should be noted that these cells can behave very differently; for example, osteoblasts are much less sensitive to shear stress.⁶¹ Osteoclasts are bone cells that remove bone tissue by a process known as “bone resorption”.^{62,63} The actin cytoskeleton of the osteoclast reorganizes into a ring known as the “sealing zone”, and the cell membrane forms a “ruffled border” at the contact with the bone tissue to facilitate dissolution of the apatite mineral followed by hydrolysis of the collagen-rich organic matrix.⁶² Vacuolar proton pumps cause demineralization of the bone matrix by acidification to a pH of ~4.5.⁶³ The organic portion of the matrix is further broken down by lysosomal cysteine proteases⁶⁴ and matrix metalloproteases (MMP).⁶² Finally, the degraded extracellular materials are removed from the resorptive lacuna and shuttled into the extracellular space and ultimately the blood.⁶² Bone resorption is essential for the growth, healing, and remodeling of adult bone and to regulate the calcium available to the body. For further information on osteoclast cells, the reader is directed to the comprehensive review by Roodman.⁶⁵

2.5. Mineralization of Bone and Its Components

Bone formation occurs biologically by one of two distinct processes, depending on the type of the bone. Intramembranous ossification is common in the development of the flat bones of the cranium and parts of the mandible and clavicle. This process involves the direct differentiation of mesenchymal progenitor cells into osteoblasts. As described below, bone formation involving mineralization from a cartilaginous template is known as endochondral ossification. Endochondral ossification is a two-step process responsible for the development of the rest of the human skeleton.⁶⁶ In the first step, a cartilaginous region is formed surrounded by a bony collar. As the cartilage is vascularized, chondrocytes (cartilage cells) undergo apoptosis, and osteoblasts migrate into the tissue. The second step is the mineralization of this cartilaginous template and the formation of new bone, which is initially deposited as woven bone, a disorganized structure with a high proportion of osteocytes. The collagen fibers in woven bone are randomly oriented. During development or after a fracture, woven bone quickly forms and is gradually replaced by slower-growing lamellar bone. Lamellar bone is stronger and filled with the cylindrical arrangements of collagen fibers known as osteons. The resulting structure is an ordered mineral-organic composite material organized into micrometers-thick lamellae with a plywoodlike structure (Figure 1).

Biomaterial nucleation and growth requires a local environment with sufficient supersaturation in the mineral precursors.¹³ Anderson has explained this in terms of matrix vesicles, which are formed and released from the outer membranes of osteoblasts and related cells.⁶⁷ It is

believed that HA is first nucleated within the vesicle. As the crystallite grows bigger, it breaks through the vesicle and is exposed to the extracellular fluid. According to this theory, the initial mineral formation (phase 1) is under cellular control, whereas mineral propagation (phase 2) is mediated by collagen in the extracellular matrix. However, matrix vesicles are not the only site of mineral nucleation.⁶⁸ Numerous *in vitro* studies have indicated that a wide variety of matrix proteins can also nucleate and control growth or agglomeration of these crystals.⁶⁸ Additional studies will be needed to resolve the contribution of these mechanisms in the formation of HA *in vivo*.

Several functional motifs within the NCPs have been noted as being particularly important for mineralization. It was postulated that the mineralization effects of BSP were only due to runs of acidic glutamate residues,⁶⁹ but later studies suggest that these groups alone are not responsible for mineral formation.⁷⁰ Hunter and Goldberg claimed that removal of phosphate groups on BSP has little or no effect on mineralization,⁶⁹ but more recently, He et al. have seen phosphorylation as the crucial component for mineralization of phosphophoryn.⁷¹ As described further in section 4, we recently demonstrated templated formation of aligned HA crystals on self-assembled nanofibers displaying phosphorylated amino acid residues.⁷² While determining the precise mechanism will require further research on the various experimental parameters (charge, phosphate ion concentration, accessibility, etc.), it seems likely that phosphorylation plays a key role in mineralization.

The formation of platelike crystals in the mineralized collagen fibrils is still not fully understood. One possible explanation for this mineral morphology in bone is that crystal growth occurs via an OCP intermediate.^{73,74} OCP has nearly the same crystal structure as HA but contains an extra hydrated layer that may be responsible for the observed plate-shaped crystals in natural bone. In contrast, Olzsta et al. infiltrated a collagen matrix with a polyanionic polymer, nucleating an amorphous mineral precursor that then entered the collagen fibrils. The subsequent crystal growth was characterized using X-ray and TEM; in this case, the mineral growth is directed and confined by the intrafibrillar “hole zones” of the collagen.¹²

The existence of a transient precursor is an ongoing controversy in the field of bone biomineralization.⁷⁵ Amorphous calcium phosphate (ACP) was also found to spontaneously precipitate to apatite at physiological values *in vitro*.⁷⁶ However, Grynopas et al.⁷⁷ could not detect the presence of ACP in young bone. Using improved methods of imaging and structure determination, stable and transient forms of amorphous precursors have since been identified in biomineralization of calcium carbonate in sea urchin spines and spicules.⁷⁸⁻⁸⁰ As a result, the role of amorphous phases in mineralization of HA in biological tissues such as bone continues to be a subject of great research interest. As a transient species, it has been claimed that ACP was difficult to identify in young bone due to its tendency to rapidly transform into an energetically more favorable phase.^{81,82} The recent work by Olzsta et al. has reintroduced the concept that an amorphous precursor could be responsible for nucleation of HA in bone.¹²

3. Enamel Mineralization

The mammalian body contains numerous mineralized tissues; the tissue with the most robust mechanical properties is enamel. Enamel is the hardest material formed by vertebrates and is the most highly mineralized skeletal tissue present in the body.⁸³ Mature enamel is composed of 95-97% carbonated HA by weight with less than 1% organic material. The high degree of mineralization makes enamel a fascinating model for understanding fundamental mineralization processes and processes that occur within an extracellular matrix. It is distinct from bone in terms of architecture, pathology, and the biological mechanisms mediating its formation. Understanding the biological formation of different mineralized structures could lead to

innovative approaches toward engineering novel scaffolds and providing new therapeutics. Additionally, unlike other biomineralized tissues, such as bone and dentin, mature enamel is acellular and does not resorb or remodel. As a result, enamel regeneration cannot occur in vivo following failure and is therefore an attractive target for future biomimetic and therapeutic approaches.

Enamel formation, or amelogenesis, is a highly regulated process involving precise genetic control as well as protein-protein interactions, protein-mineral interactions, and interactions involving the cell membrane. This section of the review focuses on the biological formation of enamel with an emphasis on protein interactions. Understanding these processes can provide insight toward designing synthetic systems to promote tissue regeneration, which is covered in detail in section 4.

3.1. Tooth Structure and Function

The mammalian tooth is made up of four distinct structures: enamel, dentin, pulp, and cementum (Figure 7).⁸⁴ The pulp contains nerves, blood vessels, fibroblasts, and lymphocytes, while the mineralized organs of the tooth include enamel, dentin, and cementum. Enamel makes up the uppermost 1-2 mm of the tooth crown and contains a high mineral content, giving it a high modulus but also making it susceptible to cracking. Dentin lies below the enamel and is tougher, forming the bulk of the tooth and absorbing stresses from enamel, preventing its fracture.⁸⁵ The composition of dentin is similar to that of bone. The cementum is the mineralized layer that surrounds the root of the tooth covering the dentin layer and some of the enamel layer. The cementum allows for the anchoring of the tooth to the alveolar bone (jawbone) through the periodontal ligament.

The primary function of the tooth is for mastication of food; however, some species use them for attacking prey and for defense. It also faces the lifelong challenge of maintaining robust mechanical properties in a bacteria-filled environment. The enamel and dentin tissues give rise to a tough, crack-tolerant, and abrasion-resistant tissue through their unique architectures and mineral compositions. Enamel is highly patterned and consists of organized interweaving bundles of crystallites (called rods or prisms). It has a higher reported toughness than that of crystalline HA, indicating that the organization of the crystallites is essential for enamel function.⁸⁶ Because of the high mineral content and minimal organic, enamel is brittle. Interestingly, the architecture of the enamel crystallites can deflect a propagating crack preventing it from reaching the dentin-enamel junction (DEJ), which also has been shown to resist delamination of the tissues despite their differences in composition.^{87,88} The mechanical properties of enamel, dentin, and the DEJ are not completely understood and are a significant area of research. Understanding the properties of these tissues could serve to motivate further engineering of more robust dental materials as well as to inspire fabrication of nonbiological materials. Extensive details on the mechanical properties of the tooth are beyond the scope of this review, and the reader is directed to the following references.⁸⁸⁻⁹¹

3.2. Hierarchy of Enamel

Similar to bone, enamel possesses a complex architecture, which can be broken into several hierarchical levels from the nanoscale to the macroscale.⁹² On the nanoscale, the protein-protein and protein-mineral interactions in the presence of supersaturated ions create a highly organized array of HA crystallites that grow preferentially along the *c*-axis.⁹³⁻⁹⁵ The sizes of these crystallites vary depending on the stage of the mineralization. The crystallites grow primarily in length during the secretory stage and continue to grow in width and thickness during the maturation stage. The assembly of amelogenin has been shown to be crucial for the proper development of enamel crystallites. Disruption of the assembly alters formation on the nanoscale, subsequently affecting larger length scales and giving rise to a diseased or

malformed enamel phenotype. This is discussed further in section 3.3.2 on amelogenin self-assembly.⁹⁶

On the mesoscale level, there are three main structural components: the rod, the interrod, and the aprismatic enamel. The main component of enamel on the mesoscale includes rods, which are bundles of aligned crystallites that are “woven” into intricate architectures that are approximately 3-5 μm in diameter, as seen in Figure 8. The individual nanoscale crystallites contained within the rods of mature human enamel are approximately 30 nm thick and 60 nm wide.⁹⁷ It is worthwhile to note that there has been a large variation in crystal sizes in literature due to “shadows” and limitations of imaging. The lengths of the rods and crystallites vary among species and can be on the order of millimeters in length—much longer than crystals in other mineralized skeletal tissues.⁸³ The second structural component of the enamel matrix is the interrod (or interprismatic) enamel, which surrounds and packs between the rods. The difference between the rod and the interrod is the orientation of HA crystals; the rod contains aligned crystallites, whereas the mineral in the interrod is less ordered. These structures coalesce to form the tough tissue of enamel, which can withstand high forces and resist damage by crack deflection.⁹⁸ The third structure, aprismatic enamel, refers to the structures containing HA crystals that show no mesoscale or macroscale alignment.

The macroscale architecture includes specific zones of enamel that have unique characteristics, which contribute to the whole tissue. The enamel adjacent to the DEJ exhibits a gradual transition from dentin to enamel. Aprismatic regions of enamel have been proposed to be primitive areas of the tooth serving as a toughening mechanism due to their flexible nature.^{98,99} Several authors have identified these aprismatic areas to be located adjacent to the DEJ and at the incisal surface of both deciduous and permanent human enamel.¹⁰⁰⁻¹⁰³ The Tomes’ process, a unique structure present at the secretory pole of an enamel-forming cell, is responsible for aligned mineral formation in the prismatic enamel. The absence of this process may give rise to the aprismatic zone in the tooth.^{83,104}

3.2.1. Amelogenesis: Cellular Processes in Formation of Enamel—Developing enamel consists of biological apatite embedded within a protein-filled organic matrix.¹⁰⁵ Two different theories have been proposed to explain the initial nucleation of enamel crystallites. One theory suggests that the earliest deposition of enamel crystallites arises from mineralized collagen fibrils, which originate during dentin formation, at the DEJ. These ribbonlike crystals could be a result of dentin crystals entering the enamel, creating a nearly seamless junction between the two tissues.^{87,106} The second theory proposes that initial nucleation is mediated extracellularly through controlled nucleation and growth of HA crystals on an organic template secreted by ameloblasts.¹⁰⁷ Regardless of the mechanism, the architecture of this mineralized tissue results from highly controlled cellular and chemical processes, which can be broken up into four stages: secretory, transition, maturation, and postmaturation.⁸³ While the details of amelogenesis are not fully understood, the cellular process can still inspire further development of biomimetic materials designed for biomineralization.

During the secretory stage, ameloblasts polarize and align in parallel arrays directed perpendicular to the DEJ. These cells migrate away from the DEJ and secrete a proteinaceous matrix (>90% amelogenin) via secretory granules that are transported from within the cell to the enamel compartment in the Tomes’ processes located along the apical side (toward the root and dentin) of the tooth.¹⁰⁴ Each ameloblast is responsible for the formation of a single crystallite bundle, or rod, which extends from the DEJ to the tooth surface. The protein deposited behind each cell gives rise to the structural rods within enamel, which undulate and weave together, indicating the migration pathway of the individual cells. Protein deposition that occurs in regions of abutting ameloblasts contributes to the interrod or interprismatic enamel. The transition stage is characterized by the reorganization of the cellular components

as well as additional protein secretion. The role of the cytoplasm, which was primarily protein secretion, changes to transportation. The cells shrink to about half the height and develop a distinct ruffled border against the mineralized layer, which serves to remove water and protein from enamel. The cells in this state are known as “maturation ameloblasts”.¹⁰⁴ Once the maturation phenotype develops, the cells begin the maturation stage, which is characterized by the removal of water and enamel matrix degradation products. Calcium, phosphate, and bicarbonate ions are introduced to the matrix and are generated by enzymes such as alkaline phosphatase (ALP) and carbonic anhydrase II.^{108,109} The crystals grow to their final width and thickness filling in the areas that were previously occupied by organic components. The crystallites grow until they come into contact with neighboring crystals, creating a mineral dense tissue. In the postmaturation stage, the enamel-producing ameloblasts retract from the matrix and emerge as low columnar cells. These cells remain dormant until the tooth erupts at which point the cells fuse with the oral epithelium.¹⁰⁴

3.3. Organic Components of Enamel

3.3.1. Amelogenin—Amelogenin is generally considered to be the most influential of the enamel matrix proteins. It is the main secretory product of ameloblasts, making up more than 90% of the organic component present in enamel (enamel consists of as little as 1% by weight organic).¹¹⁰ This protein provides a template for mineral growth and is considered somewhat analogous to collagen in other mineralizing tissues. It is by far the best-characterized protein present in the enamel protein matrix and is required for proper formation of the enamel tissue. The amelogenin-null mouse demonstrates the dramatic importance of the protein, as it exhibits a disrupted rod pattern resembling amelogenesis imperfecta. Amelogenesis imperfecta is a genetic disorder that compromises the integrity of enamel within the tooth.¹¹¹

Amelogenin is the predominant protein of the enamel matrix and is highly processed by enzymes after secretion into the extracellular environment. It is present in many isoforms due to alternative splicing and rapid proteolytic processing following secretion from the ameloblast. Table 4 is provided to clarify the nomenclature of amelogenins and their engineered constructs that are discussed in this review and in the literature.¹⁰⁵ The amelogenin sequence is highly conserved among many species;¹¹²⁻¹¹⁵ in particular, the C-terminal and N-terminal regions are conserved, indicating that these moieties play a pivotal function in enamel development and mineralization.^{83,116,117}

The amelogenin sequence can be divided into three domains, each of which serves a pivotal function in enamel development.¹¹⁷ The first domain is a 45 amino acid N-terminal domain with high tyrosine content, commonly known as tyrosine-rich amelogenin peptide (TRAP). Removing the TRAP sequence from amelogenin disrupts self-assembly in vitro and in vivo and only gives rise to monomeric forms of the protein. The tyrosyl motif in the TRAP region of amelogenin may be involved in amelogenin-cell or amelogenin-nonamelogenin interactions and is retained in mature enamel.¹¹⁰ It contains a lectin-binding motif PYPSYGYEPMGGW, which may be responsible for orienting the assembled amelogenin nanospheres as the ameloblasts retract (Figure 9).^{110,118} The second domain is the largest segment of the protein and comprises the central segment containing hydrophobic character and is made up of (X-Y-Pro) repeat motifs where X and Y are often glutamine. In contrast to the N-terminal and central domains, the C-terminal region has negatively charged acidic residues that may provide nucleation sites for calcium phosphate. Together, these three domains of amelogenin give the protein its amphiphilic characteristics determining its function and ability to self-assemble.¹⁰⁵

The leucine-rich amelogenin polypeptide (LRAP) is a naturally occurring 59 residue amelogenin that results from alternative splicing of the first 33 and the last 26 residues of the full amelogenin sequence. It has not been found to self-assemble,¹¹⁹⁻¹²¹ but it has been proposed to play a role in ameloblast differentiation, enamel growth, and formation of dentinal

tubules.¹²² There is direct evidence that the C terminus of LRAP, which is analogous to the carboxy terminus residues of amelogenin, preferentially binds to HA surfaces, indicating that amelogenin and/or LRAP likely play a significant role in mediating the shape and structure of the resulting mineral.¹²³ Additionally, LRAP has been shown to partially rescue the ability of LRAP to act as a signaling molecule to induce mineral formation.¹²⁴

High-resolution structural information of amelogenin has been difficult to obtain due to the heterogeneous mixture of amelogenin and its post-translational products in vivo. Therefore, a variety of solution-phase methods have been utilized to further characterize amelogenin. Using circular dichroism, porcine amelogenin was reported to contain three distinct regions, as described above. The N-terminal TRAP domain consists of a β -sheet structure, while the center segment was proposed to contain extended structures such as polyproline II and/or β -strand configurations, including β -turns and β -spirals. The C-terminal domain is composed of a random coil conformation.^{125,126}

Amelogenins generally have low solubility under physiological conditions due to their tendency to aggregate. Recombinant and native full-length amelogenins vary only slightly in their solubility behavior, with relatively constant solubility within a pH range from 6.0 to 9.0 and the lowest solubility being exhibited at the isoelectric point (pI ~ 8.0).¹¹⁶ TRAP was found to be insoluble, whereas LRAP was readily soluble, which can be explained by the presence of hydrophobic residues in TRAP. The 20 kDa porcine amelogenin was found to be extremely soluble at pH of 4.0-6.0 with a drastic change to insoluble forms at pH around 7.0.^{127,128} This marked difference in solubility may be significant for the binding to the enzymes to remove organic components from the enamel matrix. Changes in solubility that are dependent on pH may suggest an important role in self-assembly as well as enzymatic degradation.^{127,128}

3.3.2. Self-Assembly of Amelogenin—The amelogenin protein is mostly hydrophobic and contains a hydrophilic C terminus. It has been found to self-assemble into nanospheres,¹²⁹⁻¹³¹ which in turn give rise to higher order structures such as chains and ribbons^{58,132} that guide apatite growth.^{129,133,134} In vitro studies on amelogenin self-assembly offer great opportunities to elucidate the mechanism of in vivo enamel mineralization. In fact, amelogenin nanosphere formation has also been identified in vivo. Nanosphere assemblies of amelogenin have been visualized by both TEM and AFM. Developing murine enamel was negatively stained with uranyl acetate and imaged, revealing “circular electron-lucent regions arranged in rows parallel to the developing [enamel] crystallites.”¹³⁰ Wen et al. employed tapping mode AFM to reveal amelogenin nanospheres aligned with side faces of enamel crystallites in developing porcine enamel as seen in Figure 10.¹³⁵ However, the protein-protein and the protein-mineral interactions are particularly difficult to characterize in vivo due to the transient nature of the matrix. The self-assembly properties of amelogenin can also provide promising biomimetic approaches for nucleating biologically relevant calcium phosphates.

Recent data have demonstrated that the amelogenin assembly is entropically driven by hydrophobic collapse.¹³⁶ Amelogenin molecules can spontaneously form nanospheres under a wide variety of conditions. Du et al. discovered that amelogenin nanospheres assemble preferentially to produce birefringent microribbons.¹³³ This orientation presumably allows for the alignment of nucleated carbonated HA crystals. A proposed assembly mechanism is illustrated in Figure 11. Theoretical and experimental data reveal the presence of these aggregates as monomers, which self-associate into oligomers and “nanospheres”, which have a hydrodynamic radius of approximately 10-25 nm. These nanospheres then associate with one another through the association with monomers and oligomers to form aligned chains of a preferred length of 10-15 nanospheres. These structures were then found to further assemble into birefringent “ribbonlike” fibrous structures that were approximately 10 μ m in width and

up to hundreds of micrometers in length as described by Du et al.^{131,133} It is worthwhile to note that the amelogenin ribbon X-ray diffraction pattern in that paper contained a cellulose contaminant.¹³³ The experiment was repeated without the contaminant, and the ribbon's diffraction pattern was absent or very weak.¹³⁷ This finding did not affect the investigators' original conclusions regarding the self-assembly of the ribbon or the capability of the ribbon to nucleate aligned mineral.

Two amelogenin self-binding domains have also been identified that play a crucial role in assembly of nanospheres. The self-assembly domain A consists of the first 42 residues of the N-terminal region of native murine amelogenin. It has been found to be a site for interaction between amelogenin monomers using the two-hybrid yeast system. The yeast two-hybrid assay tests for the close contact of two proteins by restoring function of a transcription factor that has been split into two pieces. The restored activity of the transcription factor becomes a quantifiable indication of protein-protein interactions.¹³⁸ The self-assembly domain B consists of 17 amino acid residues, which border the hydrophilic C terminus and is capable of promoting amelogenin-amelogenin interactions. A time-dependent DLS analysis of amelogenin lacking the B domain results in nanospheres that form, fuse, and collapse.¹³⁹

Deletion of the A or B self-assembly domains in transgenic mice results in defective phenotypes of enamel, supporting the claim that nanosphere assembly is a critical step for enamel biomineralization.¹²¹ A knock-in study in mice of amelogenin missing self-assembly domain A or domain B showed interesting changes in tooth morphology as compared to wild-type animals as illustrated in Figure 12.^{96,140} Both of the mutants showed thinner enamel, fracturing during mastication, and morphological changes at different length scales. The mice lacking the N-terminal domain (domain A) showed no nanospheres of amelogenin by TEM and no architecture of woven rods of mineral crystallites by SEM. The mutants without the C-terminal domain (domain B) showed nanospheres that were misaligned, larger, and more disperse in size and shape than the wild-type mice. The rods were arranged abnormally, as were the crystals within each rod. Thus, the conserved self-assembly domains A and B are integral for proper enamel formation and thickness.

3.3.3. Nonamelogenin Proteins—The enamel matrix consists mainly of amelogenin, enamelin, and ameloblastin.¹¹⁶ Unlike amelogenin, enamelin and ameloblastin do not undergo extensive alternative splicing. Ameloblastin undergoes limited splicing,¹⁴¹ whereas enamelin has no identified splices,¹⁴² and only one known post-translational modification has been identified to date.¹⁴³ Despite their low abundance, the nonamelogenin proteins likely play integral roles in enamel formation through their full-length or their post-translationally modified forms. Enamel formation is highly regulated through extracellular proteolysis. Amelogenin and the main nonamelogenin proteins and proteinases are summarized in Table 5. The role of these nonamelogenin proteins in regulating enamel formation is complex and not yet fully understood. A basic overview of nonamelogenin proteins will be included in this review; a more detailed review of these proteins can be found elsewhere.¹⁴⁴

Ameloblastin (also known as amelin or sheathlin) was first identified from its proteolysis products: two polypeptides (27 and 29 kDa) cleaved from the C terminus and a number of 13-17 kDa polypeptides from the N terminus.¹⁴⁵ It is expressed by differentiating ameloblasts and stabilizes the differentiation state by acting as a cell adhesion molecule and inhibiting proliferation.^{146,147} The epithelial layer of the ameloblastin-null mouse loses polarity, detaches, and proliferates, resulting in hypoplastic enamel.¹⁴⁶ It has a possible SH3 binding domain,¹⁴⁸ DGEA motifs for integrin binding, and a VTKG motif for possible thrombospondin-like cell adhesion.¹⁴⁷

Enamelin is a glycoprotein and is the largest of the known enamel proteins. It was named for its ability to strongly adsorb to enamel crystals. Full-length enamel in has only been identified at the mineralization front (approximately 1 μm from the apical surface of the enamel). The cleavage products are concentrated within the rod and interrod.^{149,150} It is estimated to represent 1% of the total protein content of the enamel.¹¹⁶

Biglycan protein is a small proteoglycan that possibly plays a role in anchoring enamel proteins, as it has been found to interact with amelogenin, ameloblastin, and enamel in.^{144,151} In vivo, biglycan knockout animals are normal at birth but show lower growth rates and bone mass and show 3-5-fold thicker enamel when compared to wild-type animals.¹⁵²

Tuftelin is an acidic glycoprotein present in the enamel matrix and is concentrated at the DEJ. The function of tuftelins in the enamel matrix remains unclear, but it is proposed to be involved in initial enamel nucleation during tooth development, as it contains a calcium-binding domain and phosphorylated residues.¹⁵³ Using the two-yeast hybrid technique, a self-assembly domain has been identified on the tuftelin protein, implying that spatial constraints may contribute toward interaction with enamel crystallites.¹⁵⁴ Interestingly, tuftelin has been found in nonmineralizing soft tissues, indicating that it may have several roles in the body.¹⁵³ However, this fact also raises the question of its specificity in mineralization. In addition to tuftelin, several unique proteins encoded by cDNA were found to interact with tuftelin and termed tuftelin-interacting proteins (TIPs).^{155,156} TIP39 has been found to colocalize with tuftelin near the Tomes' processes of the ameloblasts, playing a possible role in mediating cellular events in the enamel mineralization process.¹⁵⁷

The proteolytic processing of the proteinaceous matrix has been shown to be an essential step of enamel biomineralization, as it removes the organic matrix and allows for the full maturation of the crystals.¹⁵⁸ This process is unique to enamel and can motivate biomimetic approaches toward achieving larger crystallites in vitro. Incorporation of enzyme-cleavable sites in synthetic constructs may prove useful for directing cell-mediated mineralization or mineralization from supersaturation solutions. MMP-20 or enamelysin is expressed during the secretory stage and is responsible for the cleaving of matrix proteins. The MMP-20 null mouse gives abnormal tooth phenotype and an altered rod pattern that results in an enamel layer that will delaminate from dentin.^{159,160} Kallikrein 4, also known as KLK-4 or ESMP1, is a serine proteinase that is expressed in enamel during the maturation stage and is believed to be responsible for the breakdown of enamel proteins.^{141,143} It is capable of the initial cleavage step of amelogenin in which the C terminus is removed.^{161,162} The cleavage products following proteolytic activity may be responsible for further self-assembly or matrix-protein interactions during crystal development; however, further research is required. It has also been shown to be capable of proteolytic processing of the other enamel matrix proteins, such as enamel in.¹⁶²

The presence of amelogenesis imperfecta phenotypes containing no relation to genetic defects in amelogenin, ameloblastin, enamel in, enamelysin, or KLK-4 has led to the recent discovery of the enamel protein amelotin.¹⁶³ Amelotin is secreted exclusively by ameloblasts unlike amelogenin, ameloblastin, and enamel in, which have shown limited expression in odontoblasts (dentin forming cells). This implies that amelotin has a specific function within the enamel organ. In the rat incisor model, this protein peaks in its RNA expression 2 weeks following birth, indicating that it plays a role in later stages of maturation.¹⁶⁴ This expression pattern is more characteristic of enzymes such as KLK-4, implying that amelotin could possibly have a role in enzymatic cleavage.

3.3.4. Other Protein-Protein Interactions—The enamel tissue is formed in the extracellular matrix, implying that protein-protein interactions play an integral role in

mineralization. A high level of control is necessary for the formation of the highly aligned and organized crystallite structure. Interactions exhibited by amelogenin self-assembly and between nonamelogenin proteins create the basic building blocks for regulation of higher order structures. Amelogenin may interact alone or in combination with other matrix molecules, such as full-length proteins or proteolytic products. For instance, it has been shown that native murine amelogenin specifically binds to recombinant and native forms of ameloblastin through the TRAP domain.¹⁶⁵ The yeast two-hybrid assay was used to show that amelogenin proteins interact with one another during the nanosphere assembly.¹²⁰ Amelogenin was also found to interact with biglycan to inhibit amelogenin expression and with CD63, a membrane receptor that may be involved in protein degradation for matrix removal as the crystallites grow.¹⁵¹

3.3.5. Protein-Mineral Interactions—In tissues with extracellular mineralization, it is generally proposed that hydrophobic molecules such as amelogenin create a space-filling system, whereas hydrophilic molecules such as the nonamelogenin proteins act as sites for nucleation and growth of mineral phases.^{105,166} Much is still unknown about the interactions between proteins present in the enamel matrix and the final crystalline phase of HA. There are several factors to consider at the organic-inorganic interface, including molecular mechanisms involved in nucleation, growth, cluster formation, crystal orientation, and fusion of the crystals. Several experiments have been conducted to investigate the role of enamel matrix proteins on nucleation and growth of HA *in vitro* by using driving forces such as supersaturation of ions in solution.

In enamel, amelogenin may act as a space-filling molecule due to its hydrophobic nature and ability to present hydrophilic groups for nucleation of mineral. The self-assembled nanosphere morphology likely increases the surface area of the hydrophilic charged C terminus of amelogenin, promoting the interaction with HA and serving as a possible nucleator for mineral.^{133,167,168} Removal of the C terminus from amelogenin yields larger nanosphere formation as compared to the full-length amelogenin. This disturbance in protein self-assembly leads to an altered interaction with HA.¹⁶⁷ Further direct evidence by solid-state NMR data showed that the charged carboxyl terminus (LRAP) is oriented adjacent to the HA surface, indicating that it plays an important role in controlling growth of the enamel crystallites.¹²³

The full-length porcine amelogenin was found at first to partially inhibit crystal growth of HA seed crystals due to adsorption onto HA surfaces when exposed to supersaturated solutions of HA.¹⁶⁹ This inhibition of the kinetics of crystal growth was also reported with recombinant mouse full-length amelogenin and was found to vary depending on protein concentration.¹³⁴ It was speculated that the concentration dependence was due to the competing effect of protein-protein interactions involved in amelogenin self-assembly and the adherence to HA. The inhibition of crystal growth kinetics that is seen in the presence of amelogenin may be due to protein adsorption to crystal faces to direct growth along the *c*-axis or due to ion binding, resulting in a decrease of supersaturation. The specific role of the full-length amelogenin and other enamel proteins in the initially formed enamel ribbons at the DEJ remains unknown.¹⁰⁵

The lower molecular weight degradation products in the enamel matrix lacked interactions with HA seeds and appeared to have little influence on crystal growth.¹⁶⁹ The 32 kDa enamelin protein and amelogenin protein were found to cooperatively reduce induction time of apatite crystal nucleation in a gelatin gel matrix as compared to either protein alone.¹⁷⁰ A similar group of phosphorylated 32 kDa proteins were found to adsorb strongly to HA and inhibit crystal growth of HA seeds.¹⁷¹

Several experiments have been performed investigating the role of amelogenin in environments that promote the formation of apatitic crystals by utilizing supersaturated solutions of ions to

promote precipitation of calcium phosphate. So far, there is no direct evidence that enamel mineralization *in vivo* occurs via heterogeneous sites of metastable calcium phosphate phases. However, native porcine amelogenin incorporated within gelatin gels promoted longer crystals with higher aspect ratios of spontaneously formed metastable OCP.⁹⁴ Incorporation of bovine amelogenin¹⁷² and purified recombinant mouse¹⁷³ amelogenin into gels reveals elongated growth of OCP crystals in a dose-dependent manner.¹⁷⁴ Amelogenin was found to interact most strongly with the (010) face, followed by the (001) and (100) faces. Furthermore, higher aspect ratio crystals were found in amelogenins in the presence or absence of the hydrophilic C terminus, indicating that the hydrophobic portions of the amelogenin protein regulate crystal shape and growth. Additionally, in the presence of supersaturated ions, monomeric forms of recombinant murine amelogenin were found to orient crystals in bundles with a preferential orientation along the *c*-axis. Monomeric forms lacking the C terminus rM166 and preassembled recombinant full-length amelogenin (rM179) nucleated mineral but failed to show an effect on crystal organization.¹⁷⁵ A more recent study utilizing a constant concentration *in vitro* crystallization system reports dramatically accelerated nucleation times and reduced induction times of OCP crystals in the presence of amelogenin in a dose-dependent manner. In this experiment, low values of supersaturation were used, and there were no crystal seeds; rather, amelogenin provided heterogeneous nucleation sites for mineralization.¹⁷⁶ Although amelogenin has been shown to interact and nucleate calcium phosphate, it is worthwhile to note that nonamelogenin proteins likely play an important role in mineralization as well.

Unique in its formation and architecture, there are many lessons to be learned from enamel. The mechanisms underlying the formation of such a hierarchical tissue can contribute to many areas of science including chemistry, biology, and materials science, ultimately providing tools for medicine and dentistry.

4. Artificial Approaches for Biomineralization

4.1. Introduction to Synthetic Bone and Enamel Mineralization

Both bone and tooth mineralization provide highly regulated signaling pathways to deposit matrix and nucleate HA mineral to provide mechanical strength to the tissues. In healthy vertebrates, bone healing and remodeling in response to minor injury occur with minimal scarring. However, this capacity for regeneration is finite, and the significant loss of bone structure due to severe injury or disease can have catastrophic implications for human health, particularly in older patients. There are also a number of medical pathologies related to the mineralization of hard tissues that can severely impair quality of life, including osteoporosis, osteogenesis imperfecta, osteomalacia, renal osteodystrophy, and amelogenesis imperfecta.¹⁰ Therefore, it is important to develop strategies to repair or regenerate these mineralized tissues. An ideal treatment would promote immediate HA mineralization, would be biodegradable, and would support or promote the formation of natural bone.

Bone grafts are commonly used as treatment for bone loss. Autologous bone grafts are taken from another part of the same patient's body, usually trabecular bone from the iliac crest of the pelvis. While immunogenic responses are minimized, the graft size is limited due to the damage caused to the donor tissue, which can be quite severe. Allografts from another donor can allow larger grafts¹⁷⁷ but have less efficient incorporation and greater potential for immune rejection or pathogen transmission.^{178,179} Xenografts carry even greater risks and are not typically considered for human bone regeneration.¹⁸⁰ To overcome the limited supply of tissue, a variety of different materials have been explored to restore bone function and regenerate tissue. Since Nicholas Senn first described the therapeutic use of demineralized bone in 1889,¹⁸¹ it has been the subject of numerous studies as a scaffold for bone regeneration.¹⁸²⁻¹⁸⁴ More recently, recombinant bone morphogenic proteins (BMPs) have been utilized in both preclinical and clinical trials.^{185,186} The growth factors are often delivered by

combining the BMP with a carrier matrix such as demineralized bone, collagen, NCPs, or synthetic constructs such as polymers, hydrogels, HA powder, or silk.¹⁸⁷ The use of BMPs could enhance or replace autologous bone grafts and perhaps even internal fixation devices. They can induce bone formation to fill a critical-sized defect and can aid with repair of long bones, craniofacial bones, and produce bony fusions in the spine.¹⁸⁵

As discussed in sections 2 and 3, the mineralization of bone and enamel is controlled by a number of regulated proteins. Delivering these proteins directly can result in rapid clearing, reducing the effectiveness of any potential therapy. Therefore, natural or synthetic polymers have been developed to sequester and retain the therapeutic agents in hydrogel networks. Because carboxylic acids and phosphorylated amino acids appear frequently in apatite-mineralizing proteins, these acidic groups are used in many of the macromolecular strategies described below. Natural polymers like collagen are useful, readily available, and generally safe for clinical use. However, the available structures are limited. Synthetic polymers offer greater diversity of chemical functionality but may be less biocompatible.

Porous metal foams can allow penetration by the biological tissue and can better match the mechanical properties of the host tissue as compared to dense metals,¹⁸⁸ but integration of the implant with the natural bone tissue remains a challenge.¹⁸⁹ Ceramics can be prepared with a variety of inorganic components, such as natural or synthetic HA. Unfortunately, these materials tend to have low tensile strength; brittleness; poor response to torsional, bending, or shear stress; complex degradation rates in vivo; and difficulties molding into arbitrary shapes. Calcium phosphate materials can be prepared with control over particle size, porosity, and composition.¹⁹⁰ However, the usefulness of these materials can be compromised by poor mechanical integrity and low macroporosity.¹⁹¹ HA-polymer composite materials have been used extensively to better match the mechanical properties of natural bone.¹⁹²⁻¹⁹⁵ Furthermore, for successful bone replacement, there must be a strong bond between the host bone as well as the growth of new bone.^{196,197} Bioactivity of inert surfaces can be improved by chemical derivatization of the surface, by coating with a thin layer of a ceramic material, or by coating with a polymer bearing appropriate functional groups. To better understand the potential for novel therapeutics and for new biomimetic mineralization strategies, the rest of this review will discuss approaches for HA mineralization.

The structure and chemical composition of HA depend strongly on the solution from which it is mineralized. To reproducibly mimic the conditions of apatite formation in vitro, "simulated body fluid" (SBF) was developed as an organic-free mixture of reagent-grade salts buffered at pH 7.4.^{198,199} As shown in Table 6, a series of improvements have been made to better reproduce the ion concentrations of human blood plasma. The most refined formulation is known as "corrected SBF".^{198,200} SBF is used to reproduce the biological environment in many of the in vitro mineralization studies on artificial substrates described throughout this section. While this solution contains the ions necessary for HA formation, additional organic or inorganic nucleators are required. To reasonably mimic the biological ion availability, the solution is typically replenished frequently with daily or weekly solvent exchanges.

4.2. Cell-Based Therapeutic Approaches

In addition to the studies described above, a number of cell-based therapeutic strategies have also been developed using a number of different cell sources.^{21,201} For example, autologous cells can be taken from the patient and expanded in vitro. The efficacy of this process can be limited by the number of available cells and the expression profiles of the proteins of interest. Xenogenic cells from a nonhuman donor can give high cellular yields but can lead to a severe immunogenic response or disease transmission. With appropriate stimulation, adult stem cells can be induced to differentiate into the cells important for tissue engineering. Mesenchymal stem cells from adult bone marrow can be induced to differentiate exclusively into the

adipocytic, chondrocytic, or osteocytic lineages.²⁰² These studies suggest great therapeutic potential for autologous MSCs combined with an appropriate delivery vehicle. In practice, engineering of musculoskeletal tissues frequently uses differentiated or progenitor cells seeded with the appropriate growth factors in three-dimensional (3D) biomaterial scaffolds that are biocompatible, biodegradable, and include structural and functional properties to mimic the native extracellular environment. In one example using electrospun polymer nanofibers, hMSCs could be induced to differentiate along adipogenic, chondrogenic, or osteogenic lineages by culturing in specific differentiation media.²⁰³ Pluripotent embryonic stem cells also offer great therapeutic potential.^{204,205} However, to be used as realistic treatment options, many scientific advances are required. For example, there need to be better methods to direct the selective differentiation, to ensure that the transplants are nontumorigenic, and to ensure immunological compatibility. In addition to controlling the medium composition, improved stem cell behavior is observed with control over the stiffness of the 3D matrix²⁰⁶ and with convection control in flow perfusion culture.²⁰⁷ The use of xenogenic cells and embryonic stem cells is further complicated by ethical and social concerns about their use.

Osteoinduction, osteoconduction, and osseointegration are used frequently but rather inconsistently in the literature.²⁰⁸ For consistency, we will briefly define each term here. Osteoinduction is the recruitment and stimulation of undifferentiated, pluripotent cells to form bone-forming cells (preosteoblasts, osteoblasts, and finally osteocytes). A common and safe strategy to test for osteoinduction is to analyze bone formation after injection into a ectopic bed, such as a muscle pouch.²⁰⁸ One of the earliest known examples of an osteoinductive material was demineralized bone.¹⁸² Osteoconduction is the growth of bone into a material. After a trauma, this growth can occur by existing preosteoblasts and osteoblasts or by differentiation into these cells (osteoinduction). The process of osteoconduction depends on the nature of the material as well as the presence of certain growth factors sufficient vascularization. Osseointegration represents the direct, microscopic contact between living bone and an implant material. While some materials show initial osteoinduction and osteoconduction, “osseointegration” implies sustained anchoring over time. Strategies to accelerate osseointegration include oxidizing or roughening the implant surface and coating the material with HA.

4.3. Protein-Based Mineralization

As discussed in the previous sections, protein-mineral interactions are essential for the formation of healthy bones and teeth. Factors such as acidity, hydrogen-bonding ability, and functional group spacing are important and should be considered in any artificial approach to biomineralization. The importance of the interactions between proteins and HA was highlighted by a recent study of protein folding on HA surfaces.²⁰⁹ They designed a de novo peptide to be unstructured in buffered saline solution, yet that undergoes induced folding at the surface of HA. The peptide folding was largely governed by the periodic positioning of γ -carboxyglutamic acid (Gla) residues within the primary sequence of the peptide. This study demonstrated the potential to use HA surfaces to trigger the intramolecular folding of designed peptides and thus represents the initial stages of defining the design rules that allow biomineral-induced peptide folding. Such studies of molecular recognition on mineral surfaces may be critical for the controlled biomimetic nucleation and growth of HA.

4.3.1. Collagen—We have discussed the structure and mineralization of collagen in natural systems in section 2. In the present section, we highlight some recent studies at the collagen-HA interface as an artificial approach to biomineralization. The fibril structure of natural collagen offer great opportunities as scaffolds to mimic autologous bone grafts.^{33,210} Thus, the in vivo and in vitro mineralization of self-assembled collagen fibrils is a fertile and active area of research. Early studies to mimic the composition and structure of bone focused on using

SBF with reconstituted type I collagen. For example, Glimcher et al. noted that HA was nucleated in the hole zones of rabbit collagen.²¹¹ More recently, Zhang et al. attempted to replicate the hierarchical self-assembly of mineralized collagen into composites of nanofibrils.²¹² HA crystals grew on the surface of triple helical fibrils such that their *c*-axes were oriented along the long axis of the fibrils, as in natural bone. The hierarchical structure of the composite was verified by conventional and high-resolution TEM (Figure 13).²¹² A recent review by Cui and Ge³³ comprehensively presents the many uses of mineralized collagen composites with a particular focus on calcium phosphate crystals for bone regeneration. The authors make special note of the expanding interest in designing novel composite materials with hierarchical structures, optimizing coassembly of organic and inorganic phases, controlling implant morphology, and predicting the behavior in biological systems.

Gelatin is a polymer obtained by partial hydrolysis of collagen.²¹³ Bigi et al. used gelatin films to mimic collagen and poly(acrylic acid) to mimic the natural acidic macromolecules.²¹⁴ After 4 days in 1.5SBF solution, the film appeared to be mineralized with spherical aggregates that resembled ACP by X-ray diffraction and by Ca/P ratio. These crystals grew with preferential orientation of their *c*-axes along the long axis of the organic molecules, indicating the potential of gelatin substrates in place of collagen in HA mineralization.

Given the importance of collagen in the formation of bone, it is an obvious scaffold on which to study the synthetic mineralization of HA. In summary, preliminary studies have shown that collagen is an important structural agent to direct HA mineralization by proteins or polymers with bonelike organization. In the subsequent sections, we will discuss similar attempts to mineralize HA using other natural and synthetic polymers.

4.3.2. Other Peptidic Biopolymers—In addition to collagen, a number of other proteins are found in high concentrations in the ECM or in blood serum. Several of these have been investigated for their interactions with HA. Albumin is the general term for water-soluble proteins that are moderately soluble in concentrated salt solutions and experience heat denaturation. Serum albumin is the most abundant blood plasma protein and has many important roles including regulating blood volume by maintaining the osmotic pressure of the blood compartment and as a carrier for lipophilic molecules. Bovine serum albumin (BSA) can at least partially block mineral formation in Hank's balanced salt solution (HBSS, a bufferless simulated inorganic plasma medium containing calcium and phosphate ions) on titanium surfaces.²¹⁵⁻²¹⁷ The role of albumin on the mineralization of HA in HBSS is more complicated. Mineralization is favored when albumin is preadsorbed and hindered when it is dissolved in HBSS, probably due to the calcium complexation by albumin early in the mineralization process. It also appears that albumin has a stabilizing effect on the formation of OCP.²¹⁸

Fibronectin is a high molecular weight extracellular matrix glycoprotein that binds to integrins and ECM components, such as collagen, fibrin, and heparan sulfate. Daculsi et al. demonstrated the ability of fibronectin to nucleate apatite crystal formation.²¹⁹ In vitro, a fibronectin network incubated with calcium phosphate crystals resulted in numerous clusters of very small particles (1 nm in diameter and 2 nm in length) by HR-TEM, whereas the control experiment on albumin revealed no crystal precipitation. In vivo, HA crystals coated with fibronectin were implanted subcutaneously into mice. After 1 or 2 weeks, HR-TEM of fibronectin immunogold labeled sections revealed the close association of the precipitated crystals with fibronectin. This nucleation could be involved in biological processes like ectopic calcification, apatite crystal nucleation in calcified tissue, and bone ingrowth on calcium phosphate ceramics.

Fibrinogen is a soluble plasma glycoprotein and is the inactive precursor for fibrin, a protein that is involved in blood clotting. A solution of SBF with or without of BSA and fibrinogen

was used to study apatite formation on a porous titania substrate *in vitro*.²²⁰ When BSA and fibrinogen were present in solution, the apatite growth kinetics were greatly slowed relative to controls. It was proposed that the presence of both albumin and fibrinogen in the SBF retards the apatite growth by decreasing the recrystallization rate of the initially formed ACP. A preadsorbed protein layer does not delay the calcium phosphate recrystallization to the same extent as when the proteins are in solution. The authors suggest that these proteins mainly influence the overall calcium phosphate nucleation and growth kinetics by adsorbing to the initial ACP.

4.4. Nonprotein Biopolymers

In addition to the proteins discussed above, there are a number of other readily available biopolymers that have been used in the biomimetic formation of HA.²¹ These are predominantly polysaccharides, such as chitin, chitosan, starch, and hyaluronic acid. These all tend to be nonimmunogenic and biocompatible but vary in their ability to form HA with good mechanical properties and bonding to native bone. We will also briefly discuss several naturally occurring polyhydroxyalkanoates and their ability to form bonelike material.

Chitin is a natural linear copolymer of *N*-acetylglucosamine and glucosamine with similar structure and reactivity to cellulose. It is biodegradable and nontoxic and can be isolated from the shells of crabs, lobsters, and other crustaceans. Chitin can be phosphorylated using H_3PO_4 and urea.²²¹ Soaking this acidic polymer with saturated $Ca(OH)_2$ solutions resulted in the growth of a thin layer of calcium phosphate. The authors suggest that the $Ca(OH)_2$ promotes hydrolysis of the phosphate groups on the polymer that first causes formation of OCP that then transformed into calciumdeficient apatite. Further soaking in 1.5SBF lead to nucleation additional mineralized calcium phosphate.

Chitosan refers to a copolymer related to chitin with less than 50% acetylation. Chitosan has found particular use for biomedical applications due to its biocompatibility, degradation, solubility, and stability in alkaline solutions. Because chitosan itself is not bioactive, it is necessary to provide an appropriate surface coating. For example, chitosan fiber-mesh scaffolds were produced by wet spinning and were sprayed with an aqueous glass-ceramic suspension.²²² Formation of an apatite layer was observed after immersion in a SBF for 1 week.²²³ More recently, chitosan microparticles were coated with calcium silicate and then soaked in SBF.²²⁴ Apatite formation could be observed in as little as 1 day. Three-dimensional HA/chitosan-gelatin networks of greater than 90% porosity have been prepared to examine the proliferation and functions of neonatal rat calvaria osteoblasts.²²⁵ With this scaffold, the cells were found to attach, proliferate, and produce extracellular matrix. Significant biomineralization was observed after 3 weeks in culture.

ChS is a linear, sulfated polysaccharide composed of a chain of alternating *N*-acetylgalactosamine and glucuronic acid. Natural ChS in cartilage provides compression resistance and allows diffusion of materials between blood and vessels. It has been suggested that ChS may have a role in regulating mineral deposition and crystal morphology during osteogenesis.²²⁶ ChS can bind to HA in a semirigid conformation.²²⁷ Light-scattering experiments were used to study the kinetics of heterogeneous HA nucleation by ChS.²²⁸ It was found that ChS assists the formation of highly ordered HA by suppressing the “supersaturation-driven interfacial structure mismatch”²²⁹ between HA crystals and the substrate. The importance of this structure matching suggests great potential to control nucleation and growth by designed substrates.

Starch is the polysaccharide $(C_6H_{10}O_5)_n$ composed of a long chain of glucose monosaccharide units joined together by glycosidic bonds. As the most consumed polysaccharide by humans and readily available from plant sources, starch has the potential to be an attractive biomaterial.

The biocompatibility and degradability of starch-based scaffolds have been well-established in the literature.²³⁰⁻²³² Pach et al. showed the potential for potato starch to nucleate the mineralization of HA with a fiberlike morphology.²³³ Gomes et al. investigated the effect of culturing conditions on the proliferation and osteogenic differentiation of bone marrow cells seeded on two different porous starch-based scaffolds in either static or flow perfusion culture conditions.²³⁴ The cell proliferation and ALP activity patterns were similar for both types of scaffolds and for both culture conditions, although the starch-polycaprolactone fiber meshes showed better interconnectivity of the pores, resulting in slightly greater proliferation as compared to the starch-ethylene vinyl alcohol meshes. Interestingly, the calcium deposition was significantly enhanced on both scaffold types cultured under flow perfusion. The authors proposed that flow perfusion culture enhanced the osteogenic differentiation of marrow stromal cells and improved their distribution in these 3D starch-based scaffolds. They also indicated that scaffold architecture and especially pore interconnectivity affect the homogeneity of the formed tissue.

Polyhydroxyalkanoates represent a class of biocompatible and biodegradable polyesters that have been developed for use in medical devices.²³⁵ Under certain growth conditions, bacteria are known to produce a number of poly(hydroxy acids), including poly(3-hydroxybutyrate) (PHB), poly(4-hydroxybutyrate) (P4HB), poly(3-hydroxybutyrate-*co*-hydroxyvalerate) (PHBV), poly(hydroxybutyrate-*co*-hydroxyhexanoate) (PHBHHx), and poly(3-hydroxyoctanoate) (PHO). In particular, PHB has shown promise for its ability to promote bone growth without inflammatory response.²³⁶ PHB-HA composites have been shown to have bonelike mechanical properties and the ability to form new bone *in vivo*.²³⁵ Furthermore, PHBHHx appears to be a good substrate for osteoblast or bone marrow stromal cell attachment. However, neither the cell attachment properties nor the mechanical properties improved as a composite with HA. It can be expected that synthetic derivatives (especially copolymers of variable composition), polymer blends, and composites will further improve the usefulness of polyhydroxyalkanoates for the formation of bonelike tissue.

The natural polymers discussed above can be used to mineralize HA and/or stimulate formation of bone and often exhibit attractive properties like biocompatibility and biodegradability. However, to be practical as a therapeutic for bone regeneration, these properties must be optimized, which is not always possible with natural materials. Therefore, synthetic strategies are also important, as we discuss below.

4.5. Synthetic Polymers

Given the importance of the extracellular matrix on cellular function and biomineralization, tissue regeneration will greatly benefit from artificial materials to control this space. In the rest of this section, we discuss a number of synthetic systems (primarily polymeric and supramolecular) that make one-dimensional (1D) structures that can mimic the fibrous texture of collagen and can induce mineralization. The use of synthetic polymers as a means for bone regeneration is attractive because the implant can act as both a scaffold for mineralization and a drug delivery device to induce bioactivity. In particular, biodegradability of many polymers allows for complete bone ingrowth with native bone tissue, eliminating the dependence on hard materials such as metals that are known to cause stress shielding and bone resorption. Furthermore, many of these materials can entrap solvent molecules to form viscoelastic hydrogels that can lead to better localization and tunable drug release profiles.²³⁷ Several representative polymers used for HA mineralization are shown in Scheme 1 and are discussed below.

4.5.1. Role of Acidic Functional Groups—As discussed previously, carboxylic acids and phosphate groups appear in many of the macromolecules responsible for HA mineralization.

Depending on the specific protein and the local biological environment, these groups can nucleate crystallite formation or promote or inhibit crystal growth. Phosphoserine and runs of aspartic acids are particularly relevant in this context. Therefore, a number of synthetic methods have been developed to incorporate these functional groups into natural and synthetic polymers. This has been accomplished by chemically introducing phosphonate, phosphate, or carboxymethyl groups.²³⁸

Dalas et al. prepared a series of aromatic amide polymers (analogous to Nomex and Kevlar) containing dimethylphosphinyl groups [PO(OMe)₂] for HA mineralization.²³⁹ At constant supersaturation, the rate of precipitation of HA increased linearly with the phosphate content of the copolymer. More recently, copolymers of 4-vinylimidazole and vinylphosphonic acid [poly(4-VIm-*co*-VPA)] were found to be substrates for HA crystallization.²⁴⁰ Varying the phosphonic acid content of the polymer from 39 to 63% increased the observed crystallization rate by a full order of magnitude. Under the sample conditions, the deposition rate was found to depend linearly on the solution supersaturation. The slope of this relationship was used to estimate the interfacial surface energy and was compared to a number of other known polymer substrates. These values can be used to compare the efficacy of nucleation by these various substrates, but they do not necessarily explain the complex physical and chemical features that contribute to the overall interfacial free energy.

4.5.2. Poly(α -hydroxyacids)—Poly(α -hydroxy acids) are among the most commonly used polymers in biomaterials as drug carriers and as sutures and staples. Commonly used examples include poly-L-lactic acid (PLLA), poly(lactic-*co*-glycolic acid) (PLGA), polyglycolic acid (PGA), and poly(2-hydroxyethyl methacrylate) (PHEMA). These polymers typically exhibit semicrystalline behavior and are synthesized by a ring-opening polymerization.⁶⁵ These polymers have also been incorporated with apatite and apatite-inducing materials by a number of investigators to assess the role of these materials in the field of hard tissue regeneration.

Composites containing both PLLA and apatite have been synthesized as porous foams that were then immersed in SBF.²⁴¹ These polymer foams were shown to form spherical microparticles of bonelike carbonated apatite, making a scaffold that could potentially induce attachment and growth of osteoprogenitor cells. Similarly, PLGA scaffolds have also been used to nucleate and grow carbonated apatite in SBF.²⁴² Porous PLGA scaffolds with an 85:15 lactide/glycolide ratio were prepared and mineralized for 16 days in SBF. Apatite crystals were observed after 6 days, and a continuous layer of mineral on the inside of the pores was formed after 16 days. Kellomäki et al. recently studied a series of different bioabsorbable materials, including PGA, PLLA, 50:50 poly-(caprolactone-*co*-lactide), and 96:4 *l/b*-lactide (PLA96) for potential bone generation and regeneration in vitro and in vivo.²⁴³ PGA and PLLA were processed into solid, self-reinforced rods that could act as scaffolds for ectopic bone formation in rabbits. A PCL/LLA copolymer film and mesh and the PLA96 mesh were found to protect the bone grafts from resorption and to guide bone formation in a cleft defect areas an application for which flexible devices are preferred over high strength.

Alkaline solutions can be used to reveal carboxylic acid²⁴⁴⁻²⁴⁶ or phosphate²⁴⁷⁻²⁴⁹ groups by partial hydrolysis of the polymer. For example, Bertozzi and co-workers used PHEMA as a hydrogel scaffold for the design and fabrication of bonelike composite materials with good mineral-polymer adhesion properties.²⁵⁰ They hydrolyze the cross-linked PHEMA polymer using a hot solution of acidic urea to expose surface carboxylic acids for the nucleation and growth of calcium phosphate. A mineral layer formed on the surface, along with extensive calcification of the hydrogel interior. Under mineralization conditions, a surface layer of several micrometers was formed. When the same conditions were applied to a hydrolysis-resistant (amide) polymer, they observed differences in both the extent of mineralization and the crystallinity of the apatite grown on the hydrogel surface. The same group also explored

cross-linked polymethacrylamide and polymethacrylate hydrogels that had been functionalized with mineral-binding ligands for the templated formation of HA.²⁵¹ Carboxylate and hydroxyl groups were found to give good adhesion between the organic and the inorganic materials. The mineral-nucleating potential of hydroxyl groups in that study suggests a potential role for hydroxylated collagen proteins in bone mineralization. It also suggests the usefulness of hydroxyl groups in biomimetic mineralization.

4.5.3. Polycaprolactone—Poly(ϵ -caprolactone) (PCL) is a semicrystalline linear polymer that is biocompatible and biodegradable and has been approved by the U.S. Food and Drug Administration for use in several medical and drug delivery devices. The use of this polymer has been somewhat limited by slow degradation and resorption, largely due to its hydrophobicity and crystallinity as compared to other aliphatic polyesters. Kweon et al. developed a more degradable porous version of this polymer by further photopolymerization of acryloylterminated PCL chains in the presence of a porogen.²⁵² To improve the mechanical and biological properties, Katti et al. investigated porous composites of PCL with HA.^{253, 254} The HA was first prepared either with (in situ) or without (ex situ) poly(acrylic acid). The composites were mixed as a 1:1 mixture with PCL in SBF for 1-4 days. Nanoindentation studies suggested that the composites prepared by the in situ method gave harder materials with higher elastic moduli as compared to the apatite grown ex situ. It is believed that nucleation in situ occurs heterogeneously by complexation of the calcium ions and the carboxylate groups of the polymer. Ex situ nucleation probably occurs heterogeneously by dissolution of the reactive apatite. Basic²⁴⁴ and oxygen plasma²⁵⁵ surface treatments have both been developed to improve the ability of PCL to nucleate formation of bonelike HA in two-dimensional (2D) and 3D scaffolds with SBF.

Rhee and co-workers have developed a PCL-silica hybrid using a sol-gel procedure.²⁵⁶ Hybrids with higher PCL content showed slower apatite formation rates and showed polymer-like ductile-tough fracture behavior, whereas lower PCL content resulted in faster apatite formation rate and more ceramic-like hard-brittle fracture behavior. In vitro studies of initial attachment and proliferation with human bone marrow stromal cells showed little difference from the tissue culture plate control. At longer times, the cells displayed even lower osteogenic differentiation than the control, presumably due to the poorly controlled growth of apatite into spireshaped granules. In contrast, good osteoconduction was observed in vivo in rabbits. The difference probably results from more control over calcium concentration by body fluids. The results suggest that precoating these surfaces before studies in vitro may be a better predictor of the results in vivo.

4.5.4. Dendrimers and Star Polymers—Polyamidoamine (PAMAM) dendrimers capped with amine, carboxylic acid, and acetamide groups have been used as “artificial proteins” and evaluated for their binding capacity and the surface charge with enamel crystals derived from rat maturation stage enamel (Figure 14).^{257,258} The uncharged acetamide group was easily removed from the crystal, indicating a low binding affinity, while the negatively charged carboxylic acid-terminated dendrimer showed a higher affinity and the positively charged amine-capped dendrimer exhibited the highest affinity. The higher affinity for the positively charged molecule can be explained by varying degrees of ionization or perhaps a higher concentration of phosphates on the surface of the mineral. These dendrimers also form nanospheres and could possibly have a role in guiding crystal growth, similar to that of amelogenin nanospheres in enamel.

In another study, star polymers were created by grafting PCL onto a poly(L-lysine) dendrimers terminated with glycolic acid groups.²⁵⁹ Preliminary studies of physical blends of organics and HA showed better film formation with the star polymer as compared to dendrimers (generations zero through six). Film formation conditions were further optimized using the star

polymers during the chemical synthesis of HA. The composite of the star polymer based on the generation 6.5 dendrimer with 20 wt % of HA exhibited mechanical properties (Young's modulus tensile strength) that were each approximately 1 order of magnitude lower than for natural bone.

Amphiphilic poly(propylene imine) dendrimers terminated with alkyl tails can be mixed with single-tail surfactants to form well-defined aggregates. These systems have been used to prepare HA composites with bonelike plastic deformation and high stiffness.²⁶⁰ With octadecylamine or CTAB as the surfactant, the resulting composite material was found to have a low organic content (9 wt % by TGA). X-ray diffraction and TEM analysis showed crystals similar to randomly oriented HA. The octylamine surfactant showed apparent needlelike crystals that were $70 \pm 25 \text{ nm} \times 10 \pm 2.8 \text{ nm}$, and the CTAB gave platelike crystals that were $125 \pm 49 \text{ nm} \times 84 \pm 35 \text{ nm}$. The resulting composite with CTAB had a Young's modulus of 90 GPa and displayed brittle fracture with an ultimate strength of 155 MPa. In the sample prepared with octadecylamine, the Young's modulus was 92 GPa and had a yield strength of 174 MPa with no brittle fracture. Further compression of the material caused strain hardening that increased the ultimate strength to 200 MPa. The authors note that the two composites give similar mechanical behavior in the elastic regime, but only the dendrimer-octadecylamine-HA composite gives bonelike yield. Under analogous conditions with SDS, the surfactant appeared to inhibit mineralization and resulted in a much lower yield of the composite (10%), with large clusters of crystals, and a high organic content (57%).

4.5.5. Mineralization within Polymer Microgels—HA has also been mineralized within the corona of aqueous microgels that can containers for its in situ mineralization.²⁶¹ The 200-500 nm microgel particles were formed from a copolymer of vinylcaprolactam and acetoacetoxyethyl methacrylate and a small proportion of vinylimidazole. As a result of mineralization, HA nanocrystals are integrated into hybrid colloids that can be formed into nanostructured films. The authors suggested that such structures could be used as injectable materials in regenerative medicine.

4.5.6. Poly(amino acids) to Nucleate HA—An interesting strategy for the mineralization of collagen was recently proposed. Using a polymer-induced liquid precursor (PILP) process,^{262,263} small amounts of poly(aspartic acid) were used to infiltrate calcium and phosphate ions into a collagen network and to induce mineralization in a nonequilibrium morphology. The observed infiltration is consistent with earlier work that showed that the presence of polyaspartate increased the amount of calcium phosphate crystals within assembling collagen fibrils.²⁶⁴ The addition of polyaspartate was also observed to greatly slow the kinetics of the amorphous-crystalline transition. Recreating the architecture of the mineralized collagen fiber from an amorphous precursor is an important step toward reproducing the hierarchical organization of natural bone. Another synthetic approach to HA mineralization uses the so-called double hydrophilic block copolymer (DHBC) with one hydrophilic block to interact with a mineral surface and another to promote solubility in an aqueous biomineralization medium.²⁶⁵ Similarly, poly(ethylene oxide)-*b*-alkylated poly(methacrylic acid) (PEO-*b*-PMAA-C12) formed calcium phosphate nanofibers with filaments oriented down the *c*-axis of HA.²⁶⁶ Aggregates trap calcium ions and are mineralized upon addition of phosphate ions. This grows in the *c*-axis direction is due to negatively charged DHBC adsorbing on the exposed surfaces parallel to the *c*-axis.

4.6. Organoapatites

Our laboratory reported in the 1980s the synthesis of a new family of materials that we termed organoapatites (OAs).²⁶⁷ These materials were synthesized by nucleation and growth of apatite crystals in media containing poly(amino acids) or synthetic organic polyelectrolytes

under strict atmospheric, temperature, and pH control. The OAs were synthesized using macromolecules such as poly(L-lysine), poly(L-glutamic acid), and poly(sodium acrylate). The materials were characterized by X-ray diffraction, scanning electron microscopy, surface area measurements, elemental analysis, and spectroscopic techniques. OAs were found to contain large surface area morphologies with nanoscale crystallites that mature slowly into HA based on analysis of Ca/P ratio. These systems were designed to mimic some aspects of apatite formation in mineralized tissues and were targeted for use as artificial materials to trigger bone regeneration at defect sites or interfaces with implants. The main biomimetic element was the use of organic macromolecules to nucleate apatite crystals and possibly regulate their sizes and shapes. The nature of the poly(amino acid) used led to significant changes in crystal morphology. For example, poly(L-lysine) generated large flat and thin single crystals, whereas poly(L-glutamic acid) generated nanoscale small crystallites (Figure 15).⁶ Because organapatite synthesis yielded powder samples, we also formulated OAs with reactive organic molecules so that pressing of two different powders could yield monolithic structures as a polymer matrix formed between apatite particles (Figure 16).²⁶⁸

We also investigated the use of OAs for bone formation in vivo.²⁶⁹ OAs were tested as implants in adult canine cortical bone for periods of 12-35 weeks. Histological analysis indicated excellent apposition of the poly(amino acid) OAs with mineralized bone but contact with fibrous tissue when synthetic polyelectrolytes were used. This suggests that the molecularly dispersed organic dopant, which was only 2-3 wt % of the microstructure, could play a critical role in the tissue response to the implant. Relative to apatite controls, poly(amino acid) OAs were also found to have greater resistance to fragmentation and revealed interfacial bioerosion accompanied by regeneration of bone. The enhanced toughness of pressed powders of OA with extremely low weight percents of organic macromolecules is also biomimetic of biogenic minerals toughened by small amounts of occluded proteins. This principle may very well apply to mature mammalian enamel, which retains a finite content of protein that is thought to enhance toughness when compared to the mineral phase alone.

OAs were also prepared using a nanopptide inspired by mussel glue proteins. These hybrid materials studied in vivo along with nanoscale apatite crystals as a control.²⁷⁰ Both materials showed good bone bonding (17 and 14% contact to bone, respectively) and resorption (as measured by the amount of osteoclast-like cells). Generally, OAs can be designed with many different organic components that may include drugs and growth factors for bone regenerative therapies. We have also coated OAs on the surfaces of metals to create implant surfaces that may be more conducive to the ingrowth of bone.²⁷¹

In the context of metal-based materials, the equiatomic nickel-titanium alloy has been found to exhibit properties such as a high damping coefficient and good fatigue resistance, making it an attractive material for bone implants and implantable stents.²⁷² In particular, these properties could help to increase the fatigue life and minimize the stress-shielding effect, for hip and other joint replacements, respectively. Titanium spontaneously forms a very stable oxide film on its surface in oxygen-rich environments, such as those found in the human body, minimizing nickel-related toxicity. However, this alloy is at best “bioinert”; it is unable to promote any particular biological function or controlled mineralization. A number of surface treatment methods (e.g., acidic, basic, or thermal) have been developed to improve the ability of these metals to mineralize bonelike HA.²⁷³⁻²⁷⁵ HA growth has been shown on silica, titania, zirconia, or alumina surfaces,²⁷⁶ but these methods typically result in changes to the functional groups on the metal surface but do not necessarily improve bioactivity. Therefore, an ideal scaffold for tissue engineering would incorporate a high porosity for cell growth and vascularization; biocompatibility; controlled biodegradation rates to match the rate of tissue growth, surface chemistries to promote cell attachment, proliferation, and differentiation; and mechanical properties to match those of the host tissue.²⁷⁷

We have investigated the influence of OA grown directly onto an L-shaped titanium mesh on preosteoblastic cellular colonization.²⁷⁸ The OA was prepared with a layer of poly(L-lysine) followed by a layer of poly(L-glutamic acid) and then cultured with MC3T3-E1 murine calvaria cells. Cells on the 3D OA-Ti mesh substrates displayed accelerated colonization and increased proliferation as compared to the bare Ti controls. Cellular differentiation, as measured by ALP and OC expression, was observed at late stages of the experiment with little difference between OA-Ti mesh and bare Ti controls. These results suggest that OA grown on porous Ti substrates is capable of inducing accelerated colonization of unseeded implant structures by osteogenic cells. Furthermore, zinc-containing OA (ZnOA) has also been used as a coating for titanium substrates to provide biomaterials that can promote new bone growth using chemical and biochemical signals. The rationale here was to deliver zinc ions to cells through the OA, given the presence of this metal ion in ALP. Preosteoblastic mouse calvaria cells were cultured in a 3D bioreactor on titanium meshes covered with ZnOA.²⁷⁹ The ZnOA-coated samples showed an earlier onset of ALP expression relative to controls as well as mineralized bone nodules by SEM.

The above methodology was adapted for the coating of titanium with a poly(L-lysine)-calcium phosphate hybrid material with a nanoscale texture.²⁸⁰ The hybrid coating was grown by nucleating seed crystals of calcium phosphate, directly on the Ti surface and followed by exposure to solutions containing Ca^{2+} , PO_4^{3-} , and poly(L-lysine). The resulting material was found to be 14 wt % poly(L-lysine). This organic component decreased greatly the dimensions of the surface features and enhanced the surface area relative to the inorganic control. The highly textured hybrid material was more susceptible to acidic and enzymatic degradation as compared to the controls. The amino acid cysteine was covalently linked to the hybrid material, demonstrating the potential for further functionalization to this type of coating.

By depositing a polylysine-coated apatite layer (OA) during the preparation of a titanium foam, we have observed an improved mechanical matching to bone tissue with a surface that is attractive to cells.²⁸¹ In a rotating bioreactor, these OA-coated titanium (OA-Ti) foams were successfully colonized by preosteoblastic cells. Finite-element analyses suggested that the ingrown tissue in these systems had improved implant performance and tissue formation through load sharing and stress distribution. The cells were shown to bind and proliferate but increase in number up to 28 days. The ALP enzyme production per cell increases an order of magnitude over this time frame, suggesting that the preosteoblasts on the OA-Ti foams did not differentiate into mature osteoblasts within 28 days.

4.7. Supramolecular Systems for Mineralization

Self-assembly offers many additional opportunities for the design of complex functional materials with tunable properties.^{282,283} One-dimensional assemblies, such as nanotubes and nanoribbons, possess a single dimension that is much longer than the others and exhibit a number of useful properties, including the potential for alignment and to integrate biological functionality. As these 1D structures entangle, they behave like linear polymers by entrapping and slowing diffusion of solvent molecules, observed macroscopically as self-supporting gels.²⁸⁴ These systems offer the possibility to become basic models for mineralization with biomimetic features since they mimic the architecture of fibrous matrices and also have potentially higher order parameters relative to polymers. The possibility of creating synthetic systems with high order parameter and 1D architecture could offer the potential for epitaxial events in synthetic systems that emulate protein-mediated mineralization. Using molecular coassembly, supramolecular systems can also be designed to multiplex biological signals combined with capacity to mineralize. This potential can create synthetic materials that create a suitable niche for regeneration of mineralized tissues. We describe below several

supramolecular systems that have been developed in our laboratories both as biomimetic mineralization models and matrices for bone regeneration.

4.7.1. Self-Assembling Peptide Amphiphiles (PAs)—In our own work, we have studied biomimetic mineralization of bone apatite using self-assembling molecules known as peptide amphiphiles.^{72,285} This supramolecular platform allows the possibility of designing nanostructures that not only incorporate bioactive epitopes but also chemistry that specifically targets mineralization processes. PAs are molecules consisting of a hydrophobic tail linked to an electrostatically charged peptide sequence (Figure 17). When the peptide sequence includes amino acids with a strong β -sheet propensity, high aspect ratio cylindrical nanofibers are observed that can mimic the architecture of collagen fibers. Self-assembly of the PA molecules is controlled by hydrophobicity of the alkyl tail and hydrogen bonding between adjacent peptides. Screening of charged groups by changing pH or ionic strength changes results in an entangled network of nanofibers, observed macroscopically as a self-supporting gel. The morphology of the PA assemblies has been extensively characterized by TEM, SEM, AFM, as well as CD, NMR, and IR spectroscopy (Figure 18).²⁸⁵⁻²⁸⁷

Using a holey carbon TEM grid on which PA nanofibers formed by self-assembly, we were able to observe a bone biomimetic mineralization process (Figure 19). By introducing dilute solutions of CaCl_2 and Na_2HPO_4 on both sides of the grid, the ultrathin film of nanostructures prepared with phosphoserine-bearing PA can template on their surfaces the formation of thin HA crystals.⁷² Energy dispersion X-ray fluorescence spectroscopy (EDS) confirmed that the HA Ca/P stoichiometry of 1.67 ± 0.08 matches the ideal value predicted for $\text{Ca}_5(\text{PO}_4)_3(\text{OH})$. Interestingly, electron diffraction established that the crystallographic *c*-axis of the HA was preferentially aligned with the long axis of the PA fibers, as in mammalian bone and dentin.²⁶ A related molecule bearing a serine in place of the phosphoserine resulted in only amorphous mineral deposits. Without the nanostructures, no mineral deposit was observed at all. We believe that the negative charge of the PA is important to establish local supersaturation of the mineral precursor.³⁰ This is consistent with the conspicuous presence of phosphoserine and aspartic acid residues in many of the proteins thought to be associated with HA mineralization.^{30,49,288} While the exact mechanism of alignment is not clear, the arrangement of the acidic groups must be responsible for the presumed epitaxial mineralization. The formation of bone biomimetic crystals of apatite in this supramolecular system is most likely possible given its 2D nature. Ions of the crystal have short diffusion distances to the nucleating surfaces of the nanostructures, which must provide a directing influence to the growing crystals.

We recently discovered a system to cooperatively template HA mineralization using a 3D PA scaffold (Figure 18).²⁸⁹ The system employs the natural enzyme alkaline phosphatase and a phosphorylated PA nanofiber gel matrix to template, in three dimensions, HA nanocrystals with size, shape, and crystallographic orientation resembling the natural bone mineral. This system relies on both temporal and spatial templating to produce the observed biomimetic nanocrystals. Enzymatic release of phosphate ions by alkaline phosphatase regulates the availability of the mineral precursor and thus the rate of nanocrystal nucleation. This regulation prevents uncontrolled mineral precipitation, biasing the system toward selective, heterogeneous nucleation on the phosphorylated PA nanofiber templates. These engineered nanofibers provide critical spatial direction to the mineralization process. Close matches between interatomic spacings of calcium ions in the (002) plane of the HA crystal lattice and measured spacings in calcium-gelled PA nanofibers suggest that the nanofibers play a critical role in directing the observed crystallographic alignment and templated mineralization of HA in this 3D system (Figure 20).

To determine the potential for using these materials in tooth regeneration, Snead and Stupp recently investigated the effect of a 3D nanofiber scaffold on dental epithelial cells during

enamel formation.²⁹⁰ Ameloblast-like cells (line LS8) and primary enamel organ epithelial (EOE) cells were seeded and cultured on or within hydrogels formed from self-assembling PAs presenting the RGD epitope on a branched peptide. The expression of amelogenin and integrin $\alpha 6$ was detected by quantitative real-time polymerase chain reaction (qPCR) and immunohistochemistry. Both LS8 and primary EOE cells responded to the branched RGD nanostructures with enhanced proliferation and enhanced expression of amelogenin. The PA material was also injected into the developing enamel matrix of embryonic mouse incisors. In this organ culture model, when the RGD-PA was injected into mouse incisors, EOE cells were found to proliferate and to differentiate into ameloblasts at the site of injection. Biochemical assays and ultrastructural analysis showed the PA nanofibers within the forming extracellular matrix and contacting the epithelial cells engaged in enamel formation. Together, these *in vitro* and *in vivo* results show that RGD-PA nanofibers may participate in integrin-mediated cell binding to the matrix and deliver instructive signals for enamel formation.

Proteinases in enamel also provide inspiration for biomimetic strategies. For instance, Jun et al. have rationally designed PAs (PAs) by integrating both a cell adhesion RGDS sequence in addition to an MMP-2 enzyme cleavable GTAGLIGQ sequence.²⁹¹ When the enzyme type IV collagenase was incubated with a self-supporting gel composed of PA, the long nanofibers became egg-shaped fibrillar aggregates, and within 1 month, the entire gel was degraded. When appropriate concentrations of the PA were used to encapsulate dental pulp cells, which produce MMP-2, the cells appeared to elongate and rearrange the nanofiber matrix over time. Without the proper concentrations of PA, the cells remained viable but only displayed a spherical phenotype.²⁹¹ This PA was then assessed for interactions with dental stem cells. The PA was used to encapsulate two types of human MSCs: One type was derived from adult third molar dental pulp (DPSC), and the other type was derived from human exfoliated deciduous teeth (SHED). SHED cells exhibited high proliferation rates and collagen production, making it more conducive for softer tissues, whereas the DPSC expressed osteoblast marker genes, an osteoblast-like phenotype, exhibited reduced proliferation rates, and deposited mineral making these cells more conducive for use in mineralized tissues.²⁹²

To covalently attach these PA nanofibers displaying the RGD epitope, we developed a general strategy for altering the surface chemistry of a NiTi substrate.²⁹³ The optimized surface treatment creates a uniform TiO₂ layer with low levels of Ni on the NiTi surface. A low-temperature vapor deposition method was developed using a TiO₂ layer substrate with an aminopropylsilane coating. The resulting amine-coated surface allows covalent attachment of PA molecules containing terminal carboxylic acid groups. Cell culture and SEM demonstrated cellular adhesion, spreading, and proliferation on these functionalized metal surfaces. These experiments also showed that covalently bonding the PA molecules to the substrate created robust coatings that lead to a confluent cell layer within 1 week.

We recently reported a method to prepare a hybrid bone implant material consisting of a Ti-6Al-4V foam filled with a PA nanofiber matrix, as shown by SEM and confocal microscopy.²⁹⁴ The method also allows the encapsulation of preosteoblastic cells within the bioactive matrix, and under appropriate conditions, the PA nanofibers can nucleate mineralization of calcium phosphate phases with a Ca/P ratio that corresponds to that of HA. A quantitative DNA assay DNA showed that the population of encapsulated cells correlated strongly with the seeding density, and SEM confirmed that the cells were able to attach and spread on the PA coating. We also explored this material *in vivo* using a bone plug model in a rat femur. Preliminary histology results after 4 weeks of implantation demonstrated *de novo* bone formation inside and around the implant and vascularization around the implant with no evidence of cytotoxicity. These studies were conducted using a 95:5 molar ratio of phosphoserine- and RGDS-bearing PAs. This approach of self-assembling PA nanofibers within the pores of metallic foams offers great potential to initiate HA mineralization and to

direct the cellular response from the host tissue into porous implants to form new bone with improved fixation, osseointegration, and long-term stability of implants.

It is also possible to control the density of bioactive epitopes by combining them with other PA molecules. The colonization of mouse preosteoblastic cells in PA-metal hybrids was investigated using different ratios of RGD and non-RGD PAs.²⁹⁵ The preosteoblasts migrated into the hybrid interior and remained viable. A plateau in cell density was reached earlier for hybrid samples that contained 15 mol % RGD as compared to samples with only 0.5 or 5% of the active epitope. Expression levels of ALP and OC showed that these cells had matured along the osteoblastic lineage by the time of the plateau (day 14).

A collagen-binding motif (CBM) with the amino acid sequence GLRSKSKKFRRPDIQYPDATDEDITSHM was synthesized based on residues 150-177 of human OP.²⁹⁶ The acidic residues (Asp and Glu) were expected to contribute to calcium binding; the hydrophobic residues (Met, Phe, and Tyr) probably contribute to the assembly of the peptide.⁴⁶ Collagen assembled with the CBM peptide showed mineralization both in vitro and within a critical defect in vivo. In contrast, no apatite nucleation was observed with collagen alone under these conditions. These results suggest that the CBM peptide sequence is sufficient for both collagen binding and HA nucleation.

4.8. Biomimetic Enamel Formation

The field of self-assembly allows for a unique approach to the field of tooth mineralization. Because the body cannot regenerate enamel de novo due to the elimination of ameloblasts during tooth maturation, it may be possible to implement the use of self-assembling molecules that promote remineralization and ultimately regeneration of mature enamel. The use of self-assembling peptides also provides a unique organic matrix that can assemble given specific physiological cues to promote the formation of inorganic HA crystals and as a scaffold for cells.²⁹² The applications of these peptides include administration to caries lesions or porous, damaged tissue.

This is still an emerging area for tooth biomineralization; however, a number of groups have developed research programs to combine self-assembly and mineralization. Kirkham, Aggeli, and co-workers²⁹⁷ have developed β -sheet-forming peptides that spontaneously self-assemble into long fibrillar structures resembling ribbons in the presence of pH less than 8.0 and/or salt. Human teeth were subjected to an acid treatment to create “carieslike” lesions, which were treated with a self-assembling peptide containing several glutamic acid residues. The samples were then subjected to cyclic pH conditions with demineralizing and remineralizing solutions to simulate the physiological environment of the tooth. In general, the peptides were shown to decrease demineralization and show a strong trend toward increasing remineralization, resulting in a net gain of mineral. Additionally, in vivo studies revealed that the peptides were able to create electron dense HA crystals de novo.

One approach toward treatment of dental caries includes the development of a dental paste, which includes inorganic components and a modified HA powder.²⁹⁸ This dental paste, when administered to small carious lesions at acidic pH, has been shown to seal the lesion site within 15 min. Upon further characterization of the microstructure, the paste was found to seal the region between the paste and the enamel tissue. Additionally, the nucleated HA structures were arranged in a densely packed 3D array within 3 min of administering the paste. This treatment could possibly replace dental fillings for early carious lesions, as it eliminates the need to remove healthy tooth for placement of a dental filling.

5. Conclusions and Outlook

Enormous progress has been made over the last few decades in understanding the process of HA biomineralization in mammalian tissues such as bone, dentin, and enamel. Some knowledge has been acquired about the role of proteins in achieving a morphologically controlled deposition of mineral as opposed to precipitation of unstructured agglomerates of crystals. The understanding is far from complete, particularly in bone. In decades to come, with advances in nanoscience and molecular biology, we will likely achieve a deeper understanding of why nature requires multiple proteins to achieve the goal of controlled mineralization. Beyond fundamental understanding of how these complex tissue matrices become the highly organized hybrids they are in biology, the field has a great deal to offer to materials chemistry. At the present time, chemistry cannot offer general synthetic methodologies to create organic-inorganic hybrid materials in which there is synergistic order established in both phases. The crystallographic alignment of apatite crystals in bone relative to the long axes of collagen fibrils is one example, as well as the spatial control of mineralization in specific locations of the organic matrix of bone. Protein-mediated control of the large-scale alignment of HA crystals in enamel, followed by degradation of most of this organic matrix, is another example of synergistic behavior. The biomimetic lesson here is that largely inorganic materials could be synthesized in an easily degraded but complex organic scaffold that may help create a hierarchical structure. The most obvious use of novel artificial materials that mimic bone and enamel mineralization would be biomaterials that can cue cells to regenerate these tissues in vitro or in vivo. However, our understanding of biomineralization in these tissues could be used to create synthetic hybrid materials with functions that are not directly related to biomedical applications but target other functions that rely heavily on mechanical, optical, magnetic, or electrical properties.

6. Acknowledgments

We are grateful to the NIH (5 R01 DE015920-04 and 5 P50 NS054287-03), DOE (DE-FG02-00ER45810), and NSF (DMR-0505772 and DMR-0605427) for financial support of our own contributions in this area. E.D.S. acknowledges support by the Department of Energy Basic Energy Sciences program at Sandia National Laboratories. Sandia is a multiprogram laboratory operated by Sandia Corporation, a Lockheed Martin Company, for the U.S. Department of Energy's National Nuclear Security Administration under Contract DE-AC04-94AL85000.

Biographies



Liam Palmer received his B.S. in Chemistry from the University of South Carolina in 1999. He completed his Ph.D. on molecular encapsulation under the supervision of Prof. Julius Rebek, Jr. at The Scripps Research Institute in 2005. Liam is now working as a Research Assistant Professor in the group of Prof. Samuel Stupp at Northwestern University. His current research focuses on strategies to control the self-assembly of amphiphilic small molecules.



Christina Newcomb graduated with a B.S. in 2005 from the University of California, San Diego. She is currently pursuing a Ph.D. in the department of Materials Science and Engineering at Northwestern University. Her doctorate studies are focused on the regeneration of hard tissues including bone and tooth under Professor Samuel I. Stupp.



Stuart R. Kaltz earned his B.S. degree at Michigan State University in 2007 and is currently pursuing his Ph.D. in Materials Science and Engineering at Northwestern University, where he is studying peptide amphiphiles for bone regeneration under Professor Samuel I. Stupp.



Erik D. Spoerke earned his B.S. in Materials Science and Engineering from Northwestern University in 1998. He continued his studies of Materials Science and Engineering at Northwestern University, earning a Ph.D. investigating biomaterials for orthopedic tissue engineering with Professor Samuel I. Stupp in 2003. Erik then served as a postdoctoral researcher at Sandia National Laboratories in Albuquerque, NM, before converting to his current position as a Senior Member of Technical Staff at Sandia. His present research efforts concentrate on nanomaterials synthesis and assembly with particular emphasis on photovoltaic materials, electrical energy storage, and active materials assembly.



Samuel I. Stupp earned his B.S. in Chemistry from the University of California at Los Angeles and his Ph.D. in Materials Science and Engineering from Northwestern University in 1977. He was a member of the faculty at Northwestern until 1980 and then spent 18 years at the University of Illinois at Urbana-Champaign where he was appointed in 1996 Swanlund Professor of Materials Science and Engineering, Chemistry, and Bioengineering. In 1999, he returned to Northwestern as a Board of Trustees professor of Materials Science, Chemistry, and Medicine and later was appointed Director of Northwestern's Institute for BioNanotechnology in Medicine. His research is focused on self-assembly of materials with special interest in regenerative medicine, cancer therapies, and solar energy technology.

7. References

- (1). Lowenstam HA. *Science* 1981;211:1126. [PubMed: 7008198]
- (2). Mann S. *Nature* 1993;365:499.
- (3). Mann S, Archibald DD, Didymus JM, Douglas T, Heywood BR, Meldrum FC, Reeves NJ. *Science* 1993;261:1286. [PubMed: 17731856]
- (4). Fritz M, Belcher AM, Radmacher M, Walters DA, Hansma PK, Stucky GD, Morse DE, Mann S. *Nature* 1994;371:49.
- (5). Shen X, Belcher AM, Hansma PK, Stucky GD, Morse DE. *J. Biol. Chem* 1997;272:32472. [PubMed: 9405458]

- (6). Stupp SI, Braun PV. *Science* 1997;277:1242. [PubMed: 9271562]
- (7). Aizenberg J, Weaver JC, Thanawala MS, Sundar VC, Morse DE, Fratzl P. *Science* 2005;309:275. [PubMed: 16002612]
- (8). Aizenberg, J. *Nanomechanics of Materials and Structures*. Chuang, T-J.; Anderson, PM.; Wu, M-K.; Hsieh, S., editors. Springer; Dordrecht, The Netherlands: 2006.
- (9). Brown WE, Chow LC. *Annu. Rev. Mater. Sci* 1976;6:213.
- (10). Boskey AL. *Elements* 2007;3:385.
- (11). Verdelis K, Lukashova L, Wright JT, Mendelsohn R, Peterson MG, Doty S, Boskey AL. *Bone* 2007;40:1399. [PubMed: 17289453]
- (12). Olszta MJ, Cheng XG, Jee SS, Kumar R, Kim YY, Kaufman MJ, Douglas EP, Gower LB. *Mater. Sci. Eng., R* 2007;58:77.
- (13). Weiner S, Dove PM. *Rev. Mineral Geochem* 2003;54:1.
- (14). Barralet J, Best S, Bonfield W. *J. Biomed. Mater. Res* 1998;41:79. [PubMed: 9641627]
- (15). Koutsopoulos S. *J. Biomed. Mater. Res* 2002;62:600. [PubMed: 12221709]
- (16). Zhan JH, Tseng YH, Chan JCC, Mou CY. *Adv. Funct. Mater* 2005;15:2005.
- (17). Elliott, JC. *Structure and Chemistry of the Apatites and Other Calcium Orthophosphates*. Elsevier; Amsterdam: 1994.
- (18). LeGeros, RZ. *Calcium Phosphates in Oral Biology & Medicine*. Karger; Basel: 1991.
- (19). Tas AC. *Biomaterials* 2000;21:1529.
- (20). Liu DM, Troczynski T, Tseng WJ. *Biomaterials* 2001;22:1721. [PubMed: 11396875]
- (21). Salgado AJ, Coutinho OP, Reis RL. *Macromol. Biosci* 2004;4:743. [PubMed: 15468269]
- (22). Manolagas SC. *Endocr. Rev* 2000;21:115. [PubMed: 10782361]
- (23). Weiner S, Wagner HD. *Annu. Rev. Mater. Sci* 1998;28:271.
- (24). Mann, S. *Biomaterialization Principles and Concepts in Bioinorganic Materials Chemistry*. Oxford University Press; Oxford, United Kingdom: 2001.
- (25). Fernandez-Moran H, Engstrom A. *Biochim. Biophys. Acta* 1957;23:260. [PubMed: 13412720]
- (26). Traub W, Arad T, Weiner S. *Proc. Natl. Acad. Sci. U.S.A* 1989;86:9822. [PubMed: 2602376]
- (27). Feng JQ, Ward LM, Liu S, Lu Y, Xie Y, Yuan B, Yu X. *Nat. Genet* 2006;38:1311.
- (28). Schmidt WJ. *Naturwissenschaften* 1936;24:361.
- (29). Burger C, Zhou H, Wang H, Sics I, Hsiao BS, Chu B, Graham L, Glimcher M. *Biophys. J* 2008;95:1985. [PubMed: 18359799]
- (30). Weiner S, Addadi L. *J. Mater. Chem* 1997;7:689.
- (31). Rho JY, Kuhn-Spearing L, Zioupos P. *Medi. Eng. Phys* 1998;20:92.
- (32). Prockop DJ, Kivirikko KI. *Annu. Rev. Biochem* 1995;64:403. [PubMed: 7574488]
- (33). Cui FZ, Li Y, Ge J. *Mater. Sci. Eng., R* 2007;57:1.
- (34). Kadler KE, Holmes DF, Trotter JA, Chapman JA. *Biochem. J* 1996;316:1. [PubMed: 8645190]
- (35). Bella J, Brodsky B, Berman HM. *Structure* 1995;3:893. [PubMed: 8535783]
- (36). Bella J, Eaton M, Brodsky B, Berman HM. *Science* 1994;266:75. [PubMed: 7695699]
- (37). Landis WJ, Song MJ, Leith A, McEwen L, McEwen BF. *J. Struct. Biol* 1993;110:39. [PubMed: 8494671]
- (38). Landis WJ, Hodgens KJ, Arena J, Song MJ, McEwen BF. *Microsc. Res. Tech* 1996;33:192. [PubMed: 8845518]
- (39). Weiner S, Traub W, Wagner HD. *J. Struct. Biol* 1999;126:241. [PubMed: 10475685]
- (40). Wenk HR, Heidelberg F. *Bone* 1999;24:361. [PubMed: 10221548]
- (41). White SW, Hulmes DJS, Miller A, Timmins PA. *Nature* 1977;266:421. [PubMed: 859610]
- (42). Landis WJ. *J. Ultrastruct. Mol. Struct. Res* 1986;94:217. [PubMed: 3027205]
- (43). Landis WJ, Hodgens KJ, Song MJ, Arena J, Kiyonaga S, Marko M, Owen C, McEwen BF. *J. Struct. Biol* 1996;117:24. [PubMed: 8776885]
- (44). Toroian D, Lim JE, Price PA. *J. Biol. Chem* 2007;282:22437. [PubMed: 17562713]
- (45). Ganss B, Kim RH, Sodek J. *Crit. Rev. Oral Biol. Med* 1999;10:79. [PubMed: 10759428]

- (46). Sodek J, Ganss B, McKee MD. *Crit. Rev. Oral Biol. Med* 2000;11:279. [PubMed: 11021631]
- (47). Hauschka PV, Lian JB, Cole DE, Gundberg CM. *Physiol. Rev* 1989;69:990. [PubMed: 2664828]
- (48). Oldberg A, Franzen A, Heinegard D. *J. Biol. Chem* 1988;263:19430. [PubMed: 3198635]
- (49). Addadi L, Weiner S. *Proc. Natl. Acad. Sci. U.S.A* 1985;82:4110. [PubMed: 3858868]
- (50). Addadi L, Weiner S, Geva M. *Z. Kardiol* 2001;90(Suppl 3):92. [PubMed: 11374040]
- (51). Bianco P, Fisher LW, Young MF, Termine JD. *Calcif. Tissue Int* 1991;49:421. [PubMed: 1818768]
- (52). Hunter GK, Hauschka PV, Poole AR, Rosenberg LC, Goldberg HA. *Biochem. J* 1996;317:59. [PubMed: 8694787]
- (53). Termine JD, Kleinman HK, Whitson SW, Conn KM. *Cell* 1981;26:99. [PubMed: 7034958]
- (54). Romberg RW, Werness PG, Riggs BL, Mann KG. *Biochemistry* 1986;25:1176. [PubMed: 3008822]
- (55). Gericke A, Qin C, Spevak L, Fujimoto Y, Butler WT, Sørensen ES, Boskey AL. *Calcif. Tissue Int* 2005;77:45. [PubMed: 16007483]
- (56). Weinreb M, Shinar D, Rodan GA. *J. Bone Miner. Metab* 1990;5:831.
- (57). Ducy P, Desbois C, Boyce B, Pinero G, Story B, Dunstan C, Smith E, Bonadio J, Goldstein S, Gundberg C, Bradley A, Karsenty G. *Nature* 1996;382:448. [PubMed: 8684484]
- (58). Ecarot-Charrier B, Glorieux FH, Vanderrest M, Pereira G. *J. Cell Biol* 1983;96:639. [PubMed: 6833375]
- (59). Balcerzak M, Hamade E, Zhang L, Pikula S, Azzar G, Radisson J, Bandorowicz-Pikula J, Buchet R. *Acta Biochim. Pol* 2003;50:1019. [PubMed: 14739992]
- (60). Lanyon LE. *Calcif. Tissue Int* 1993;53(Suppl 1):S102. [PubMed: 8275362]
- (61). Bonewald LF, Johnson ML. *Bone* 2008;42:606. [PubMed: 18280232]
- (62). Väänänen HK, Zhao H, Mulari M, Halleen JM. *J. Cell Sci* 2000;113:377. [PubMed: 10639325]
- (63). Teitelbaum SL. *Science* 2000;289:1504. [PubMed: 10968780]
- (64). Gowen M, Lazner F, Dodds R, Kapadia R, Feild J, Tavaría M, Bertocello I, Drake F, Zavarselk S, Tellis I, Hertzog P, Debouck C, Kola I. *J. Bone Miner. Res* 1999;14:1654. [PubMed: 10491212]
- (65). Roodman GD. *Endocr. Rev* 1996;17:308. [PubMed: 8854048]
- (66). Mackie EJ. *Int. J. Biochem. Cell Biol* 2003;xxx:xxx.
- (67). Anderson HC. *Clin. Orthop. Relat. R* 1995:266.
- (68). Boskey AL. *Connect. Tissue Res* 1996;xxx:xxx.
- (69). Hunter GK, Goldberg HA. *Biochem. J* 1994;302:175. [PubMed: 7915111]Part 1
- (70). Stubbs JT, Mintz KP, Eanes ED, Torchia DA, Fisher LW. *J. Bone Miner. Res* 1997;12:1210. [PubMed: 9258751]
- (71). He G, Ramachandran A, Dahl T, George S, Schultz D, Cookson D, Veis A, George A. *J. Biol. Chem* 2005;280:33109. [PubMed: 16046405]
- (72). Hartgerink JD, Beniash E, Stupp SI. *Science* 2001;294:1684. [PubMed: 11721046]
- (73). Brown WE, Smith JP, Frazier AW, Lehr JR. *Nature* 1962;196:1050.
- (74). Weiner S, Traub W. *FASEB J* 1992;6:879. [PubMed: 1740237]
- (75). Grynepas M. *Bone* 2007;41:162. [PubMed: 17537689]
- (76). Eanes ED, Gillesen IH, Posner AS. *Nature* 1965;208:365. [PubMed: 5885449]
- (77). Grynepas MD, Bonar LC, Glimcher MJ. *Calcif. Tissue Int* 1984;36:291. [PubMed: 6432293]
- (78). Addadi L, Raz S, Weiner S. *Adv. Mater* 2003;15:959.
- (79). Politi Y, Arad T, Klein E, Weiner S, Addadi L. *Science* 2004;306:1161. [PubMed: 15539597]
- (80). Politi Y, Levi-Kalisman Y, Raz S, Wilt FH, Addadi L, Weiner S, Sagi I. *Adv. Funct. Mater* 2006;16:1289.
- (81). Weiner S. *Bone* 2006;39:431. [PubMed: 16581322]
- (82). Weiner S, Sagi I, Addadi L. *Science* 2005;309:1027. [PubMed: 16099970]
- (83). Robinson, C.; Kirkham, J.; Shore, R., editors. *Dental Enamel Formation to Destruction*. CRC Press; Boca Raton, FL: 1995.
- (84). Tamerler C, Sarikaya M. *MRS Bull* 2008;33:504.

- (85). Ten Cate, AR. Oral Histology. Development, Structure, and Function. 4th ed.. Mosby; St. Louis, MO: 1994.
- (86). White SN, Luo W, Paine ML, Fong H, Sarikaya M, Snead ML. J. Dent. Res 2001;80:321. [PubMed: 11269723]
- (87). Lin CP, Douglas WH, Erlandsen SL. J. Histochem. Cytochem 1993;41:381. [PubMed: 8429200]
- (88). Imbeni V, Kruzic JJ, Marshall GW, Marshall SJ, Ritchie RO. Nat. Mater 2005;4:229. [PubMed: 15711554]
- (89). Habelitz S, Marshall SJ, Marshall GW, Balooch M. Arch. Oral Biol 2001;46:173. [PubMed: 11163325]
- (90). Lin CP, Douglas WH. J. Dent. Res 1994;73:1072. [PubMed: 8006234]
- (91). Tesch W, Eidelman N, Roschger P, Goldenberg F, Klaushofer K, Fratzl P. Calcif. Tissue Int 2001;69:147. [PubMed: 11683529]
- (92). Paine ML, White SN, Luo W, Fong H, Sarikaya M, Snead ML. Matrix Biol 2001;20:273. [PubMed: 11566262]
- (93). Kirkham J, Zhang J, Brookes SJ, Shore RC, Wood SR, Smith DA, Wallwork ML, Ryu OH, Robinson C. J. Dent. Res 2000;79:1943. [PubMed: 11201043]
- (94). Wen HB, Moradian-Oldak J, Fincham AG. J. Dent. Res 2000;79:1902. [PubMed: 11145363]
- (95). Wen X, Lei YP, Zhou YL, Okamoto CT, Snead ML, Paine ML. Cell. Mol. Life Sci 2005;62:1038. [PubMed: 15868102]
- (96). Zhu DH, Paine ML, Luo W, Bringas P, Snead ML. J. Biol. Chem 2006;281:21173. [PubMed: 16707492]
- (97). Daculsi G, Kerebel B. J. Ultrastruct. Res 1978;65:163. [PubMed: 731784]
- (98). White SN, Paine ML, Luo W, Sarikaya M, Fong H, Yu ZK, Li ZC, Snead ML. J. Am. Ceram. Soc 2000;83:238.
- (99). Wang RZ, Weiner S. J. Biomech 1998;31:135. [PubMed: 9593206]
- (100). Whittaker DK. Arch. Oral Biol 1982;27:383. [PubMed: 6956250]
- (101). Boyde, A. Handbook of Microscopic Anatomy. Oksche, ALV., editor. Springer-Verlag; Berlin: 1989.
- (102). Kodaka T, Nakajima F, Higashi S. Caries Res 1989;23:290. [PubMed: 2766312]
- (103). Gwinnett AJ. Oper. Dent 1992;10. [PubMed: 1470538]
- (104). Garant, P. Oral Cells and Tissues. Quintessence Publishing Co. Inc.; Chicago: 2003.
- (105). Margolis HC, Beniash E, Fowler CE. J. Dent. Res 2006;85:775. [PubMed: 16931858]
- (106). Landis WJ, Burke GY, Neuringer JR, Paine MC, Nanci A, Bai P, Warshawsky H. Anat. Rec 1988;220:233. [PubMed: 2834985]
- (107). Diekwisch TGH, Berman BJ, Gentner S, Slavkin HC. Cell Tissue Res 1995;279:149. [PubMed: 7895256]
- (108). Gomez S, Boyde A. Microsc. Res. Tech 1994;29:29. [PubMed: 8000082]
- (109). Toyosawa S, Ogawa Y, Inagaki T, Ijuhin N. Cell Tissue Res 1996;285:217. [PubMed: 8766158]
- (110). Ravindranath RM, Moradian-Oldak J, Fincham AG. J. Biol. Chem 1999;274:2464. [PubMed: 9891017]
- (111). Gibson CW, Yuan ZA, Hall B, Longenecker G, Chen EH, Thyagarajan T, Sreenath T, Wright JT, Decker S, Piddington R, Harrison G, Kulkarni AB. J. Biol. Chem 2001;276:31871. [PubMed: 11406633]
- (112). Gibson C, Golub E, Herold R, Risser M, Ding W, Shimokawa H, Young M, Termine J, Rosenbloom J. Biochemistry 1991;30:1075. [PubMed: 1989679]
- (113). Hu CC, Bartlett JD, Zhang CH, Qian Q, Ryu OH, Simmer JP. J. Dent. Res 1996;75:1735. [PubMed: 8955667]
- (114). Salido EC, Yen PH, Koprivnikar K, Yu LC, Shapiro LJ. Am. J. Hum. Genet 1992;50:303. [PubMed: 1734713]
- (115). Snead ML, Lau EC, Zeichner-David M, Fincham AG, Woo SL, Slavkin HC. Biochem. Biophys. Res. Commun 1985;129:812. [PubMed: 4015654]
- (116). Fincham AG, Moradian-Oldak J, Simmer JP. J. Struct. Biol 1999;126:270. [PubMed: 10441532]

- (117). Toyosawa S, O'Huigin C, Figueroa F, Tichy H, Klein J. *Proc. Natl. Acad. Sci. U.S.A* 1998;95:13056. [PubMed: 9789040]
- (118). Paine ML, White SN, Luo W, Fong H, Sarikaya M, Snead ML. *Matrix Biol* 2001;20:273. [PubMed: 11566262]
- (119). Moradian-Oldak J. *Matrix Biol* 2001;20:293. [PubMed: 11566263]
- (120). Paine ML, Snead ML. *J. Bone Miner. Res* 1997;12:221. [PubMed: 9041053]
- (121). Paine ML, Zhu DH, Luo W, Bringas P, Goldberg M, White SN, Lei YP, Sarikaya M, Fong HK, Snead ML. *J. Struct. Biol* 2000;132:191. [PubMed: 11243888]
- (122). Ravindranath RM, Devarajan A, Bringas P. *Arch. Oral Biol* 2007;52:1161. [PubMed: 17679105]
- (123). Shaw WJ, Campbell AA, Paine ML, Snead ML. *J. Biol. Chem* 2004;279:40263. [PubMed: 15299015]
- (124). Warotayanont R, Zhu D, Snead ML, Zhou Y. *Biochem. Biophys. Res. Commun* 2008;367:1. [PubMed: 18086559]
- (125). Goto Y, Kogure E, Takagi T, Aimoto S, Aoba T. *J. Biochem* 1993;113:55. [PubMed: 8454575]
- (126). Matsushima N, Izumi Y, Aoba T. *J. Biochem* 1998;123:150. [PubMed: 9504422]
- (127). Tan J, Leung W, Moradian-Oldak J, Zeichner-David M, Fincham AG. *Connect. Tissue Res* 1998;38:215. [PubMed: 11063029]
- (128). Tan J, Leung W, Moradian-Oldak J, Zeichner-David M, Fincham AG. *J. Dent. Res* 1998;77:1388. [PubMed: 9649167]
- (129). Fincham AG, Moradian-Oldak J, Simmer JP, Sarte P, Lau EC, Diekwisch T, Slavkin HC. *J. Struct. Biol* 1994;112:103. [PubMed: 8060728]
- (130). Fincham AG, Moradian-Oldak J, Diekwisch TGH, Lyaruu DM, Wright JT, Bringas P, Slavkin HC. *J. Struct. Biol* 1995;115:50. [PubMed: 7577231]
- (131). Moradian-Oldak J, Goldberg M. *Cells Tissues Organs* 2005;181:202. [PubMed: 16612086]
- (132). Veis A. *Science* 2005;307:1419. [PubMed: 15746414]
- (133). Du C, Falini G, Fermani S, Abbott C, Moradian-Oldak J. *Science* 2005;307:1450. [PubMed: 15746422]
- (134). Moradian-Oldak J, Tan J, Fincham AG. *Biopolymers* 1998;46:225. [PubMed: 9715666]
- (135). Wen HB, Fincham AG, Moradian-Oldak J. *Matrix Biol* 2001;20:387. [PubMed: 11566273]
- (136). Lakshminarayanan R, Fan D, Du C, Moradian-Oldak J. *Biophys. J* 2007;93:3664. [PubMed: 17704165]
- (137). Moradian-Oldak J, Du C, Falini G. *Eur. J. Oral Sci* 2006;114(Suppl 1):289. [PubMed: 16674701]
- (138). Fields S, Song O. *Nature* 1989;340:245. [PubMed: 2547163]
- (139). Moradian-Oldak J, Paine ML, Lei YP, Fincham AG, Snead ML. *J. Struct. Biol* 2000;131:27. [PubMed: 10945967]
- (140). Ignelzi MA, Liu YH, Maxson RE, Snead ML. *Crit. Rev. Oral Biol. Med* 1995;6:181. [PubMed: 8785260]
- (141). Hu CC, Fukae M, Uchida T, Qian Q, Zhang CH, Ryu OH, Tanabe T, Yamakoshi Y, Murakami C, Dohi N, Shimizu M, Simmer JP. *J. Dent. Res* 1997;76:648. [PubMed: 9062558]
- (142). Hu CC, Fukae M, Uchida T, Qian Q, Zhang CH, Ryu OH, Tanabe T, Yamakoshi Y, Murakami C, Dohi N, Shimizu M, Simmer JP. *J. Dent. Res* 1997;76:1720. [PubMed: 9372788]
- (143). Simmer JP, Hu JC. *Connect. Tissue Res* 2002;43:441. [PubMed: 12489196]
- (144). Bartlett JD, Ganss B, Goldberg M, Moradian-Oldak J, Paine ML, Snead ML, Wen X, White SN, Zhou YL. *Curr. Top. Dev. Biol* 2006;74:57. [PubMed: 16860665]
- (145). Fukae M, Tanabe T. *Calcif. Tissue Int* 1987;40:286. [PubMed: 3034388]
- (146). Fukumoto S, Kiba T, Hall B, Iehara N, Nakamura T, Longenecker G, Krebsbach PH, Nanci A, Kulkarni AB, Yamada Y. *J. Cell Biol* 2004;167:973. [PubMed: 15583034]
- (147). Cerny R, Slaby I, Hammarström L, Wurtz T. *J. Bone Miner. Res* 1996;11:883. [PubMed: 8797107]
- (148). Lee SK, Kim SM, Lee YJ, Yamada KM, Yamada Y, Chi JG. *Mol Cells* 2003;15:216. [PubMed: 12803485]
- (149). Fukae M, Tanabe T, Murakami C, Dohi N, Uchida T. *Adv. Dent. Res* 1996;10:111. [PubMed: 9206327]

- (150). Uchida T, Tanabe T, Fukae M, Shimizu M. *Arch. Histol. Cytol* 1991;54:527. [PubMed: 1793666]
- (151). Wang H, Tannukit S, Zhu D, Snead ML, Paine ML. *J. Bone Miner. Res* 2005;20:1032. [PubMed: 15883644]
- (152). Xu TS, Bianco P, Fisher LW, Longenecker G, Smith E, Goldstein S, Bonadio J, Boskey A, Heegaard AM, Sommer B, Satomura K, Dominguez P, Zhao CY, Kulkarni AB, Robey PG, Young MF. *Nat. Genet* 1998;20:78. [PubMed: 9731537]
- (153). Deutsch D, Leiser Y, Shay B, Fermon E, Taylor A, Rosenfeld E, Dafni L, Charuvi K, Cohen Y, Haze A, Fuks A, Mao Z. *Connect. Tissue Res* 2002;43:425. [PubMed: 12489194]
- (154). Paine ML, Deutsch D, Snead ML. *Connect. Tissue Res* 1996;35:157. [PubMed: 9084654]
- (155). Paine CT, Paine ML, Snead ML. *Connect. Tissue Res* 1998;39:257. [PubMed: 11063006]
- (156). Paine ML, Krebsbach PH, Chen LS, Paine CT, Yamada Y, Deutsch D, Snead ML. *J. Dent. Res* 1998;77:496. [PubMed: 9496923]
- (157). Paine CT, Paine ML, Luo W, Okamoto CT, Lyngstadaas SP, Snead ML. *J. Biol. Chem* 2000;275:22284. [PubMed: 10806191]
- (158). Bartlett JD, Simmer JP. *Crit. Rev. Oral. Biol. Med* 1999;10:425. [PubMed: 10634581]
- (159). Caterina JJ, Skobe Z, Shi J, Ding YL, Simmer JP, Birkedal-Hansen H, Bartlett JD. *J. Biol. Chem* 2002;277:49598. [PubMed: 12393861]
- (160). Beniash E, Skobe Z, Bartlett JD. *Eur. J. Oral Sci* 2006;114:24. [PubMed: 16674658]
- (161). Simmer JP, Fukae M, Tanabe T, Yamakoshi Y, Uchida T, Xue J, Margolis HC, Shimizu M, DeHart BC, Hu CC, Bartlett JD. *J. Dent. Res* 1998;77:377. [PubMed: 9465170]
- (162). Tanabe T, Fukae M, Uchida T, Shimizu M. *Calcif. Tissue Int* 1992;51:213. [PubMed: 1422965]
- (163). Iwasaki K, Bajenova E, Somogyi-Ganss E, Miller M, Nguyen V, Nourkeyhani H, Gao Y, Wendel M, Ganss B. *J. Dent. Res* 2005;84:1127. [PubMed: 16304441]
- (164). Trueb B, Taeschler S, Schild C, Lang NP. *Int. J. Mol. Med* 2007;19:49. [PubMed: 17143547]
- (165). Ravindranath HH, Chen LS, Zeichner-David M, Ishima R, Ravindranath RM. *Biochem. Biophys. Res. Commun* 2004;323:1075. [PubMed: 15381109]
- (166). Weiner S. *Crit. Rev. Biochem. Mol* 1986;20:365.
- (167). Moradian-Oldak J, Bouropoulos N, Wang L, Gharakhanian N. *Matrix Biol* 2002;21:197. [PubMed: 11852235]
- (168). Tarasevich BJ, Howard CJ, Larson JL, Snead ML, Simmer JP, Paine M, Shaw WJ. *J. Cryst. Growth* 2007;304:407.
- (169). Aoba T, Fukae M, Tanabe T, Shimizu M, Moreno EC. *Calcif. Tissue Int* 1987;41:281. [PubMed: 2825935]
- (170). Bouropoulos N, Moradian-Oldak J. *J. Dent. Res* 2004;83:278. [PubMed: 15044499]
- (171). Tanabe T, Aoba T, Moreno EC, Fukae M, Shimizu M. *Calcif. Tissue Int* 1990;46:205. [PubMed: 2106381]
- (172). Iijima M, Moriwaki Y, Takagi T, Moradian-Oldak J. *J. Cryst. Growth* 2001;222:615.
- (173). Iijima M, Moriwaki Y, Wen HB, Fincham AG. *J. Dent. Res* 2002;81:69. [PubMed: 11820371]
- (174). Iijima M, Moradian-Oldak J. *Calcif. Tissue Int* 2004;74:522. [PubMed: 15354860]
- (175). Beniash E, Simmer JP, Margolis HC. *J. Struct. Biol* 2005;149:182. [PubMed: 15681234]
- (176). Wang L, Guan X, Du C, Moradian-Oldak J, Nancollas GH. *J. Phys. Chem. C* 2007;111:6398.
- (177). Mankin HJ, Gebhardt MC, Jennings LC, Springfield DS, Tomford WW. *Clin. Orthop. Relat. R* 1996:86.
- (178). Buck BE, Malinin TI, Brown MD. *Clin. Orthop. Relat. R* 1989:129.
- (179). Mankin HJ, Hornicek FJ, Raskin KA. *Clin. Orthop. Relat. R* 2005:210.
- (180). Butler D. *Nature* 1998;391:320. [PubMed: 9450734]
- (181). Senn N. *Am. J. Med. Sci* 1889;98:219.
- (182). Urist MR. *Science* 1965;150:893. [PubMed: 5319761]
- (183). Mulliken JB, Glowacki J, Kaban LB, Folkman J, Murray JE. *Ann. Surg* 1981;194:366. [PubMed: 7023397]
- (184). Kubler N, Michel C, Zoller J, Bill J, Muhling J, Reuther J. *J. Cranio. Maxill. Surg* 1995;23:337.

- (185). White AP, Vaccaro AR, Hall JA, Whang PG, Friel BC, McKee MD. *Int. Orthop* 2007;31:735. [PubMed: 17962946]
- (186). Nakashima M, Reddi AH. *Nat. Biotechnol* 2003;21:1025. [PubMed: 12949568]
- (187). Kirker-Head CA. *Adv. Drug Delivery Rev* 2000;43:65.
- (188). Thelen S, Barthelat F, Brinson LC. *J. Biomed. Mater. Res. A* 2004;69A:601. [PubMed: 15162401]
- (189). Spoerke ED, Murray NGD, Li H, Brinson LC, Dunand DC, Stupp SI. *J. Biomed. Mater. Res. A* 2008;84A:402. [PubMed: 17618479]
- (190). LeGeros RZ. *Clin. Orthop. Relat. R* 2002:81.
- (191). Karageorgiou V, Kaplan D. *Biomaterials* 2005;26:5474. [PubMed: 15860204]
- (192). Bonfield W, Grynblas MD, Tully AE, Bowman J, Abram J. *Biomaterials* 1981;2:185. [PubMed: 6268209]
- (193). Roeder RK, Converse GL, Kane RJ, Yue WM. *JOM* 2008;60:38.
- (194). Rezwani K, Chen QZ, Blaker JJ, Boccaccini AR. *Biomaterials* 2006;27:3413. [PubMed: 16504284]
- (195). Mano JF, Sousa RA, Boesel LF, Neves NM, Reis RL. *Compos. Sci. Technol* 2004;64:789.
- (196). Neo M, Nakamura T, Ohtsuki C, Kokubo T, Yamamuro T. *J. Biomed. Mater. Res* 1993;27:999. [PubMed: 8408128]
- (197). Neo M, Kotani S, Nakamura T, Yamamuro T, Ohtsuki C, Kokubo T, Bando Y. *J. Biomed. Mater. Res* 1992;26:1419. [PubMed: 1447227]
- (198). Kokubo T. *Biomaterials* 1991;12:155. [PubMed: 1878450]
- (199). Kokubo T, Takadama H. *Biomaterials* 2006;27:2907. [PubMed: 16448693]
- (200). Ohtsuki C, Kushitani H, Kokubo T, Kotani S, Yamamuro T. *J. Biomed. Mater. Res* 1991;25:1363. [PubMed: 1797808]
- (201). Heath CA. *Trends Biotechnol* 2000;18:17. [PubMed: 10631775]
- (202). Pittenger MF, Mackay AM, Beck SC, Jaiswal RK, Douglas R, Mosca JD, Moorman MA, Simonetti DW, Craig S, Marshak DR. *Science* 1999;284:143. [PubMed: 10102814]
- (203). Li WJ, Tuli R, Huang XX, Laquerriere P, Tuan RS. *Biomaterials* 2005;26:5158. [PubMed: 15792543]
- (204). Buttery LD, Bourne S, Xynos JD, Wood H, Hughes FJ, Hughes SP, Episkopou V, Polak JM. *Tissue Eng* 2001;7:89. [PubMed: 11224927]
- (205). Duplomb L, Dagouassat M, Jourdon P, Heymann D. *Stem Cells* 2007;25:544. [PubMed: 17095705]
- (206). Engler AJ, Sen S, Sweeney HL, Discher DE. *Cell* 2006;126:677. [PubMed: 16923388]
- (207). Bancroft GN, Sikavitsast VI, van den Dolder J, Sheffield TL, Ambrose CG, Jansen JA, Mikos AG. *Proc. Natl. Acad. Sci. U.S.A* 2002;99:12600. [PubMed: 12242339]
- (208). Albrektsson T, Johansson C. *Eur. Spine J* 2001;10(Suppl 2):S96. [PubMed: 11716023]
- (209). Capriotti LA, Beebe TP, Schneider JP. *J. Am. Chem. Soc* 2007;129:5281. [PubMed: 17397165]
- (210). Landis WJ, Silver FH, Freeman JW. *J. Mater. Chem* 2006;16:1495.
- (211). Glimcher MJ. *Phil. Trans. R. Soc. London, Ser. B* 1984;304:479. [PubMed: 6142489]
- (212). Zhang W, Liao SS, Cui FZ. *Chem. Mater* 2003;15:3221.
- (213). Chang MC, Ko CC, Douglas WH. *Biomaterials* 2003;24:2853. [PubMed: 12742723]
- (214). Bigi A, Boanini E, Panzavolta S, Roveri N. *Biomacromolecules* 2000;1:752. [PubMed: 11710207]
- (215). Serro AP, Fernandes AC, Saramago B, Lima J, Barbosa MA. *Biomaterials* 1997;18:963. [PubMed: 9212191]
- (216). Lima J, Sousa SR, Ferreira A, Barbosa MA. *J. Biomed. Mater. Res* 2001;55:45. [PubMed: 11426397]
- (217). Liu Y, Hunziker EB, Randall NX, de Groot K, Layrolle P. *Biomaterials* 2003;24:65. [PubMed: 12417179]
- (218). Marques P, Serro AP, Saramago BJ, Fernandes AC, Magalhaes MCF, Correia RN. *Biomaterials* 2003;24:451. [PubMed: 12423600]
- (219). Daculsi G, Pilet P, Cottrel M, Guicheux G. *J. Biomed. Mater. Res* 1999;47:228. [PubMed: 10449634]

- (220). Areva S, Peltola T, Sailynoja E, Laajalehto K, Linden M, Rosenholm JB. *Chem. Mater* 2002;14:1614.
- (221). Yokogawa Y, Reyes JP, Mucalo MR, Toriyama M, Kawamoto Y, Suzuki T, Nishizawa K, Nagata F, Kamayama T. *J. Mater. Sci.: Mater. Med* 1997;8:407. [PubMed: 15348722]
- (222). Tuzlakoglu K, Alves CM, Mano JF, Reis RL. *Macromol. Biosci* 2004;4:811. [PubMed: 15468275]
- (223). Tuzlakoglu K, Reis RL. *J. Mater. Sci.: Mater. Med* 2007;18:1279. [PubMed: 17431748]
- (224). Leonor IB, Baran ET, Kawashita M, Reis RL, Kokubo T, Nakamura T. *Acta Biomater* 2008;4:1349. [PubMed: 18400572]
- (225). Zhao F, Yin Y, Lu WW, Leong JC, Zhang W, Zhang J, Zhang M, Yao K. *Biomaterials* 2002;23:3227. [PubMed: 12102194]
- (226). Embery G, Hall R, Waddington R, Septier D, Goldberg M. *Crit. Rev. Oral Biol. Med* 2001;12:331. [PubMed: 11603505]
- (227). Lindahl U, Hook M. *Annu. Rev. Biochem* 1978;47:385. [PubMed: 354500]
- (228). Jiang H, Liu XY, Zhang G, Li Y. *J. Biol. Chem* 2005;280:42061. [PubMed: 16251185]
- (229). Liu XY, Lim SW. *J. Am. Chem. Soc* 2003;125:888. [PubMed: 12537485]
- (230). Mendes SC, Reis RL, Bovell YP, Cunha AM, van Blitterswijk CA, de Bruijn JD. *Biomaterials* 2001;22:2057. [PubMed: 11426886]
- (231). Gomes ME, Reis RL, Cunha AM, Blitterswijk CA, de Bruijn JD. *Biomaterials* 2001;22:1911. [PubMed: 11396897]
- (232). Marques AP, Reis RL, Hunt JA. *Biomaterials* 2002;23:1471. [PubMed: 11829443]
- (233). Pach L, Duncan S, Roy R, Komarneni S. *J. Mater. Sci* 1996;31:6565.
- (234). Gomes ME, Sikavitsas VI, Behravesch E, Reis RL, Mikos AG. *J. Biomed. Mater. Res. A* 2003;67:87. [PubMed: 14517865]
- (235). Chen GQ, Wu Q. *Biomaterials* 2005;26:6565. [PubMed: 15946738]
- (236). Doyle C, Tanner ET, Bonfield W. *Biomaterials* 1991;12:841. [PubMed: 1764555]
- (237). Estroff LA, Hamilton AD. *Chem. Rev* 2004;104:1201. [PubMed: 15008620]
- (238). Filmon R, Grizon F, Basle MF, Chappard D. *Biomaterials* 2002;23:3053. [PubMed: 12069348]
- (239). Dalas E, Kallitsis JK, Koutsoukos PG. *Langmuir* 1991;7:1822.
- (240). Doğan O, Öner M. *Langmuir* 2006;22:9671. [PubMed: 17073495]
- (241). Zhang RY, Ma PX. *J. Biomed. Mater. Res* 1999;45:285. [PubMed: 10321700]
- (242). Murphy WL, Kohn DH, Mooney DJ. *J. Biomed. Mater. Res* 2000;50:50. [PubMed: 10644963]
- (243). Kellomäki M, Niiranen H, Puumanen K, Ashammakhi N, Waris T, Törmälä P. *Biomaterials* 2000;21:2495. [PubMed: 11071599]
- (244). Oyane A, Uchida M, Choong C, Triffitt J, Jones J, Ito A. *Biomaterials* 2005;26:2407. [PubMed: 15585244]
- (245). Murphy WL, Mooney DJ. *J. Am. Chem. Soc* 2002;124:1910. [PubMed: 11866603]
- (246). Chen JL, Chu B, Hsiao BS. *J. Biomed. Mater. Res. A* 2006;79A:307. [PubMed: 16817203]
- (247). Li Q, Wang J, Shahani S, Sun DDN, Sharma B, Elisseeff JH, Leong KW. *Biomaterials* 2006;27:1027. [PubMed: 16125222]
- (248). Wang DA, Williams CG, Yang F, Cher N, Lee H, Elisseeff JH. *Tissue Eng* 2005;11:201. [PubMed: 15738675]
- (249). Wang DA, Williams CG, Li QA, Sharma B, Elisseeff JH. *Biomaterials* 2003;24:3969. [PubMed: 12834592]
- (250). Song J, Saiz E, Bertozzi CR. *J. Am. Chem. Soc* 2003;125:1236. [PubMed: 12553825]
- (251). Song J, Malathong V, Bertozzi CR. *J. Am. Chem. Soc* 2005;127:3366. [PubMed: 15755154]
- (252). Kweon H, Yoo MK, Park IK, Kim TH, Lee HC, Lee HS, Oh JS, Akaike T, Cho CS. *Biomaterials* 2003;24:801. [PubMed: 12485798]
- (253). Verma D, Katti K, Katti D. *J. Biomed. Mater. Res. A* 2006;77:59. [PubMed: 16355408]
- (254). Verma D, Katti K, Katti D. *J. Biomed. Mater. Res. A* 2006;78:772. [PubMed: 16739180]
- (255). Oyane A, Uchida M, Yokoyama Y, Choong C, Triffitt J, Ito A. *J. Biomed. Mater. Res. A* 2005;75:138. [PubMed: 16044403]

- (256). Rhee SH. *Biomaterials* 2004;25:1167. [PubMed: 14643590]
- (257). Chen H, Banaszak Holl M, Orr BG, Majoros I, Clarkson BH. *J. Dent. Res* 2003;82:443. [PubMed: 12766196]
- (258). Chen H, Clarkson BH, Sun K, Mansfield JF. *J. Colloid Interface Sci* 2005;288:97. [PubMed: 15927567]
- (259). Boduch-Lee KA, Chapman T, Petricca SE, Marra KG, Kumta P. *Macromolecules* 2004;37:8959.
- (260). Donners J, Nolte RJM, Sommerdijk N. *Adv. Mater* 2003;15:313.
- (261). Schachschal S, Pich A, Adler HJ. *Langmuir* 2008;24:5129. [PubMed: 18363417]
- (262). Olszta MJ, Douglas EP, Gower LB. *Calcif. Tissue Int* 2003;72:583. [PubMed: 12616327]
- (263). Olszta MJ, Odom DJ, Douglas EP, Gower LB. *Connect. Tissue Res* 2003;44:326. [PubMed: 12952217]
- (264). Bradt JH, Mertig M, Teresiak A, Pompe W. *Chem. Mater* 1999;10:2694.
- (265). Yu SH, Colfen H. *J. Mater. Chem* 2004;14:2124.
- (266). Antonietti M, Breulmann M, Goltner CG, Colfen H, Wong KKW, Walsh D, Mann S. *Chem. Eur. J* 1998;4:2493.
- (267). Stupp SI, Ciegler GW. *J. Biomed. Mater. Res* 1992;26:169. [PubMed: 1569112]
- (268). Stupp SI, Mejicano GC, Hanson JA. *J. Biomed. Mater. Res* 1993;27:289. [PubMed: 8360199]
- (269). Stupp SI, Hanson JA, Eurell JA, Ciegler GW, Johnson A. *J. Biomed. Mater. Res* 1993;27:301. [PubMed: 8360200]
- (270). Müller-Mai CM, Stupp SI, Voigt C, Gross U. *J. Biomed. Mater. Res* 1995;29:9. [PubMed: 7713964]
- (271). Hwang JJ, Jaeger K, Hancock J, Stupp SI. *J. Biomed. Mater. Res* 1999;47:504. [PubMed: 10497285]
- (272). Shabalovskaya SA. *Bio-Med. Mater. Eng* 2002;12:69.
- (273). Habibovic P, Barrere F, van Blitterswijk CA, de Groot K, Layrolle P. *J. Am. Ceram. Soc* 2002;85:517.
- (274). Kim HM, Miyaji F, Kokubo T, Nakamura T. *J. Mater. Sci.: Mater. Med* 1997;8:341. [PubMed: 15348733]
- (275). Nishiguchi S, Kato H, Neo M, Oka M, Kim HM, Kokubo T, Nakamura T. *J. Biomed. Mater. Res* 2001;54:198. [PubMed: 11093179]
- (276). Li PJ, Ohtsuki C, Kokubo T, Nakanishi K, Soga N, Degroot K. *J. Biomed. Mater. Res* 1994;28:7. [PubMed: 8126031]
- (277). Nather, A.; Aziz, S. *Bone Grafts and Bone Substitutes: Basic Science and Clinical Applications*. Nather, A., editor. World Scientific; Hackensack, NJ: 2005.
- (278). Spoerke ED, Stupp SI. *J. Biomed. Mater. Res. A* 2003;67:960. [PubMed: 14613245]
- (279). Storrie H, Stupp SI. *Biomaterials* 2005;26:5492. [PubMed: 15860205]
- (280). Spoerke ED, Stupp SI. *Biomaterials* 2005;26:5120. [PubMed: 15792538]
- (281). Spoerke ED, Murray NG, Li H, Brinson LC, Dunand DC, Stupp SI. *Acta Biomater* 2005;1:523. [PubMed: 16701832]
- (282). Hartgerink JD, Zubarev ER, Stupp SI. *Curr. Opin. Solid State Mater. Sci* 2001;5:355.
- (283). Palmer LC, Velichko YS, de la Cruz MO, Stupp SI. *Phil. Trans. R. Soc. A* 2007;365:1417. [PubMed: 17428769]
- (284). Zubarev ER, Pralle MU, Sone ED, Stupp SI. *Adv. Mater* 2002;14:198.
- (285). Hartgerink JD, Beniash E, Stupp SI. *Proc. Natl. Acad. Sci. U.S.A* 2002;99:5133. [PubMed: 11929981]
- (286). Behanna HA, Donners JJM, Gordon AC, Stupp SI. *J. Am. Chem. Soc* 2005;127:1193. [PubMed: 15669858]
- (287). Jiang HZ, Guler MO, Stupp SI. *Soft Matter* 2007;3:454.
- (288). George A, Bannon L, Sabsay B, Dillon JW, Malone J, Veis A, Jenkins NA, Gilbert DJ, Copeland NG. *J. Biol. Chem* 1996;271:32869. [PubMed: 8955126]
- (289). Spoerke ED, Anthony SG, Stupp SI. *Adv. Mater.* in press

- (290). Huang Z, Sargeant T, Hulvat JF, Mata A, P. Bringas J, Koh C-Y, Stupp SI, Snead ML. *J. Bone Miner. Res.* 2008;DOI: 10.1359/jbmr.080705
- (291). Jun HW, Yuwono V, Paramonov SE, Hartgerink JD. *Adv. Mater* 2005;17:2612.
- (292). Galler KM, Cavender A, Yuwono V, Dong H, Shi S, Schmalz G, Hartgerink JD, D'Souza RN. *Tissue Eng. A* 2008;14;DOI: 10.1089/ten.tea.2007.0413
- (293). Sargeant TD, Rao MS, Koh CY, Stupp SI. *Biomaterials* 2008;29:1085. [PubMed: 18083225]
- (294). Sargeant TD, Guler MO, Oppenheimer SM, Mata A, Satcher RL, Dunand DC, Stupp SI. *Biomaterials* 2008;29:161. [PubMed: 17936353]
- (295). Sargeant TD, Oppenheimer SM, Dunand DC, Stupp SI. *J. Tissue Eng. Regen. Med.* 2008;DOI: 10.1002/term.117
- (296). Lee JY, Choo JE, Choi YS, Park JB, Min DS, Lee SJ, Rhyu HK, Jo IH, Chung CP, Park YJ. *Biomaterials* 2007;28:4257. [PubMed: 17604098]
- (297). Kirkham J, Firth A, Vernals D, Boden N, Robinson C, Shore RC, Brookes SJ, Aggeli A. *J. Dent. Res* 2007;86:426. [PubMed: 17452562]
- (298). Yamagishi K, Onuma K, Suzuki T, Okada F, Tagami J, Otsuki M, Senawangse P. *Nature* 2005;433:819. [PubMed: 15729330]
- (299). Finean JB, Engstrom A. *Biochim. Biophys. Acta* 1957;23:202. [PubMed: 13412700]
- (300). Wachtel E, Weiner S. *J. Bone Miner. Res* 1994;9:1651. [PubMed: 7817813]
- (301). Weiner S, Price PA. *Calcif. Tissue Int* 1986;39:365. [PubMed: 3026591]
- (302). Gamble, JE. *Chemical Anatomy, Physiology and Pathology of Extracellular Fluid.* Harvard University Press; Cambridge: 1967.
- (303). Kokubo T, Kushitani H, Sakka S, Kitsugi T, Yamamuro T. *J. Biomed. Mater. Res* 1990;24:721. [PubMed: 2361964]
- (304). Oyane A, Kim HM, Furuya T, Kokubo T, Miyazaki T, Nakamura T. *J. Biomed. Mater. Res. A* 2003;65A:188. [PubMed: 12734811]
- (305). Takadama H, Hashimoto M, Mizuno M, Kokubo T. *Phosphorus Res. Bull* 2004;17:119.

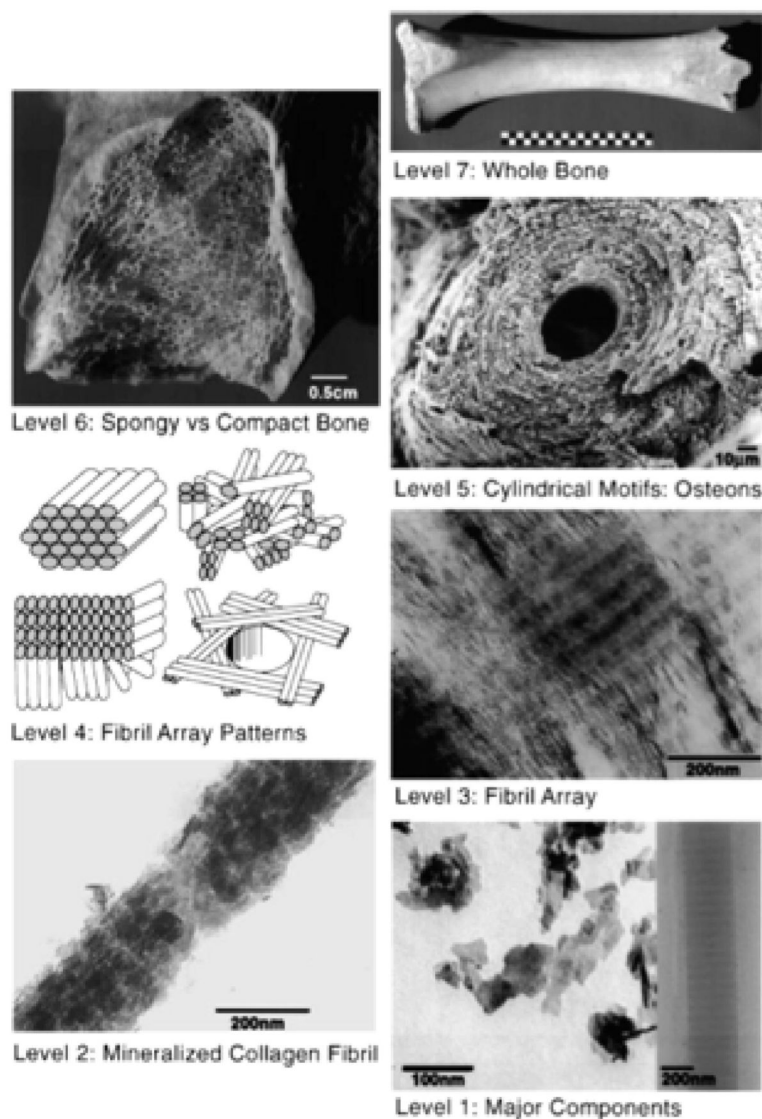


Figure 1. Seven hierarchical levels of organization of the bone family of materials as proposed by Weiner and Wagner. Reprinted with permission from *Ann. Rev. Mater. Sci.*, ref ²³. Copyright 1998 Annual Reviews (<http://www.annualreviews.org>).

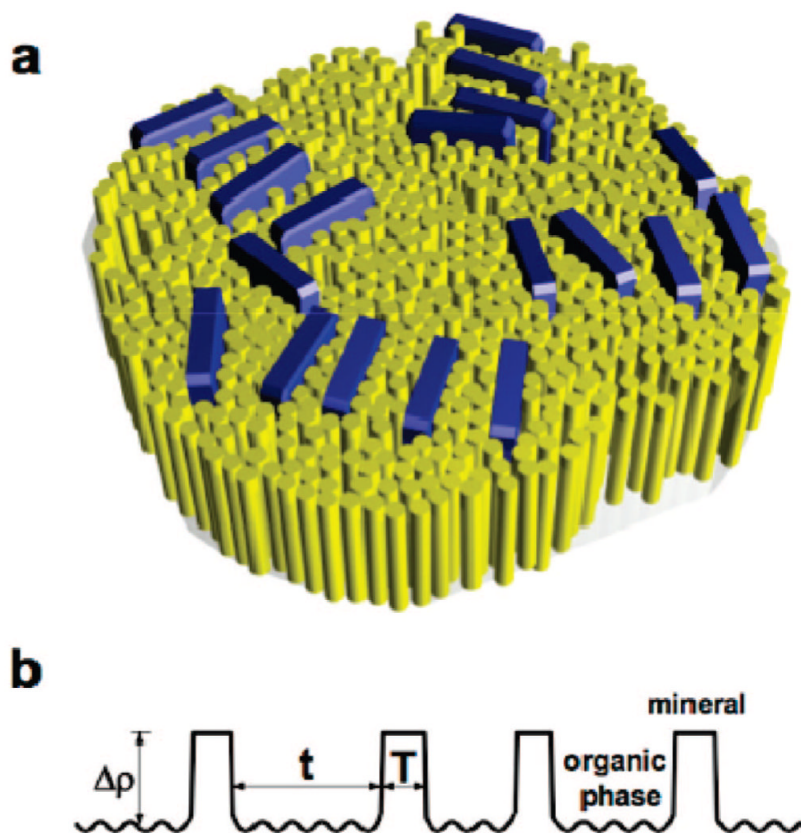


Figure 2.

(a) Schematic illustration of the lateral packing of mineral crystals in the collagen matrix. Thin apatite platelets are aligned nearly parallel within the stacks. The crystals are typically about 2 nm thick, 20 nm wide, and 30 nm high. (b) Map of the electron density projected onto the normal of a stack of mineral platelets. T is the thickness of individual crystals, and t is the thickness of organic layers between the neighboring crystals. The density of the mineral phase is assumed to be uniform, but there are small density fluctuations in the organic phase that are much smaller than the density contrast ($\Delta\rho$) between the mineral and the organic phases. Reprinted with permission from *Biophys. J.*, ref ²⁹. Copyright 2008 Biophysical Society.

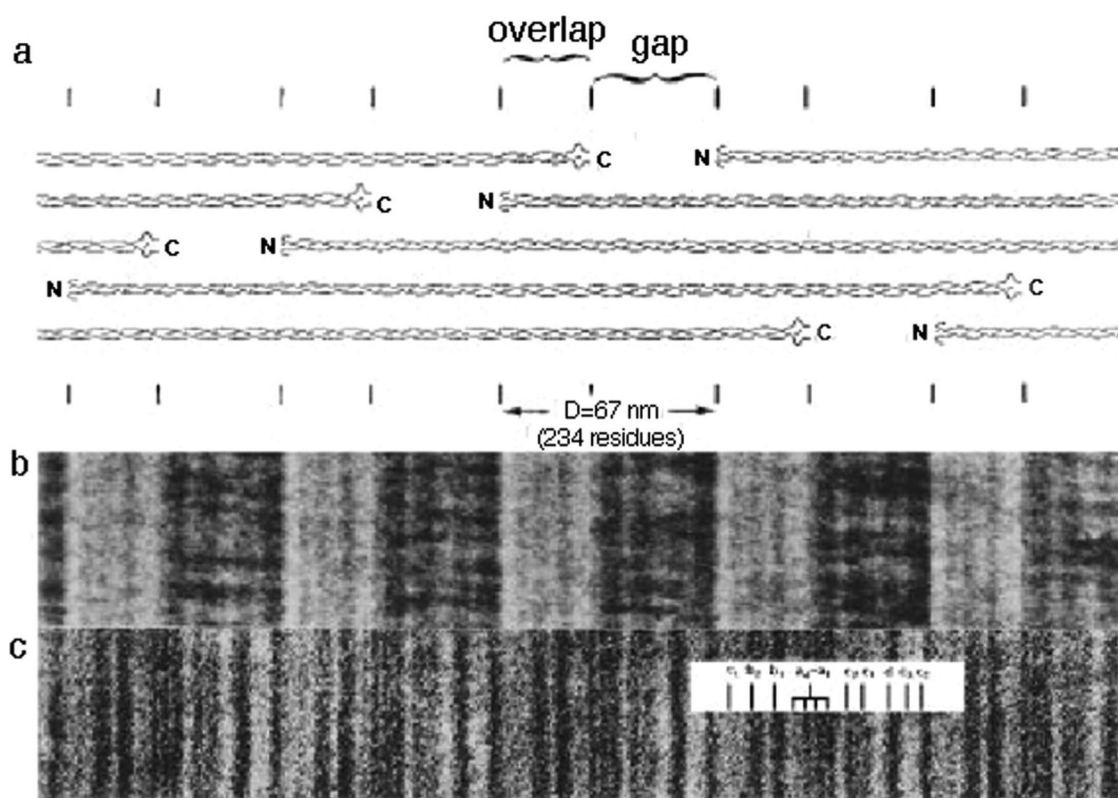


Figure 3.

Axial structure of D-periodic collagen fibrils. (a) Schematic representation of the axial packing arrangement of triple-helical collagen molecules in a fibril, as derived from analysis of the negative (b) and positive (c) staining patterns. (b) Collagen fibril negatively stained with sodium phosphotungstic acid (1%, pH 7). The fibril is from a gel of fibrils reconstituted from acetic acid-soluble calfskin collagen. The repeating broad dark and light zones are produced by preferential stain penetration into regions of lowest packing (the gap regions). (c) Similar fibril positively stained with phosphotungstic acid (1%, pH 3.4) and then uranyl acetate (1%, pH 4.2). The darkly staining transverse bands are the result of uptake of electron dense heavy-metal ions from the staining solutions onto charged residue side groups of collagen. Reprinted with permission from *Biochem. J.*, ref ³⁴. Copyright 1996 Portland Press.

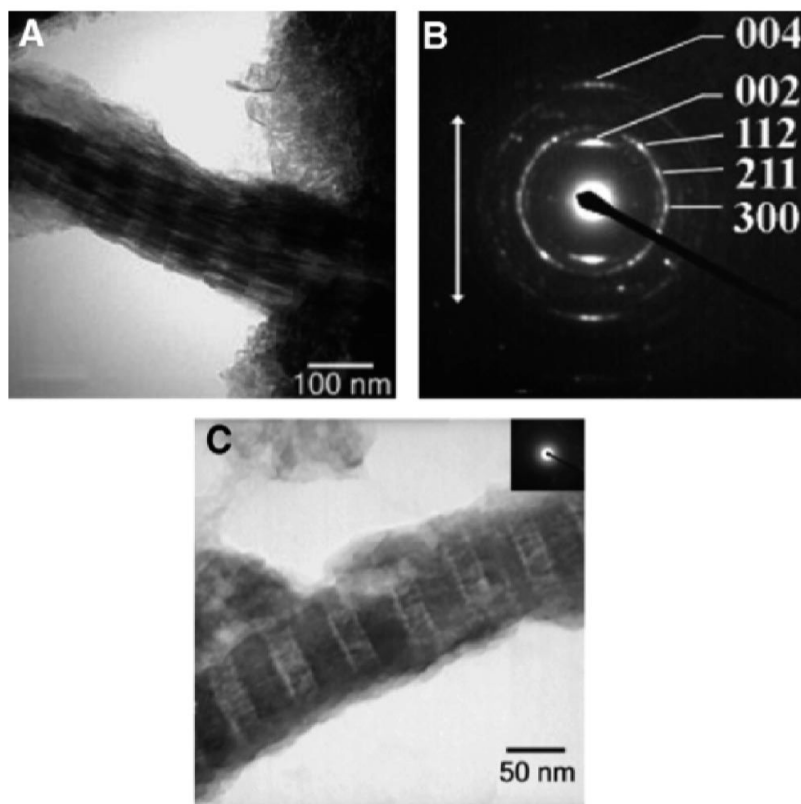


Figure 4.

Electron micrographs of equine cortical bone. (A) TEM brightfield image demonstrating intrafibrillar mineralization of type I collagen fibrils in natural bone. The native banding pattern of type I collagen is due to the infiltration of electron dense mineral, and staining was therefore unnecessary. The striated appearance results from HA platelets aligned parallel to the long axis of the collagen. Scale bar = 100 nm. (B) Selected area electron diffraction (SAED) of a single fibril of crushed equine bone. The arcing of the (002) and (004) planes, which are parallel to the long axis of the collagen fibrils (white arrow), is characteristic of bone. The (112), (211), and (300) planes, indexed using d -spacings and angles relative to the (002) plane, form three arcs that nearly overlap, combining into what appears to be a ring; however, there is a gap in the ring just behind the (002) arc because it is not really a powder ring but three distinct sets of planes that have very close d -spacings. The appearance of these three planes simultaneously indicates that there is more than one orientation of the HA platelets in the a-b plane. (C) TEM brightfield image of an isolated collagen fibril showing the banding pattern of that is characteristic of type I collagen. The SAED pattern (inset) of this fibril demonstrates that the fibril does not diffract, suggesting that the electron dense phase, which is the only thing providing contrast (the sample was not stained), is amorphous CaP. Scale bar = 50 nm. Reprinted with permission from *Mater. Sci. Eng., R*, ref¹². Copyright 2007 Elsevier.

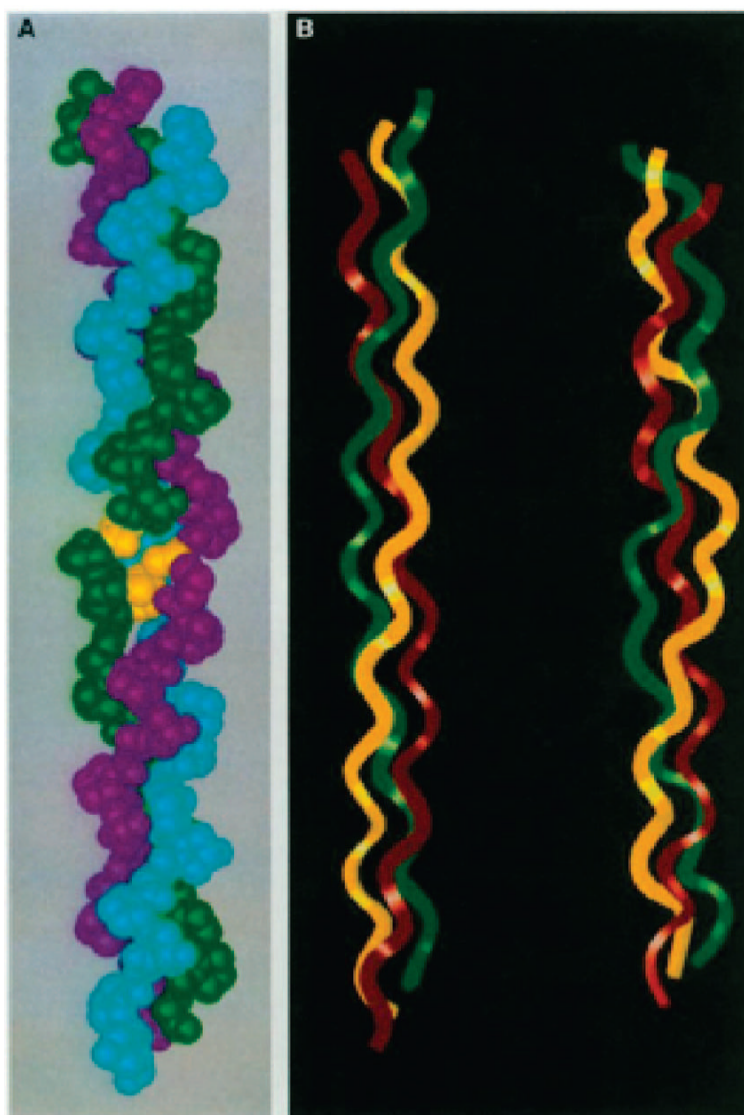


Figure 5. (a) Space-filling model of Gly→Ala collagen crystal structure and (b) ribbon diagram comparison of native collagen 10₇ helix (left) and the Gly→Ala peptide (right). Reprinted with permission from *Science* (<http://www.sciencemag.org>), ref ³⁶. Copyright 1994 AAAS.

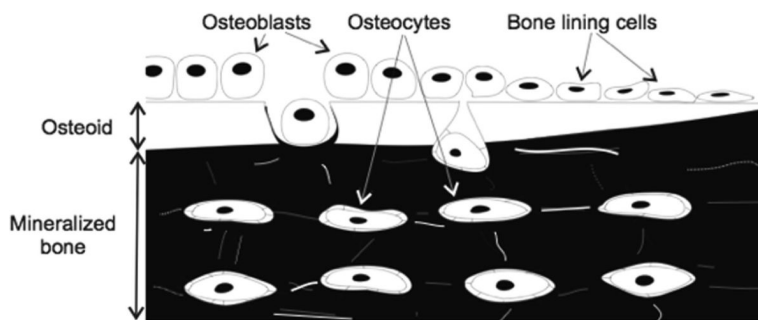


Figure 6. Schematic of the topographic relationship among bone cells. The osteoblasts are located on the lining layer of bone surface, actively producing uncalcified matrix (osteoid tissue). Osteocytes are the most mature or terminally differentiated cells of the osteoblast lineage and are embedded in the bone matrix. Reprinted with permission from *Acta Biochim. Pol.*, ref ⁵⁹. Copyright 2003 *Acta Biochim. Pol.*

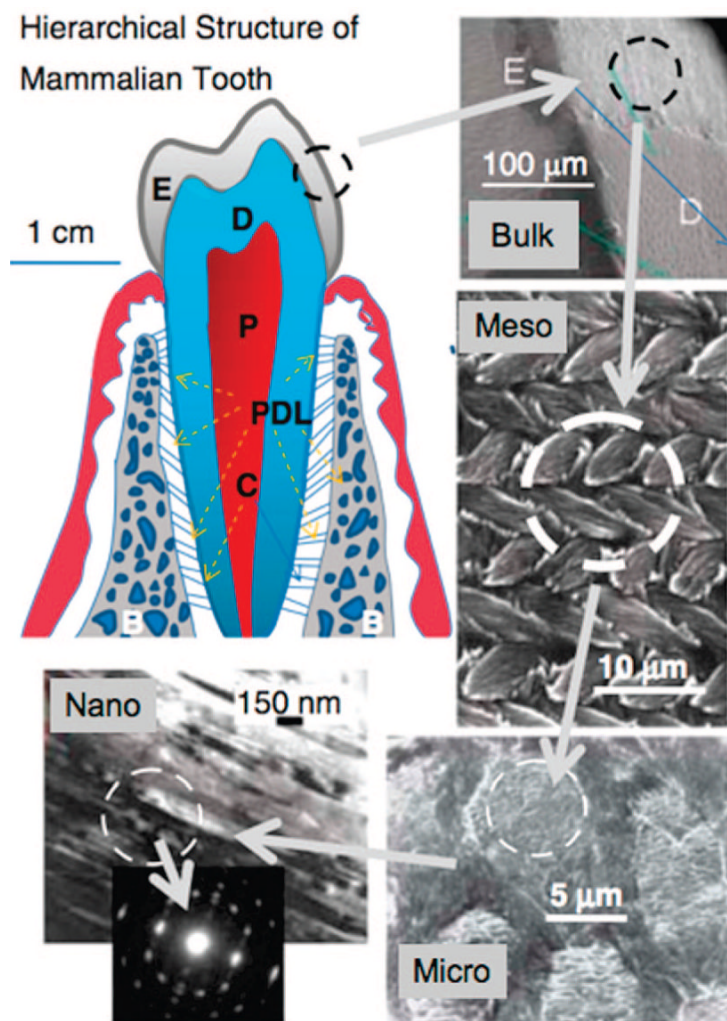


Figure 7. Hierarchical architecture of mammalian enamel. Enamel (E) is the outermost layer at the crown of the tooth and resides above the dentin (D). The pulp (P) contains nerves and blood vessels, while the cementum (C) is the outermost layer of mineralized tissue surrounding the root of the tooth allowing the tooth to be anchored to the jawbone through the periodontal ligament (PDL). The bulk image depicts the enamel organ, the transition across the dentino-enamel junction, and the dentin below. On the mesoscale level, prismatic enamel consisting of weaving of rods (or prisms) that range from 3 to 5 μm in diameter can be visualized. Upon further magnification, the micrometer scale shows the composition of a single rod. The nanometer scale reveals a highly organized array of individual HA crystallites (approximately 30 nm thick, 60 nm wide, and several millimeters in length), which are preferentially aligned along the *c*-axis. Adapted with permission from *MRS Bull.*, ref ⁸⁴. Copyright 2008 Materials Research Society (www.mrs.org/bulletin).

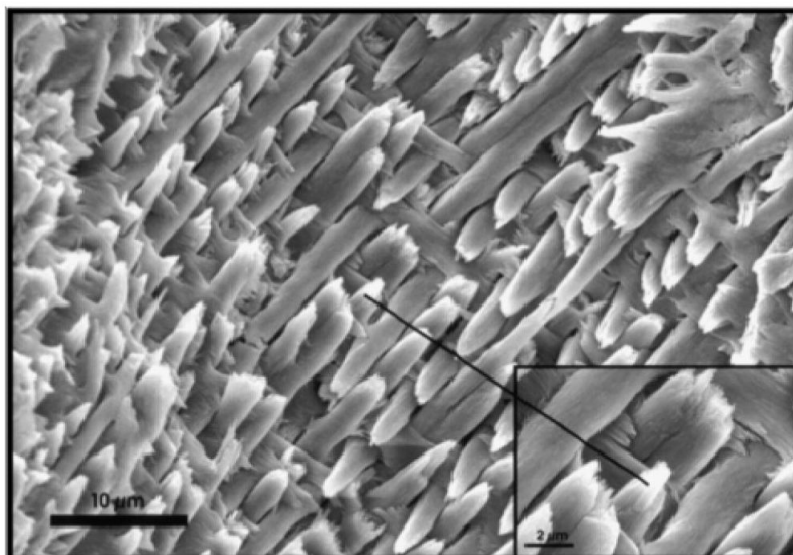


Figure 8. Organization of prismatic dental enamel on the mesoscale showing interweaving crystallite bundles termed as prisms or rods. This scanning electron micrograph shows an acid-etched ground section of mature mouse incisal dental enamel. Reprinted with permission from *J. Struct. Biol.*, ref ¹¹⁶. Copyright 1999 Elsevier.

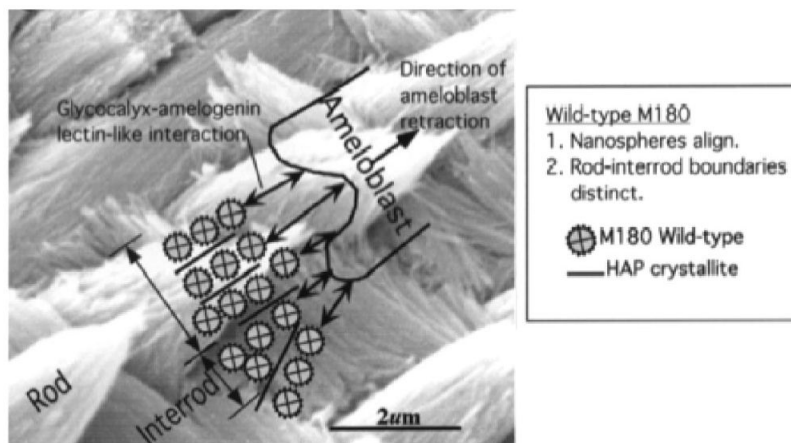


Figure 9. Organization of prismatic dental enamel on the mesoscale showing interweaving crystallite bundles termed as prisms or rods. This scanning electron micrograph shows an acid-etched and ground section of mature mouse incisal dental enamel. Reprinted with permission from *J. Struct. Biol.*, ref ¹⁵⁷. Copyright 1999 Elsevier.

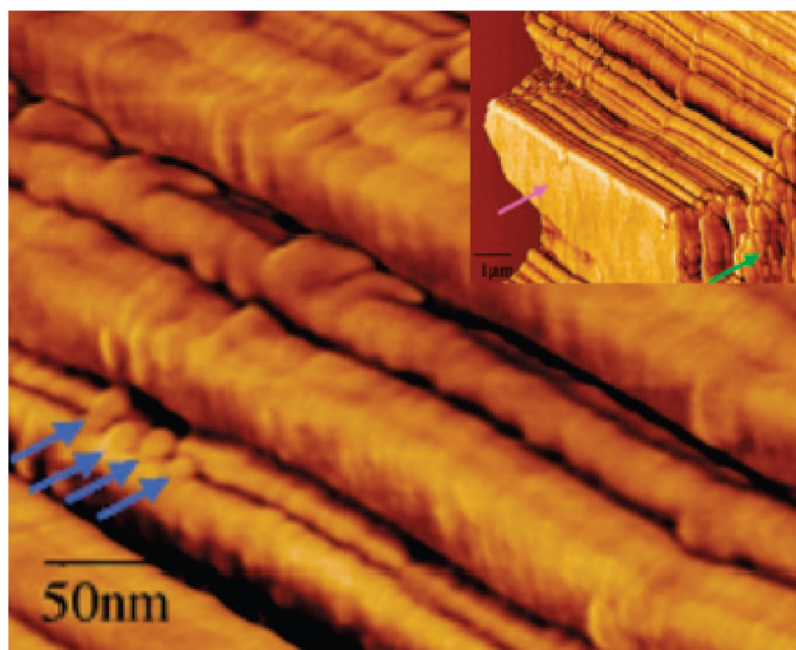


Figure 10. Amelogenin nanospheres aligned in a “chain” of porcine enamel aligned along the side of enamel crystallite imaged via AFM. The purple arrow indicates the 100 face of enamel, the green arrow indicates organic, and the blue arrows indicate the nanospheres. Reprinted with permission from *Matrix Biol.*, ref ¹³⁵. Copyright 2001 Elsevier.

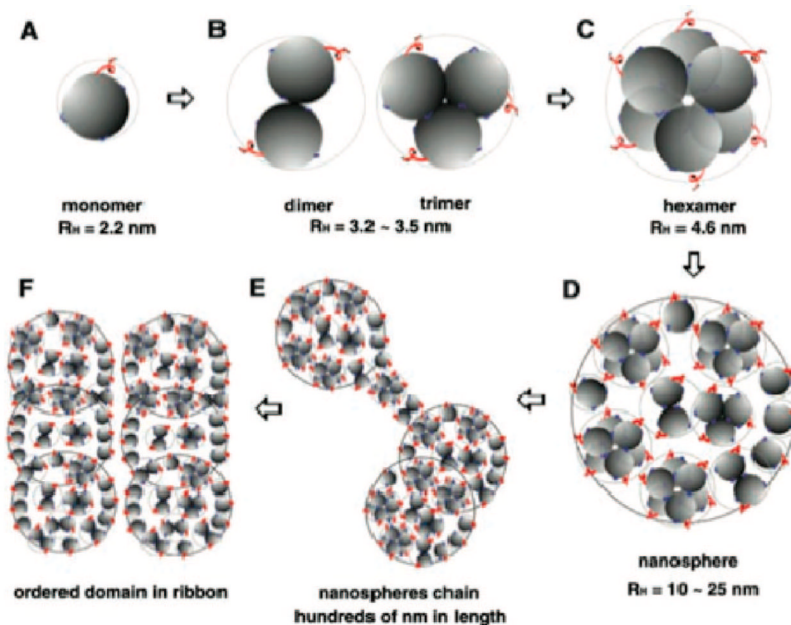


Figure 11.

Schematic model of amelogenin self-assembly based on DLS analysis, TEM, SEM, and AFM observations. (A) The amelogenin molecule folds into a globular form that preserves the bipolar nature derived from the protein's primary structure. The hydrophilic C-terminal (-Thr-Lys-Arg-Glu-Glu-Val-Asp) "tail" (red thread) is flexible and exposed on the surface of otherwise hydrophobic molecule. (B and C) Hydrophobic interactions drive oligomerization of the amelogenin into higher order aggregates. The apparent radii for the ideal hard sphere type of oligomers are calculated to be 3.5 nm for a dimer or a trimer and 4.2 nm for a hexamer. (D) Nanosphere structures form by further association of the monomers and oligomers. (E) The nanospheres can then assemble linear chains of 10-15 nanospheres. In water, this process was facilitated by increasing amelogenin concentration or adding a hydrophilic ingredient such as PEG. (F) The bipolar nature of the amelogenin can facilitate the formation and/or the reorganization of the chain structures and eventually to a ribbon structure. Reprinted with permission from *Science* (<http://www.sciencemag.org>), ref ¹³³. Copyright 2005 AAAS.

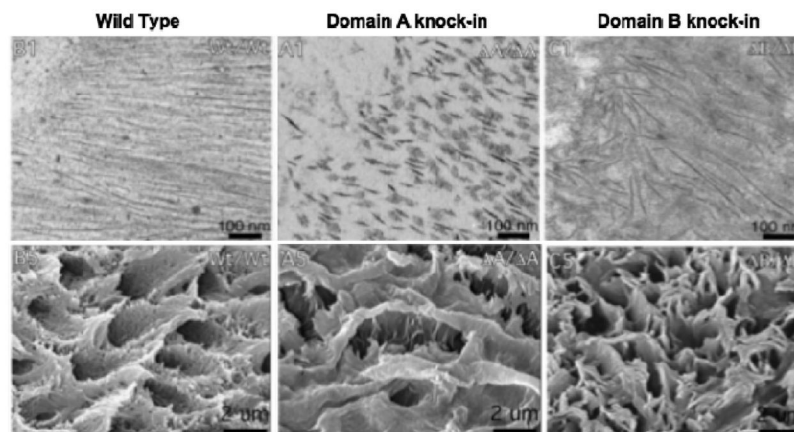


Figure 12.

Row 1: TEM images of new enamel crystallites of wild-type, knock-in self-assembly Domain A knock-in and knock-in self-assembly Domain B knock-in mice. Shorter crystallites can be seen with knock-in A and disruption of the enamel pattern due to collapse of amelogenin nanospheres can be seen in the knock-in B. Row 2: Magnified SEM images of resulting crystallites of wild-type, knock-in A, and knock-in B. Knock-in A exhibits short and enlarged crystallites, while knock-in B exhibits numerous but smaller crystallites as compared to wild-type. Reprinted with permission from *J. Biol. Chem.*, ref⁹⁶. Copyright 2006 American Society for Biochemistry and Molecular Biology.

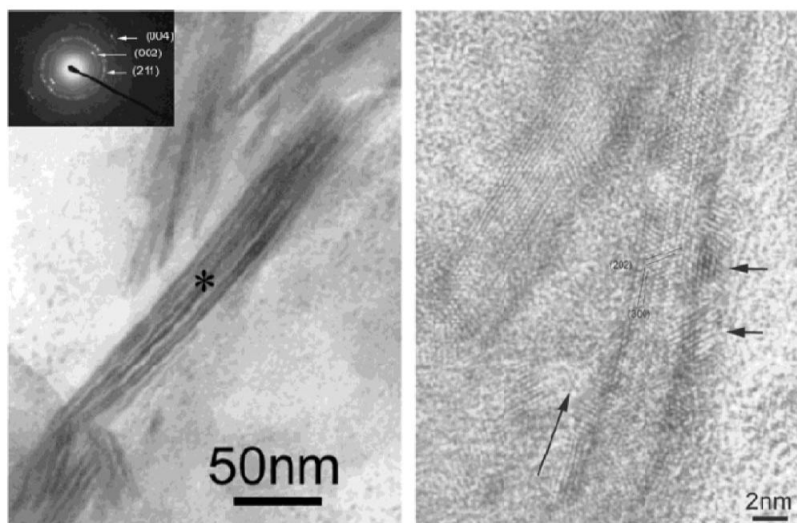


Figure 13.

(a) High magnification of the mineralized collagen fibrils. The insert is the selected area electron diffraction pattern of the mineralized collagen fibrils. The asterisk is the center of the area, and the diameter of the area is about 200 nm. (b) HR-TEM image of mineralized collagen fibrils. The long arrow indicates the longitude direction of collagen fibril. Two short arrows indicate two HA nanocrystals. Reprinted with permission from ref ²¹². Copyright 2003 American Chemical Society.

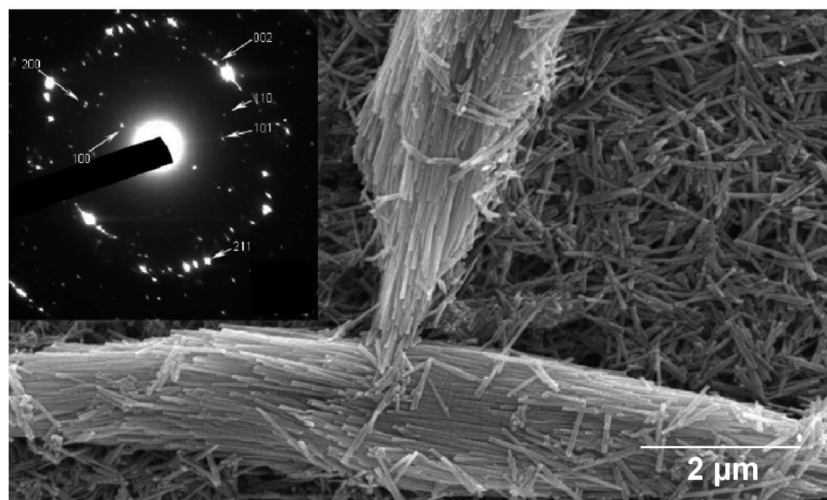


Figure 14. SEM image of rat enamel prisms and enamel crystals. (Inset) SAED pattern of enamel crystals. Lattice planes are indicated in the pattern by arrows. Reprinted with permission from *J. Colloid Interface Sci.*, ref ²⁵⁸. Copyright 2005 Elsevier.

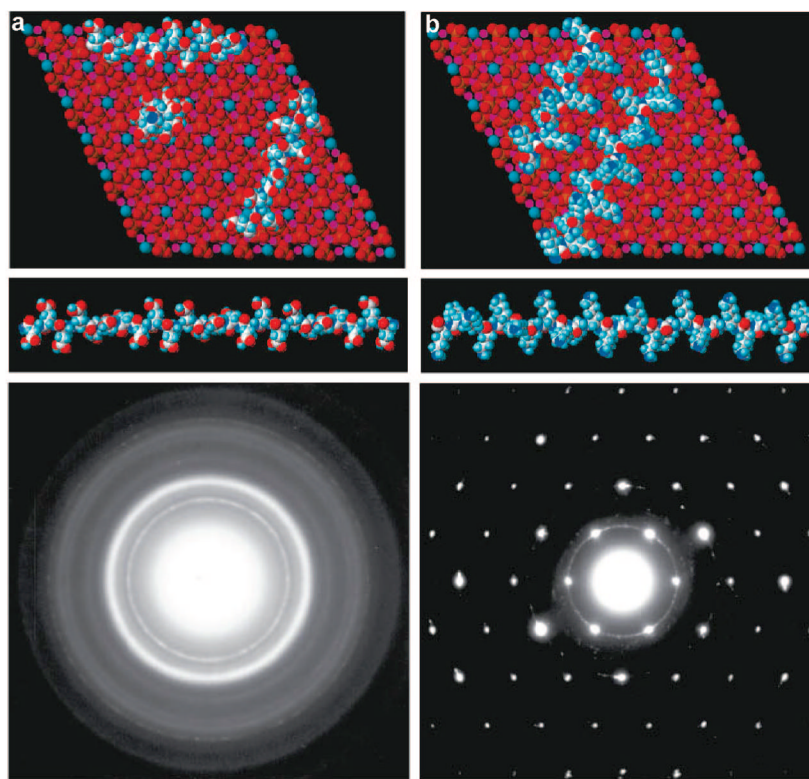


Figure 15.

In synthetic OAs, very small amounts of poly(amino acids) can manipulate microstructure by forming either (a) polycrystalline aggregates of apatite nanocrystals with poly(L-glutamic acid) or (b) large, flat single crystals (micrometers in cross-section and nanometers in thickness), or poly(L-lysine) is present in the mother liquor. Note the coherence between the apatite crystal lattice and the amino groups of the poly(L-lysine) chain in part b. Reprinted with permission from *Science* (<http://www.sciencemag.org>), ref ⁶. Copyright 1997 AAAS.

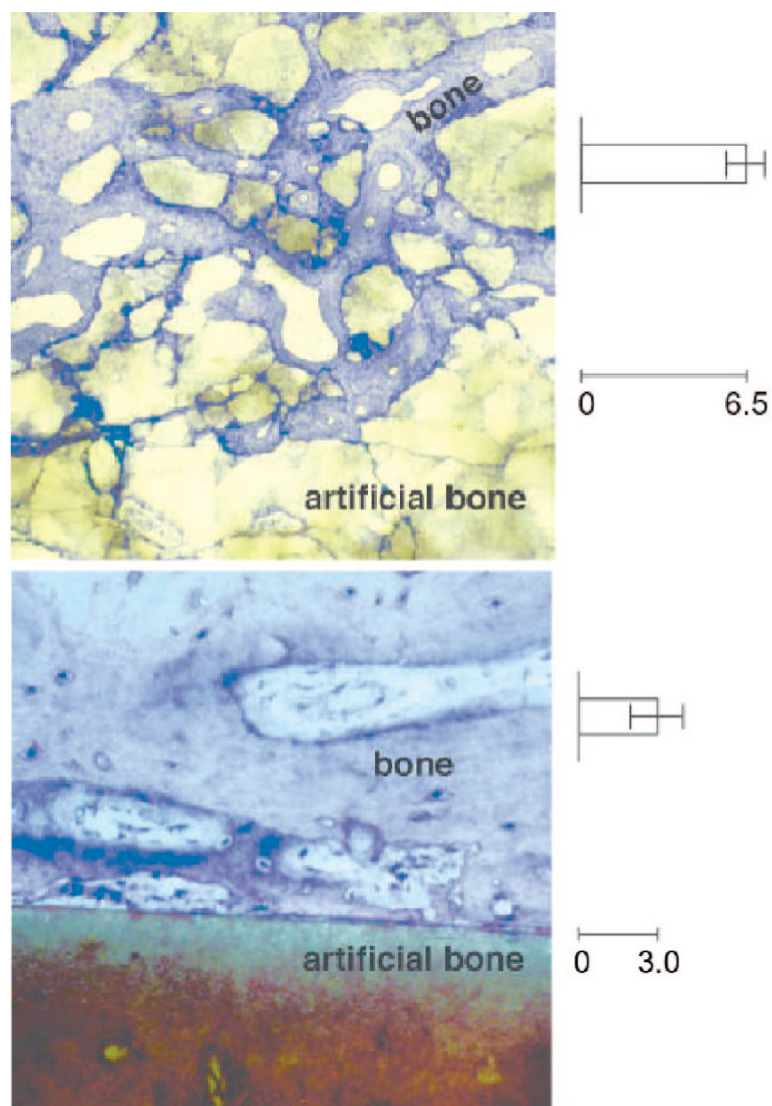


Figure 16. Brittleness of an apatite-based artificial bone material is revealed by the common fragmentation of cylindrical objects implanted in bone (top), whereas mechanically toughened implants can be synthesized by manipulation of the mineral's growth and particle sintering with only 2-3 weight % organic macromolecules (bottom). The fragmentation index is given on the right-hand side of each figure. Reprinted with permission from *Science* (<http://www.sciencemag.org>), ref ⁶. Copyright 1997 AAAS.

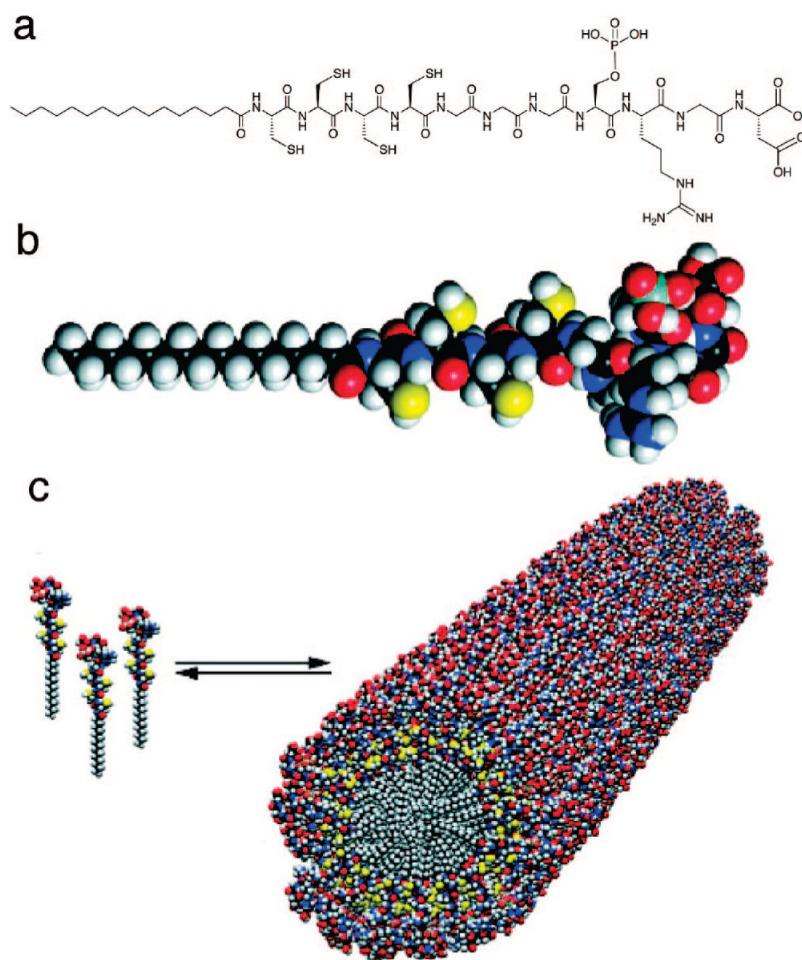


Figure 17.

(a) Chemical structure of the PA, consisting of a hydrophobic alkyl tail; four cysteine residues that when oxidized may form disulfide bonds to polymerize the self-assembled structure; a flexible linker region of three glycine residues to provide the hydrophilic head group flexibility from the more rigid cross-linked region; a single phosphorylated serine residue that was designed to interact strongly with calcium ions and help direct mineralization of HA; and the cell adhesion ligand RGD. (b) Molecular model of the PA showing the overall conical shape of the molecule going from the narrow hydrophobic tail to the bulkier peptide region. (c) Schematic showing the self-assembly of PA molecules into a cylindrical micelle. Reprinted with permission from *Science* (<http://www.sciencemag.org>), ref ⁷⁹. Copyright 2001 AAAS.

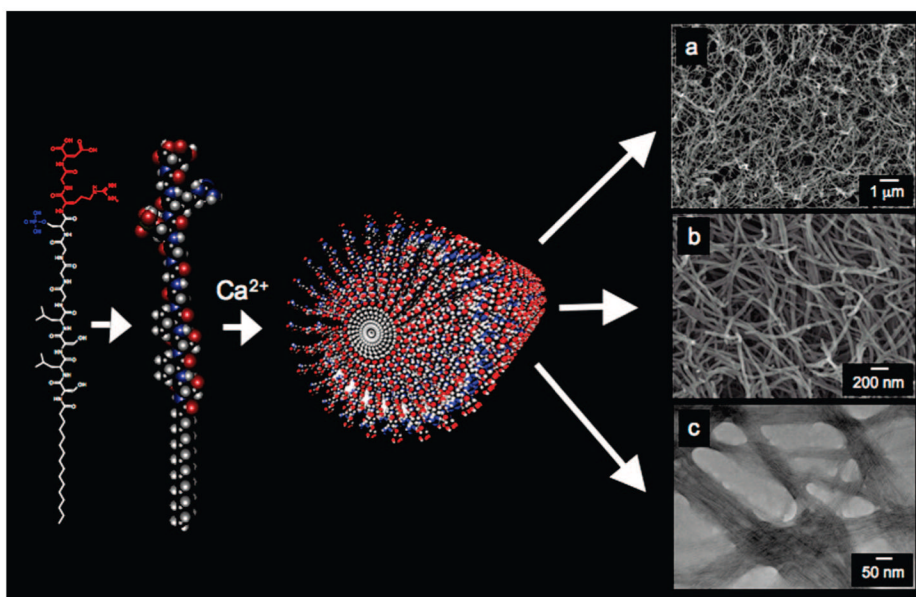


Figure 18. Schematic illustration of the RGD-PA and its self-assembly into a nanofiber. The low magnification (a) and high magnification (b) scanning electron micrographs and the transmission electron micrograph (c) show fibrous bundles, made up of PA nanofibers approximately 5-7 nm in diameter. The scanning electron micrographs were taken of a critical point dried PA gel, while the transmission electron micrograph was taken of nanofibers dried on a TEM grid and stained with phosphotungstic acid.

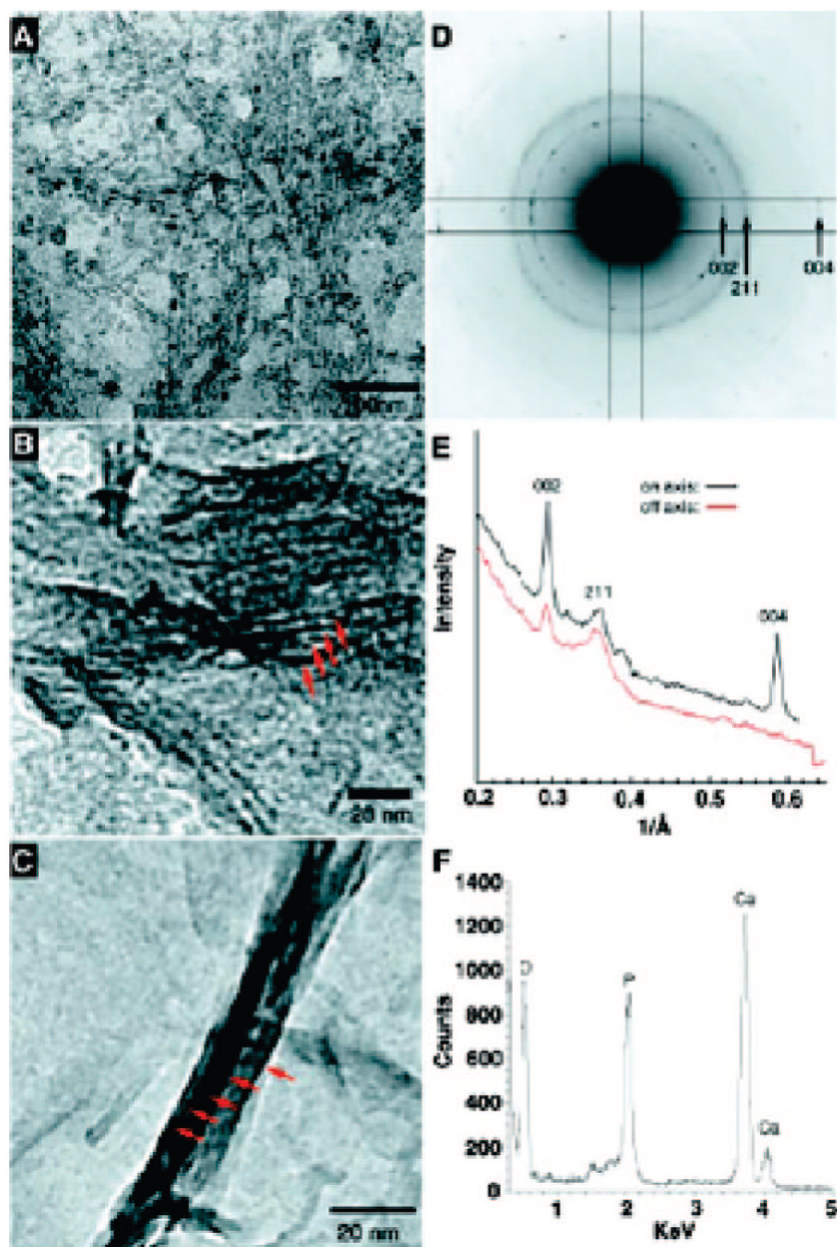


Figure 19. (a) TEM micrographs of the unstained, cross-linked peptide-amphiphile fibers incubated for 10 min in CaCl_2 and Na_2HPO_4 solution. (b) After 20 min, forming HA crystals (red arrows) are observed in parallel arrays on some of the PA fibers. (c) After 30 min, mature HA crystals (red arrows) completely cover the PA fibers. (d) Electron diffraction pattern taken from a mineralized bundle of PA fibers after 30 min of exposure to calcium and phosphate. The presence and orientation of the diffraction arcs corresponding to the 002 and 004 planes (whose intensities are enhanced with respect to the 211 family of reflections) indicate preferential alignment of the crystals with their *c*-axes along the long axis of the bundle. (e) Plot of intensity vs inverse angstroms reveals that the 002 and 004 peaks of HA are strongly enhanced along the peptide-amphiphile fiber axis. (f) EDS profile of mineral crystals after 30 min of incubation

reveals a Ca/P ratio of 1.67 ± 0.08 , as expected for HA. Reprinted with permission from *Science* (<http://www.sciencemag.org>), ref ⁷⁹. Copyright 2001 AAAS.

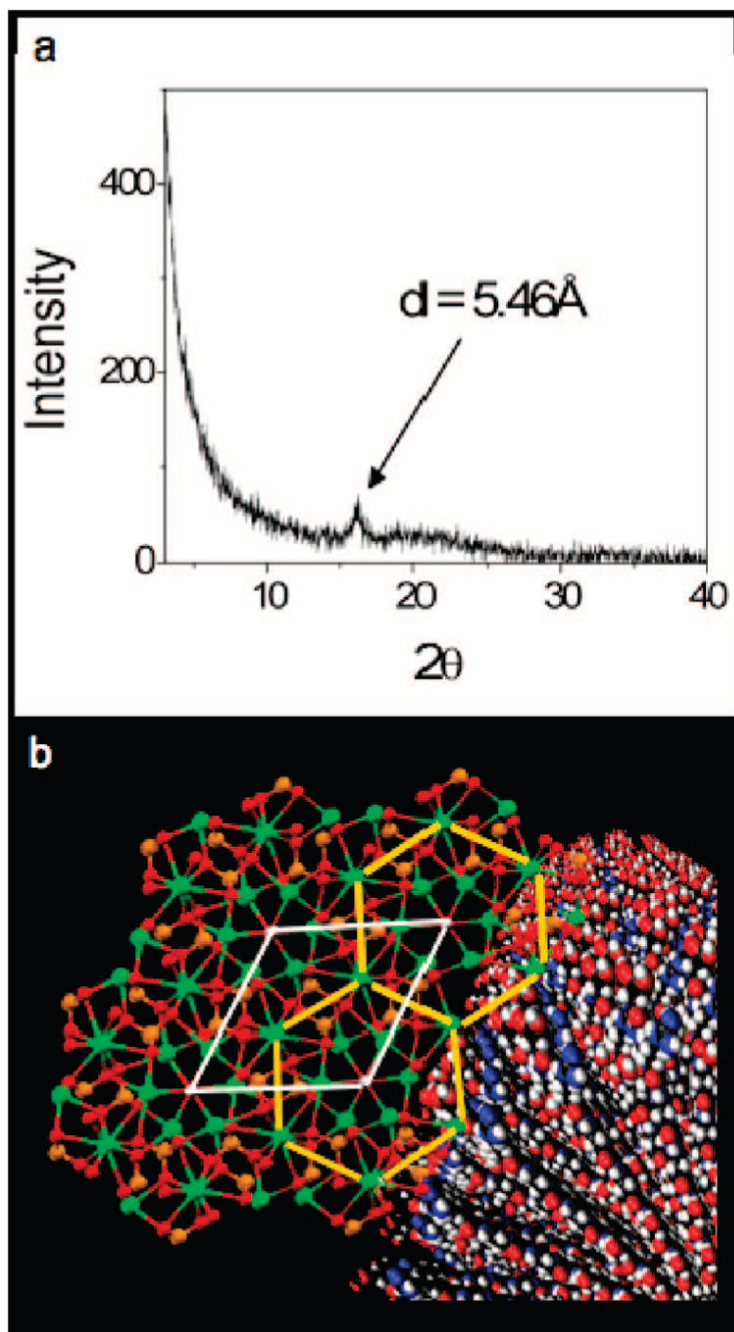
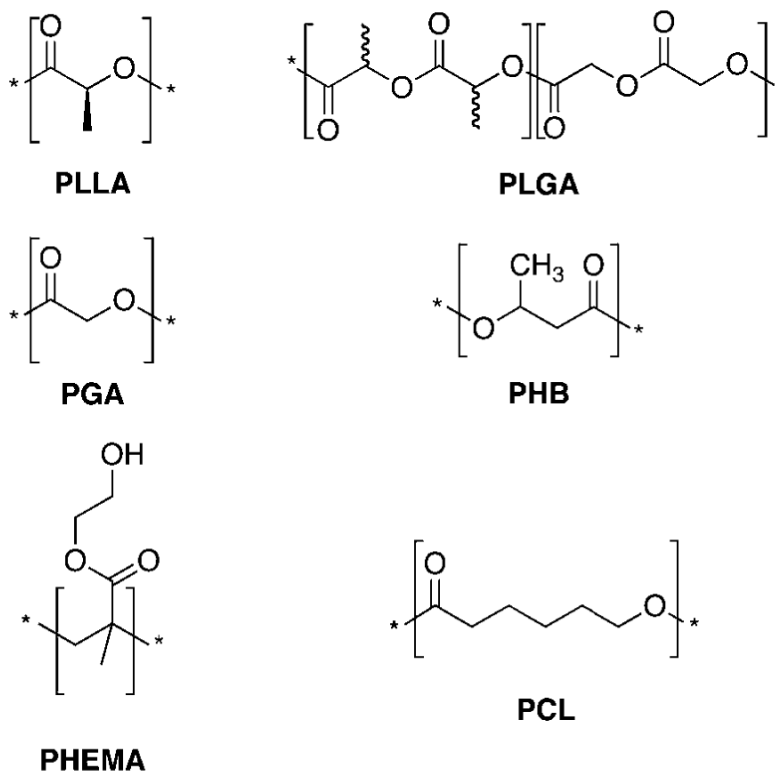


Figure 20.

(a) Powder XRD scan of calcium-gelled PA showing a significant peak at 5.46 Å. Peaks corresponding to HA were not observed, and this peak was not present in PA not exposed to calcium ions. (b) A visualization of a HA crystal nucleating off calcium ions spaced 5.46 Å apart on the PA nanofiber. Calcium ions are shown in green, phosphorus in orange, oxygen in red, and hydrogen in white, while white lines depict the borders of the HA unit cell. The HA crystal is shown with its *c*-axis parallel to the long axis of the PA nanofiber. Yellow lines trace the 5.45 Å interatomic spacings of calcium ions arranged hexagonally throughout the 002 planes of the HA crystal.



Scheme 1. Chemical Structures of Selected Polymers Useful for HA Mineralization

Table 1

Biologically Relevant Calcium Phosphate Minerals^a

mineral	chemical formula	Ca/P ratio	crystallographic characteristics	solubility product (log K_{sp})
monocalcium phosphate monohydrate (MCPM)	$\text{Ca}(\text{H}_2\text{PO}_4)_2 \cdot \text{H}_2\text{O}$	0.5	triclinic P1	highly soluble
dicalcium phosphate dihydrate (DCPD) (brushite)	$\text{CaHPO}_4 \cdot \text{H}_2\text{O}$	1.0	monoclinic C2/c	-6.4
OCP	$\text{Ca}_8\text{H}_2(\text{PO}_4)_6 \cdot 5\text{H}_2\text{O}$	1.33	triclinic P1	-46.9
tricalcium phosphate (TCP)	α - and β - $\text{Ca}_3(\text{PO}_4)_2$	1.5	β = rhombohedral R3c	-29.5
HA	$\text{Ca}_{10}(\text{PO}_4)_6(\text{OH})_2$	1.67	hexagonal P6 ₃ /m	-114.0
fluoroapatite	$\text{Ca}_{10}(\text{PO}_4)_6\text{F}_2$	1.67	hexagonal P6 ₃ /m	-118.0

^aThis table was adapted from refs 15 and 24.

Table 2
Characterization of Bone Crystallites Using Different Analytical Methods

analytical method	crystal dimensions	ref
TEM	3-6 nm diameter × 20 nm long	25
XRD	10-35 nm long	299
SAXS	50 nm × 25 nm × 1.5-4 nm	300, 301
SAXS and TEM	30 nm × 20 nm × 1.5-2 nm	29

Table 3

Organic Components of Bone

name	function in bone mineralization
collagen bone sialoprotein (BSP) osteonectin (ON) and osteopontin (OP) chondroitin sulfate (ChS) and keratan sulfate	structural protein found in many tissues acid protein with poly(glutamic acid) run and RGD binds calcium glycoproteins that may either nucleate or block HA mineralization large molecular weight, sulfated glycosaminoglycans that are found in cartilage and bone tissues
osteocalcin (OC) biglycan and decorin	inhibits bone formation; does not appear to affect HA mineralization proteoglycans that bind to type I collagen and are involved in assembly of bone matrix; decorin specifically interacts with the d and e bands of collagen; biglycan consists of leucine-rich repeats and two glycosaminoglycans; these proteins also interact with thrombospondin and fibronectin.
thrombospondin and fibronectin	matrix glycoproteins that bind to integrins and ECM components (collagen, fibrin, etc.)

Table 4
Recombinant and Native Forms of Amelogenin and Its Cleavage Products

protein description	species	nomenclature	comments
full-length amelogenin	murine	M180	native murine amelogenin
		rM179 (sometimes called rM180)	recombinant-compared with native, lacks Met from N terminus, and phosphorylation on Ser 16
	porcine	P173 (25 kDa)	native porcine amelogenin
		rP172	recombinant-compared with native, lacking Met from N terminus
full-length lacking 13 residue C terminus	murine	M164/M169	native cleavage products
		rM166	recombinant-removed 13 C terminus residues from rM179
full-length lacking 25 C terminus residues	porcine	P148 (20 kDa)	native porcine amelogenin lacking 25 residues of C terminus
tyrosine-rich amelogenin peptide (TRAP)	porcine conserved	P45 (5 kDa)	45 amino acid N-terminal domain
leucine-rich amelogenin peptide (LRAP)	highly conserved	TRAP	
self-assembly domain A	determined from murine	LRAP	
	M180		contains first 33 and last 26 residues of amelogenin residues 1-42, N-terminal region of M180
self-assembly domain B			residues 157-173, C-terminal region of M180

Table 5

Predominant Enamel Matrix Proteins

protein name(s)	description
amelogenin	This is the major protein in enamel that exhibits self-assembly presumably to aid in guiding and templating HA. Ameloblastin maintains the differentiation state of ameloblasts and inhibits proliferation. It may also play a role in cell adhesion, and ameloblastin-null mouse causes the enamel to detach and lose polarity.
ameloblastin, amelin, or sheathelin	
enamelin	Enamelin makes up 1% of the total protein in enamel and is the largest protein in the enamel matrix. Full-length enamelin is located at the mineralization front, while the proteolytic products are concentrated in the rod and interrod.
enamelysin or matrix metalloproteinase-20 (MMP-20)	A proteinase that cleaves amelogenin to produce TRAP as well as a number of other proteolytic products. It is expressed in early stages of amelogenesis (secretory stage), and the MMP-20 null mouse gives rise to a disrupted rod pattern.
kallikrein-4 (KLK-4), enamel matrix serine protease 1 (EMSP-1), or serine protease 17	This is a serine protease that cleaves both amelogenins and nonamelogenins. It is specifically responsible for initial amelogenin cleave and is expressed in later stages of enamel formation.

Table 6

Ion Concentration of SBF^a

	ion concentration (mM)								ref
	Na ⁺	K ⁺	Mg ²⁺	Ca ²⁺	Cl ⁻	HCO ₃ ⁻	H ₂ PO ₄ ⁻	SO ₄ ²⁻	
human blood plasma	142.0	5.0	1.5	2.5	103.0	27.0	1.0	0.5	302
SBF	142.0	5.0	1.5	2.5	148.8	4.2	1.0	0	303
corrected SBF	142.0	5.0	1.5	2.5	147.8	4.2	1.0	0.5	198, 200
revised SBR	142.0	5.0	1.5	2.5	103.0	27.0	1.0	0.5	304
new improved SBF	142.0	5.0	1.5	2.5	103.0	4.2	1.0	0.5	305
1.5SBF	213.2	7.5	2.3	3.8	186.8	40.5	1.5	0.75	221

^aThis table was adapted from ref 199.